**The Thesis Committee for Robert Francis Fimognari, Jr.**
**Certifies that this is the approved version of the following thesis:**

# Development of Functional Materials for Extraction, Sequestration, and Separation Applications

**APPROVED BY**
**SUPERVISING COMMITTEE:**

**Supervisor:**

Jonathan L. Sessler

Bruce Moyer

# Development of Functional Materials for Extraction, Sequestration, and Separation Applications

**by**

**Robert Francis Fimognari, Jr.**

**Thesis**

Presented to the Faculty of the Graduate School of

The University of Texas at Austin

in Partial Fulfillment

of the Requirements

for the Degree of

**Master of Arts**

**The University of Texas at Austin**

**May 2018**

# Acknowledgements

I would first like to thank Professor Jonathan L. Sessler for so graciously accepting me into his research group when misfortune struck me. And to the Sessler lab group members for being so welcoming and inclusive. I also want to thank all of the Holliday lab group members who helped me along the way with my chemistry, or for just being a friend, especially Matt Moore, Kory Mueller, and Sarah Moench. Without your support, none of this would have been possible. I need to also thank my mom and dad for their unwavering love and support. Even though it was from afar, it meant the world to me. And finally, Katie, thank you for being with me on this journey, and showing me through the dark when I couldn't see. You will always be the light in my life.

# Abstract

## Development of Functional Materials for Extraction, Sequestration, and Separation Applications

Robert Francis Fimognari, Jr., M.A.

The University of Texas at Austin, 2018

Supervisor: Jonathan L. Sessler

The separation and purification of elements, ions, and molecules are of great importance to a wide arrays of chemical industries. To this end, materials are continuously being designed to effect and improve upon these separations. Herein are described three classes of materials for the separation of specific analytes of interest. Polymeric extractants were developed based on the incorporation of selective ligands through ring-opening metathesis polymerization, and polymers bearing picolinic acid functionalized pendant groups were shown to selectively extract Cu(II) over a panel of transition metal ions. This material shows promise in radiomedicine, for the purification of Cu radioisotopes. Rigidified picolinamides were shown to selectively extract Am(III) over Eu(III), and were shown to have potential for application in nuclear fuel reprocessing. Finally, polymeric materials for the sequestration of radioiodine are presented and were successfully prepared, containing pendant imidazolium groups for binding Ag(I). These materials may serve as solid sorbents for the fixation of volatile radioiodine from nuclear fuel waste.

# Table of Contents

# List of Tables

# List of Figures

# List of Schemes

# CHAPTER 1: SYNTHESIS OF NORBORNENE-TYPE CONJUGATE MONOMERS FOR POLYMERIZATION BY RING-OPENING METATHESIS POLYMERIZATION, APPLICATIONS TOWARDS THE SELECTIVE BINDING OF COPPER

## 1.1 Introduction

The production and processing of Cu is vital to a wide variety of consumer goods and industries. Therefore, the demand for efficient processes to extract selectively Cu from its ores and waste streams is of immense importance. Traditionally, mined Cu was purified via pyrometallurgy. Unfortunately, the attendant processes require harsh handling conditions, generate large amounts of waste, and produce significant quantities of slag byproduct, which may contain up to 1.5% Cu.[1,2] This slag must be treated via pyrometallurgical and hydrometallurgical processes several times, not only to maximize Cu recovery, but also to meet environmental standards. In addition, waste from electrowinning refinement and metal surface treatment industries contains significant amounts of Cu, which must be separated from other heavy metals to achieve sufficient purity for further use.[3,4] Alternative hydrometallurgical processes, such as solvent extraction, have been explored for Cu purification. In this context, extractants containing carboxylic acid, phosphoric acid, and hydroxyoxime moieties have seen commercial applications in the separation and recycling of Cu from a wide range of other metals (Figure 1.1).[5,6]

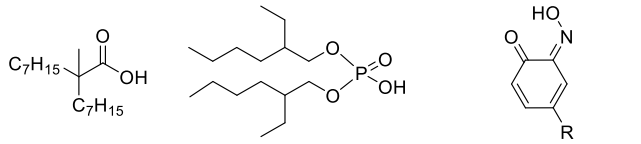


**1.1:** Versatic Acid **1.2:** D2EHPA **1.3:** LIX Hydroxyoxime

**Figure 1.1:** Extractants and functionalities that are selective for copper cations over other metal ions

To improve the working conditions for solvent extraction, these ligands are often immobilized on a solid support, which allows the extraction to be performed with only one liquid phase.[7] Polymeric supports and materials have been utilized in the recognition and separation of metal ions, and the incorporation of certain extractant molecules into polymeric resins has been shown to permit the selective binding and extraction of divalent metal ions.[8,9] Examples of such materials include molecularly-imprinted polymers (MIPs), which have allowed the selective preconcentration of a range of organic substrates and metal ions.[10–12] Unfortunately, the choice of monomer and crosslinker is critical and typically must be optimized for each substrate. Moreover, the molecularly-imprinting template must be stripped from the polymer after fabrication. This can lead to a breakdown in the polymeric structure and affect adversely its ability to recognize and bind analytes of interest.[13]

The introduction of pendant functional groups onto polymer backbones has also been explored as an approach to obtaining polymers that target analytes selectivity.[14] One approach to obtaining such systems involves the use of radical-initiated polymerization methods (e.g., production of polymethyl methacrylates). These strategies are attractive due to the general ease of monomer synthesis and their broad functional group tolerance.[15,16]

However, the polymers produced in this way are often irregular and characterized by broad dispersities. They can also require significant optimization (monomer and initiator choice, solvent, use of a metal catalyst, temperature) in order to achieve a more living character.[17] Ring-opening metathesis polymerization (ROMP) is another polymerization technique that is attractive in the context of producing materials suitable for extraction. ROMP is not prone to chain transfer or termination events, which allows for highly controllable, living polymerizations.[18] The catalysts used for ROMP also have high functional group tolerance. Finally, the requisite monomers can often be synthesized readily by combining a recognition group with a norbornyl moiety to generate precursors that undergo the actual polymerization.[19] To date, several polymers bearing pendant chelating moieties bound to the polymer have been synthesized via ROMP and have been used to achieve selective metal ion binding.[20,21] However, systems appropriate for selective copper extraction remain to be prepared.

Holliday and coworkers previously reported polymers synthesized by ROMP that could be used to separate actinides from simulated spent nuclear fuel waste.[22] These systems were prepared by conjugating a selective ligand to the polymer backbone. Building off this prior success, we sought an easily functionalized moiety that is capable of complexing metal ions in reversible fashion. In this context, controlling metal complexation by pH appeared attractive; in principle, it could allow the affinities to be tuned with high precision. To achieve the desired pH dependence, we elected to explore carboxylic acids as the cation chelating group, in part because carboxylate anions display a preference for Cu(II) over other divalent transition metal cations.[23] For instance, work

by Tasaki and coworkers served to confirm that Cu(II) could be extracted in a pH dependent fashion in competition over other transition metal ions when 2-ethylhexyl picolinic acid was used as their extractant (Figure 1.2).[24]

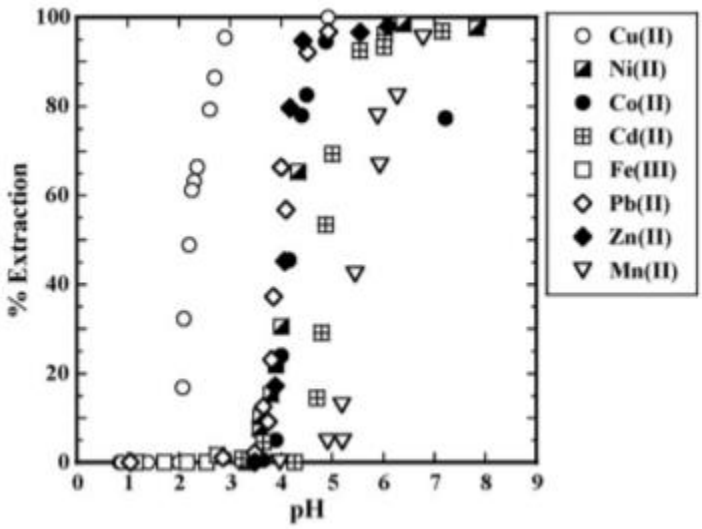


**Figure 1.2:** pH dependent extraction data for 2-ethylhexyl picolinic acid against a panel of transition metal ions.[24]

The observed selectivity was attributed to the stability of the 2:1 metal complex formed between the ligand and Cu(II), as well as the inherent preference for the Cu(II) displayed by carboxylate anions, as the corresponding ester has not shown any extraction ability. This functional handle is a moiety that should be readily amenable for use in ROMP-based approaches to supported extractant development (Figure 1.3).

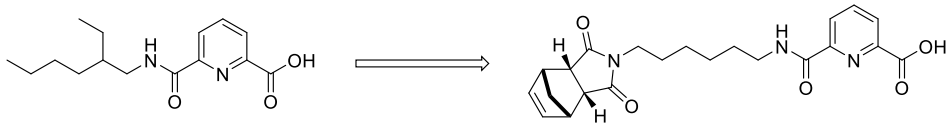

**1.4**: EHPA **1.5**

**Figure 1.3:** Picolinic acid extractant EHPA selective for Cu(II) at low pH (**1.4**) and proposed monomer for use in preparing a Cu(II) selective ROMP-derived polymer (**1.5**)

## 1.2 Results and Discussion

### 1.2.1 MONOMER AND POLYMER SYNTHESIS

The monomer **1.5** was synthesized as shown in Scheme 1.1. Starting from the known norbornyl anhydride **1.6**, the primary amine **1.7** was prepared via condensation with 1,6-diaminohexane in acetic acid.[25] Intermediate **1.7** was then condensed with dimethyl pyridine-2,6-dicarboxylate using catalytic acetic acid to give the amide-ester **1.8** in 91% yield. Base hydrolysis of this compound using lithium hydroxide followed by acidic aqueous workup gave the free acid **1.5** in 89% yield. Overall the monomer **1.5** was synthesized in a total yield of 64% over three steps.

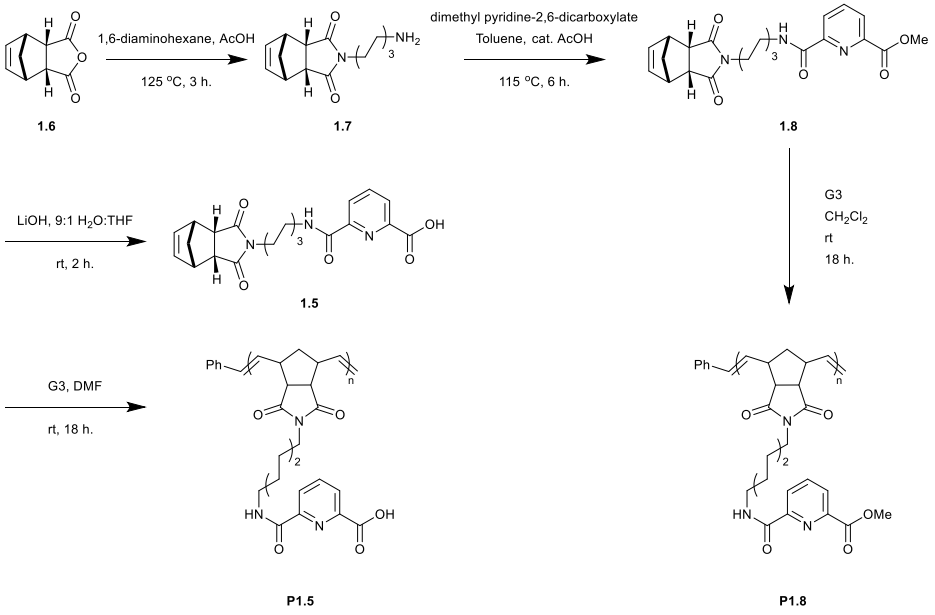


**Scheme 1.1:** Synthesis of monomers **1.5** and **1.8** and their respective polymers, **P1.5** and **P1.8**

To confirm the binding stoichiometry of our monomer and metal ions, metal complexes were synthesized by stirring **1.5** in an EtOH/$H_2O$ (3:1 v/v) solution containing NaOH and various divalent metal dichloride test salts. The chlorides of Cu(II), Ni(II),

Zn(II), Mn(II), Fe(II), Co(II), Pb(II), and Cd(II) were investigated. Crystals suitable for X-ray diffraction were obtained for **1.5**, as well as complexes with Cu(II), Ni(II), Zn(II), and Pb(II). These crystal structures are shown in Figures 1.4-1.8. The structures of complexes with Cu(II), Ni(II), and Zn(II) are all octahedral, with coordination occurring through the carboxylate oxygen, pyridine nitrogen, and amide carbonyl oxygen atoms. In each of the complexes, the bond length between the amide oxygen and the metal is longer than between the carboxylate oxygen and the metal. This indicates that this bond may be slightly labile, and acts as a coordinating ligand due to proximity within the inner coordinating sphere. This makes good sense, as the ionic interaction between the carboxylate oxygen and the metal is expected to be stronger than neutral σ-donor.

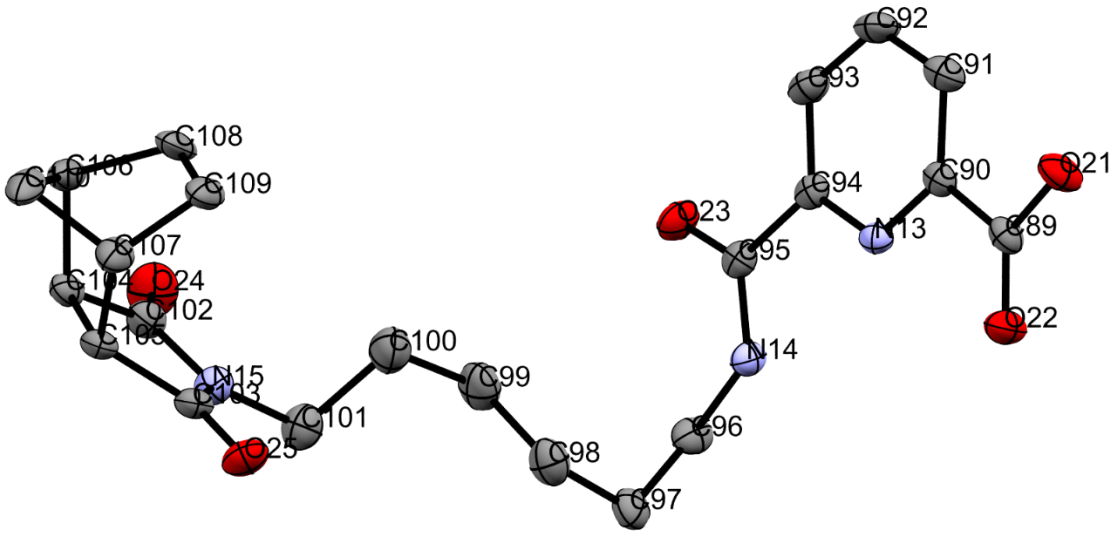


**Figure 1.4:** Molecular structure of **1.5**. The atom labeling scheme is shown. Displacement ellipsoids are shown at the 50% probability level

There is some distortion seen in the Cu(II) complex, most likely due to Jahn-Teller distortions as result of the asymmetrically-filled $d^9$ orbital set.[26] The Ni(II) complex shows similar bond lengths between the two ligands and does not exhibit any distortion.

Presumably, this reflects its $d^8$ electron count. While the Zn(II) complex should not be distorted on the basis of orbital energy stabilization, there is a fair amount of asymmetry between the two ligands, resulting in a "twisted" orientation. Zn(II) is a $d^{10}$ metal ion, and therefore is not stabilized in any geometry. This leads to 4-, 5-, and 6-coordinate complexes being common.[27] As stated above, the longer bond length of the amide oxygen may lead to potential lability. In the case of Zn(II), that may lead to some distortion as the complex is expected to be between 5- and 6-coordinate in solution, with the 6-coordinate complex being observed in the solid state, albeit with increased bond lengths. The Pb(II) complex

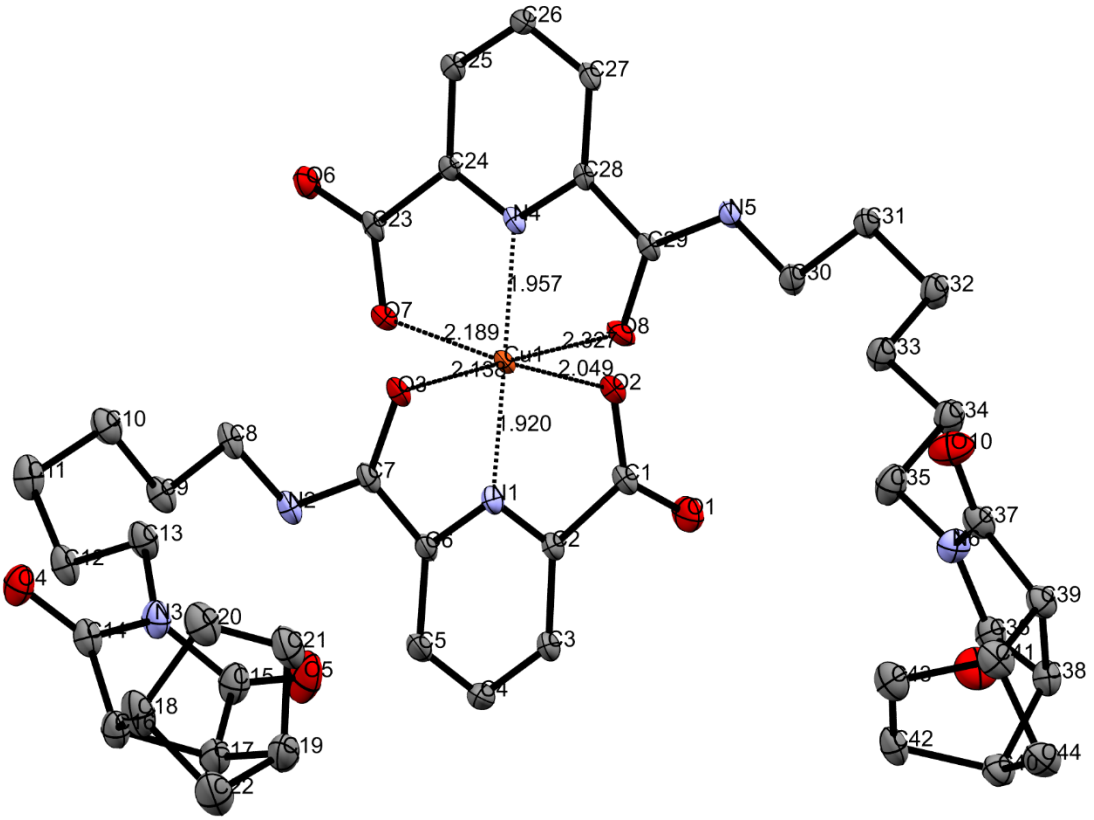


**Figure 1.5:** Crystal structure of **1.5** with Cu(II). The atom labeling scheme is shown. Displacement ellipsoids are shown at the 50% probability level

adopts a hemi-directed geometry, as a result of its filled 6*s* orbital. Interestingly, this complex is completely symmetric with respect to ligand bond lengths. This may be due to reduced steric crowding around the significantly larger Pb(II) ion.

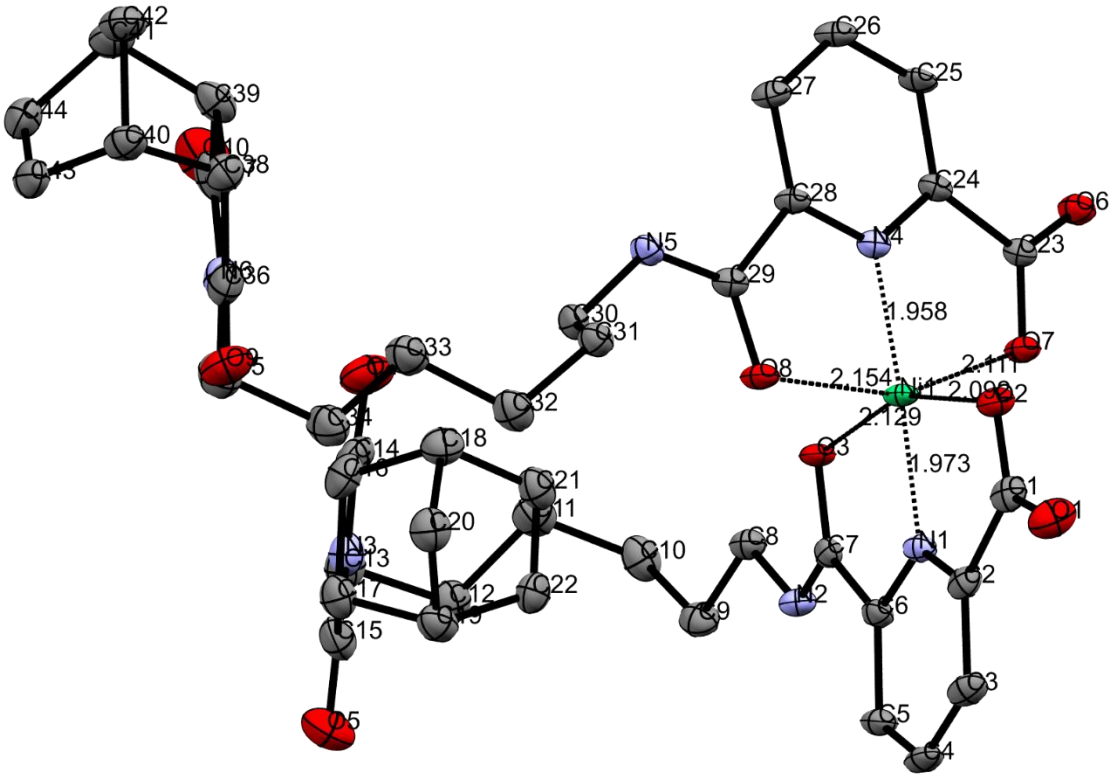


**Figure 1.6:** Crystal structure of **1.5** with Ni(II). The atom labeling scheme is shown. Displacement ellipsoids are shown at the 50% probability level

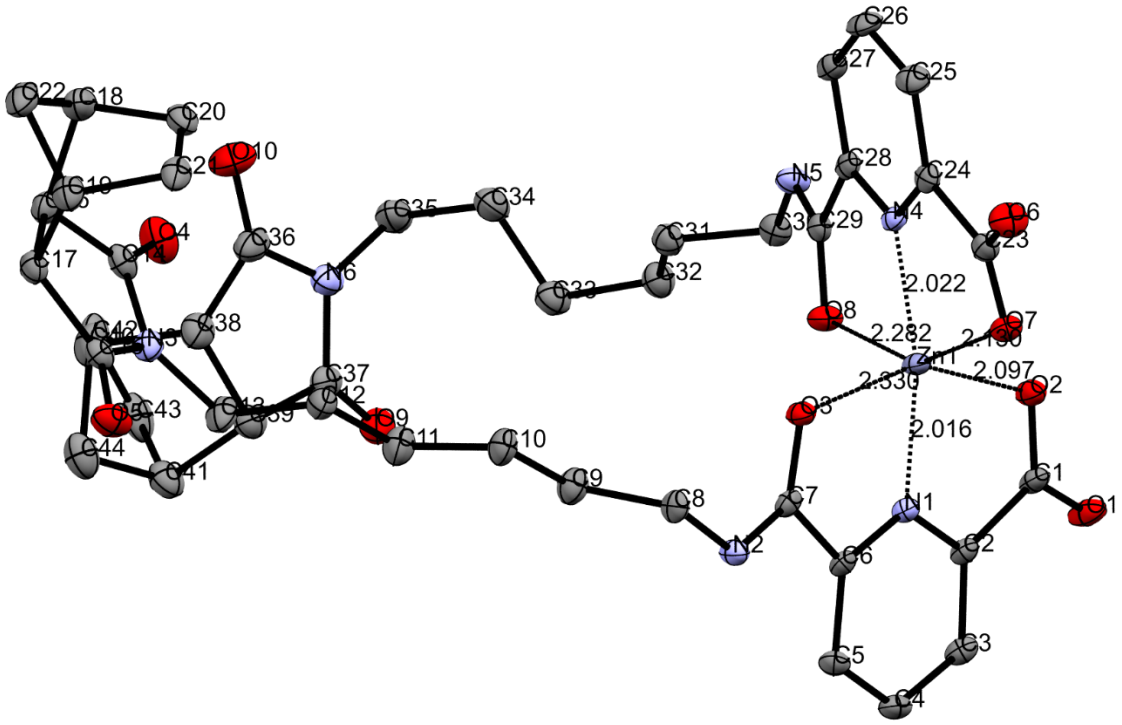


**Figure 1.7:** Crystal structure of **1.5** with Zn(II). The atom labeling scheme is shown. Displacement ellipsoids are shown at the 50% probability level

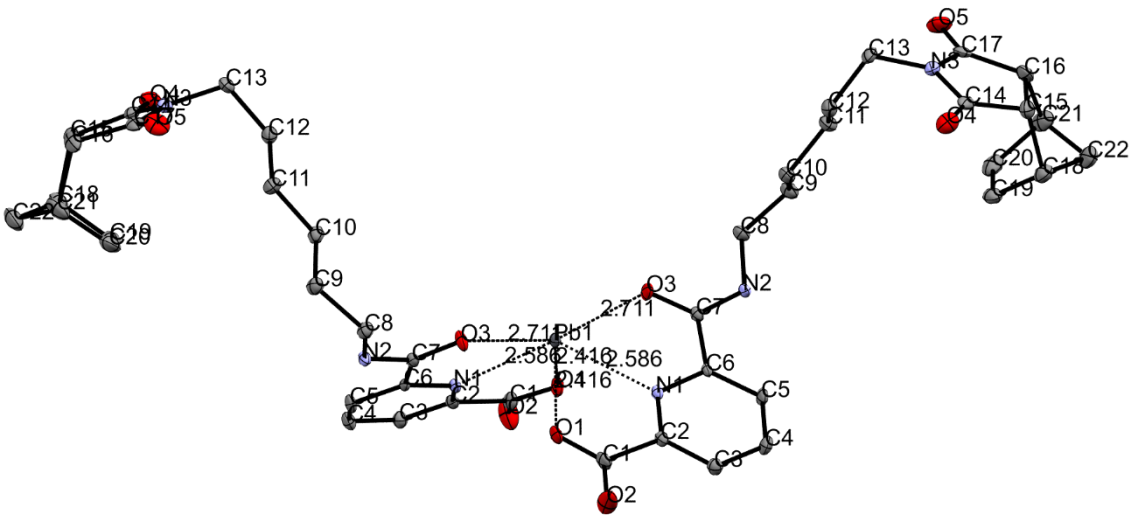


**Figure 1.8:** Crystal structure of **1.5** with Pb(II). The atom labeling scheme is shown. Displacement ellipsoids are shown at the 50% probability level

All polymer samples were prepared by stirring either the monomer of choice dissolved in methylene chloride or dimethylformamide (0.2 M) with a solution of either the Grubbs 2nd or the Grubbs 3rd generation catalyst (0.02 M) and adjusting the solution volume to control the chain length as desired. After stirring overnight under an inert atmosphere, the polymerization was terminated by adding excess (2-3 mL) ethyl vinyl ether and stirring for 30 min. The solvent was removed *in vacuo*, and the crude residue redissolved in a minimal quantity of methylene chloride or dimethylformamide. The resulting solution was rapidly added to either excess methanol or diethyl ether to precipitate the polymer, a process that was repeated at least three more times. Polymers were found to be pure as inferred from NMR spectroscopic analysis after 3-4 precipitations. Initial studies were performed with **1.5** using Grubbs 2nd generation catalyst in dichloromethane. This resulted in incomplete consumption of the starting monomer, most likely due to the

precipitation of short chain oligomers. We rationalized this result in terms of the propagation of the growing chain leading to increasing insolubility of the oligomer/polymer, due to the highly polar pendant carboxylic acid group on our monomer. Changing the solvent to DMF prevented this precipitation, but still resulted in poor control over the molecular weight. Our next thought was that the Grubbs catalyst was not initiating fast enough to allow for living polymerization. Therefore, the $PCy_3$ ligand of the catalyst was exchanged for 3-bromopyridine, which is a better leaving group and promotes faster catalyst initiation.[18] Using this catalyst in DMF resulted in good control of molecular weight, but only up to ca. n = 50 repeat units (approximately 20.7 kD). This result led us to consider that there may be a secondary polymer structure at play, which would orient the polar carboxylic acid moieties towards the solvent and seclude the more hydrophilic polymer backbone. This was problematic, as the secluded backbone would hinder the rate of polymerization, resulting in the poor molecular weight control seen at higher degrees of polymerization. Additionally, this could also increase the likelihood that chain-transfer or -termination events would occur.

To mitigate these putative problems, polymerizations with **1.8** were also attempted. Reaction in dichloromethane using Grubbs 2$^{nd}$ generation catalyst gave polymers of the desired molecular weight. However, to allows comparison with **1.5**, the Grubbs 3$^{rd}$ generation catalyst was used for most polymerization studies. Representative NMR spectra of **P1.8 and P1.5** are shown in Figure 1.9.

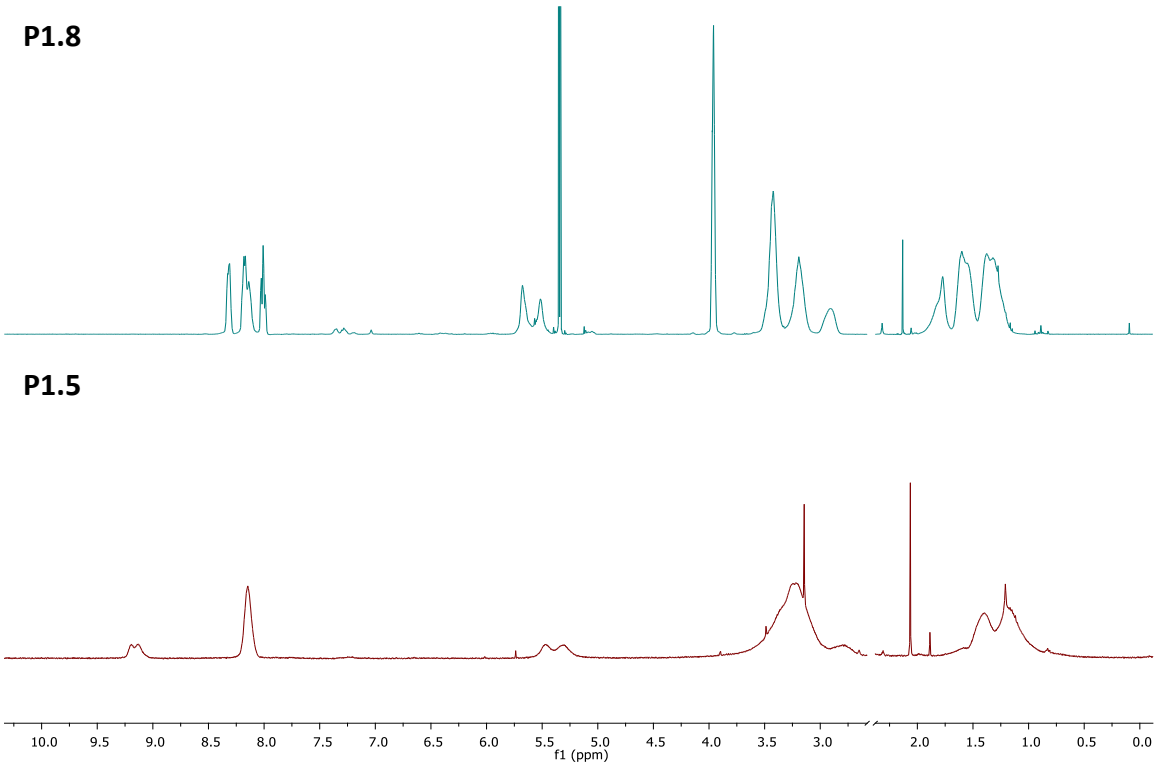


**Figure 1.9:** Representative NMR spectra for **P1.8** in $CD_2Cl_2$ and **P1.5** in DMSO-$d_6$. The region around the residual DMSO solvent peak (ca. 2.5 ppm) has been omitted for clarity

We then wanted to determine the living character of the polymerization of **1.8**. This was done by varying the amount of catalyst added and observing the theoretical and actual molecular weights obtained. Molecular weights were determined from the relative integration of the region corresponding to the terminal phenyl group of the polymer, as illustrated in Figure 1.10**.** Figure 1.11 shows a comparison between the theoretical and actual molecular weights ranging from 25 to 250 repeat units. Since the slope is almost unity, we concluded that the polymerization was living.

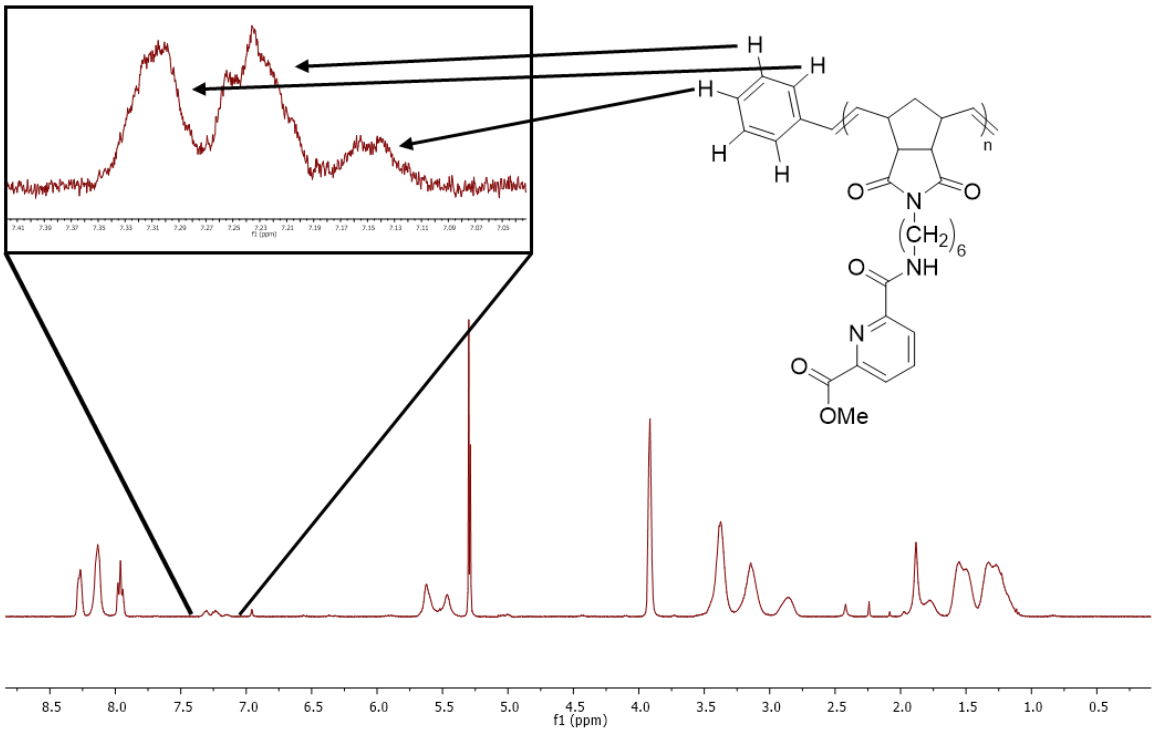


**Figure 1.10:** Determination of polymer molecular weight ($M_n$) by NMR spectroscopy. Integrating the 7.15-7.40 ppm region as 5H gives the relative number of monomer repeat units within the polymer

Additional characterization of samples of **P1.5** and **P1.8** samples was attempted using Gel permeation chromatography (GPC). However, the data collected was insufficient to characterize the dispersity (Đ) of these two samples. Poor light scattering of this polymer type led to very low signal-to-noise ratios, and values for $M_w$ and $M_n$ could not be determined.

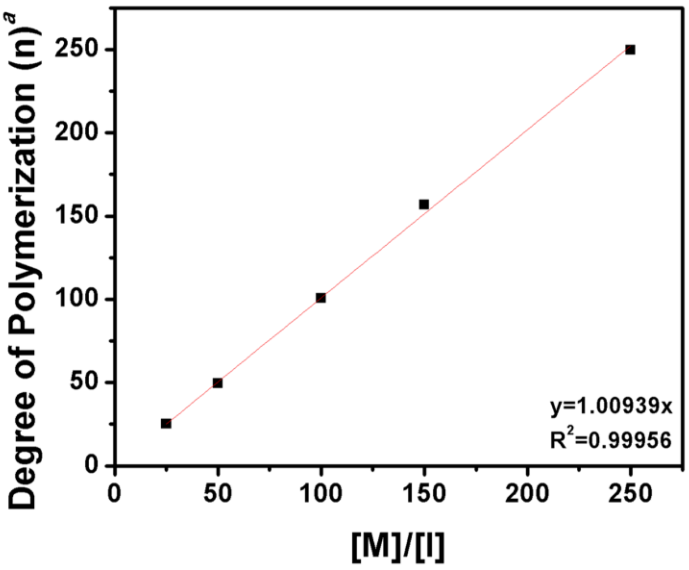


**Figure 1.11:** Living polymerization plot for **P1.8**. A slope of near-unity is consistent with a living polymerization. [a]Determined by NMR Spectroscopy

Work by Viéville and coworkers has shown that polymer samples can be characterized by diffusion-ordered NMR spectroscopy (DOSY), based on the relative diffusion coefficients of the bulk polymer and the end-groups.[28,29] This work has shown a correlation between these diffusion coefficients and polymer dispersity for a broad variety of polymer types, ranging from poly(styrene) and poly(ethylene oxide) to DNA and proteins. DOSY spectra were recorded for **P1.8** over a range of molecular weights (10-50 kD). Polymer sizes larger than 50 kD did not provide good signals due to instrument limitations. Polymer dispersities were calculated using eq. 1.1:

$$Đ = \left(\frac{<D_w>}{<D_n>}\right)^{-d_f} \qquad (1.1)$$

where $<D_w>$ represents the mean diffusion coefficient of the polymer backbone, $<D_n>$ is

the diffusion coefficient of the endgroup, and $d_f$ is the fractal dimension of the polymer.[28] A representative DOSY spectrum of **P1.8** is shown in Figure 1.12, with the corresponding peaks for $<D_w>$ and $<D_n>$ shown. The fractal dimension is equal to the inverse of the Flory exponent, δ, which is a quantitative measure of the conformation that the polymer takes in solution. The fractal dimension may be determined from eq. 1.2:

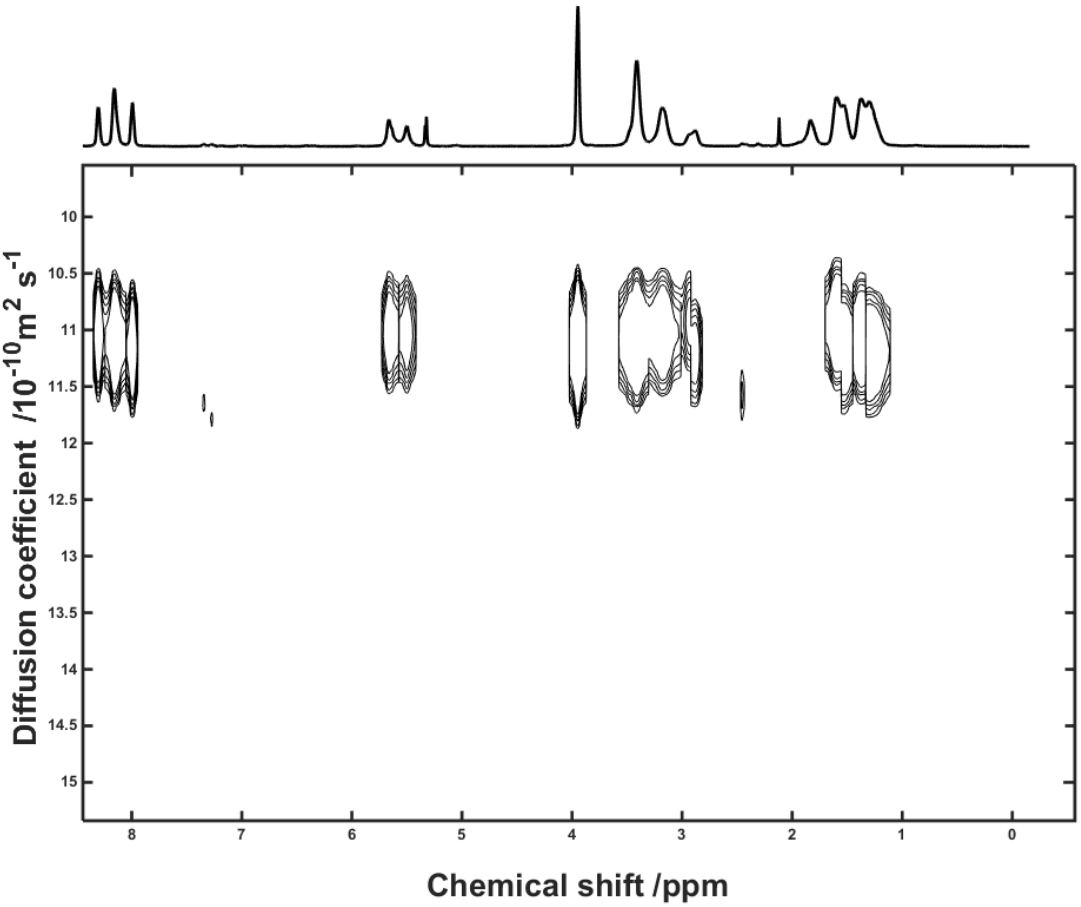


**Figure 1.12:** Representative DOSY spectrum of **P1.8**. $<D_w>$ may be obtained from the peaks of the polymer backbone (ca. $11*10^{-10}$ $m^2s^{-1}$), and $<D_n>$ from the peaks corresponding to the end-group (ca. $11.75*10^{-10}$ $m^2s^{-1}$)

$$M_n \approx \left(\frac{C_r}{D_r}\right)^{d_f} \quad (2)$$

where $M_n$ is the molecular weight of the polymer, $C_r$ is a calibration constant for the "family" of polymers in question, $D_r$ is the diffusion coefficient of the polymer backbone, and $d_f$ is the fractal dimension.[29] A logarithmic fit of eq. 1.2 is shown in Figure 1.13. The

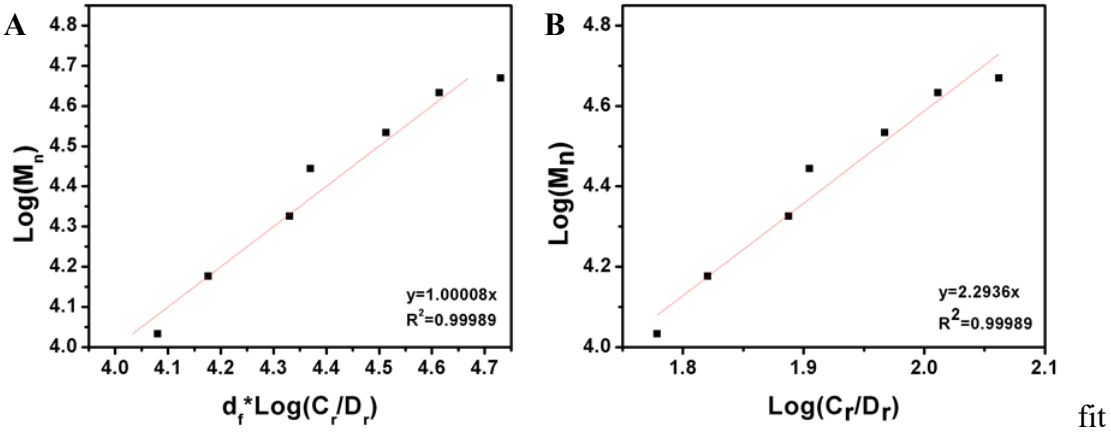


fit

**Figure 1.13:** Logarithmic fit of **P1.8** DOSY data to eq. 1.2 using $d_f$*log($C_r$/$D_r$) vs. log($M_n$) (A) and log($C_r$/$D_r$) vs. log($M_n$) (B). Fitting these two plots gave a value for $C_r$ of 540. The value of $d_f$ may be obtained from the slope of the plot of log($C_r$/$D_r$) vs. log($M_n$)

gives a value of 2.29 for $d_f$, which when used in eq. 1.1 gives Đ values for **P1.8** in the range of 1.02-1.26. This value for $d_f$ of 2.29 corresponds to a Flory exponent of 0.437, meaning that the polymer essentially undergoes a random walk in solution, but still favors polymer-polymer over polymer-solvent interactions to some degree. Similar studies were conducted with **P1.5**, but did not yield a good linear fit. This failure may reflect the intrinsically higher viscosity of DMSO compared to dichloromethane, which would interfere with the

DOSY experiments. Or, it could reflect secondary ordering of the polymer, arising from relatively increased hydrogen bonding.

In order to access **P1.15, P1.8** was saponified using conditions analogous used in preparing **1.5**. The resulting polymer was suspended in a $H_2O$:THF mixutre (9:1 v/v) containing NaOH. The reaction was eemed complete once all the polymer had dissolved (monitored by NMR spectroscopy). Addition of HCl to reprotonate the carboxylic acids served to precipitate **P1.5**. Figure 1.14 compares the NMR spectra of **P1.8** with **P1.5**,

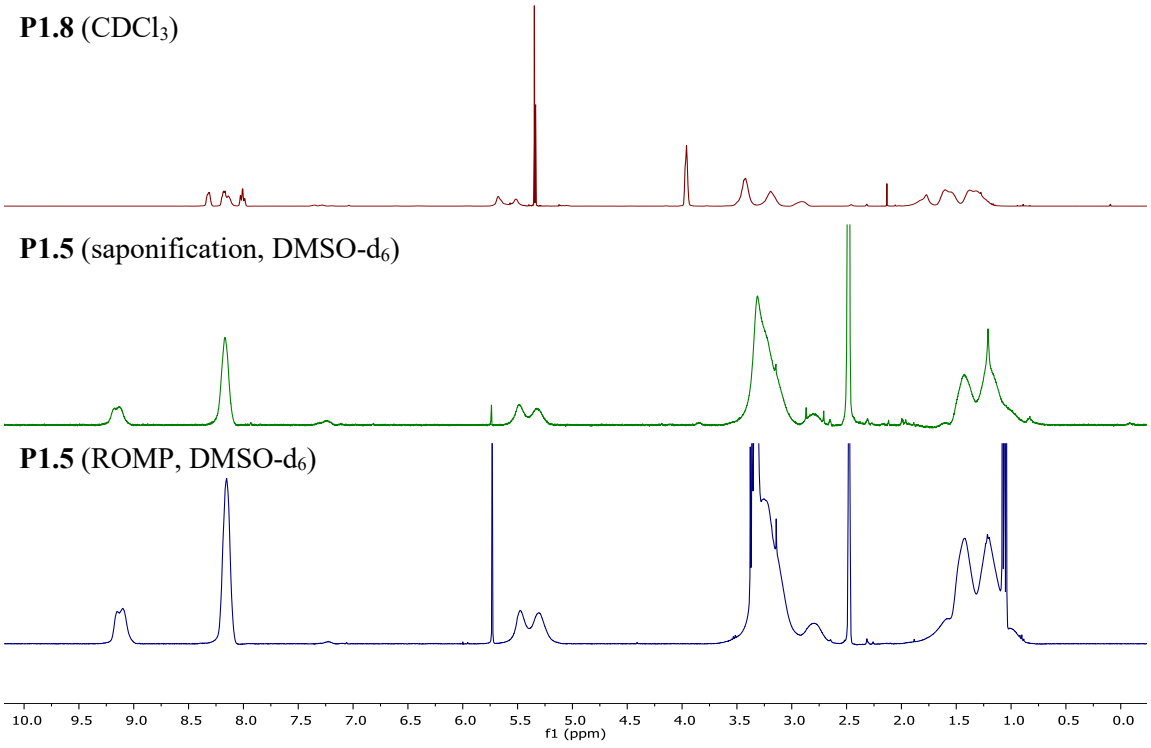


**Figure 1.14:** $^1$H NMR spectra of **P1.8** (top), and **P1.5** produced as a result of the base hydrolysis of **P1.8** (middle), and **P1.5** synthesized in dimethylformamide with Grubbs 3$^{rd}$ generation catalyst (bottom). The disappearance of the peak at ca. 4 ppm is taken as evidence that hydrolysis of the methyl ester has occurred.

synthesized by saponification and by ROMP. After saponification, the peak corresponding to the methyl ester at ca. 4 ppm is no longer visible. This was taken as evidence that the desired carboxylic acid as been formed. Comparison of the NMR spectra of **P1.5** synthesized by saponification and by ROMP does not show many discernable differences, providing further evidence of the success of the saponification reaction.

### 1.2.2 Extraction Studies

Initial extraction studies began with **1.5**, using a procedure similar to that used by Tasaki and coworkers.[30] This previous work was focused on the extraction of metal ions in a noncompetitive system. Therefore, our efforts were focused on investigating a panel of metal ions in the same solution. That is, we wanted to see how **1.5** performed in extractions when exposed to a panel of metal ions at the same time. For simplicity, we chose the same metal salts from the work of Tasaki and coworkers: $CuCl_2$, $NiCl_2$, $ZnCl_2$, $FeCl_2$, $MnCl_2$, $CoCl_2$, $CdCl_2$, and $PbCl_2$. These salts were dissolved at 1 mM each in 1 M aqueous $NH_4Cl$. The $NH_4Cl$ was added to help to drive metal complex formation and ultimately ion extraction. To provide sufficient excess for metal ion extraction, 3.3 equivalents of ligand per metal ion were dissolved in toluene. The pH of the aqueous solutions used for the extraction studies was adjusted with concentrated HCl and $NH_4OH$ to give a range of pH values from 1-7. Extractions were carried out for 24 hours, and involved contacting equal volumes of the aqueous and organic phases. The phases were separated and the aqueous phase was analyzed for its metal ion concentration. The extraction efficiency was calculated based on the mass balance between the two phases.

The results of this study are shown in Figure 1.15. The data is plotted as both the initial pH before extraction as well as the equilibrium pH measured after extraction. In the case of Cu(II) essentially complete extraction still occurs at ca. pH 2. In contrast, appreciable extraction of the other potentially competitive divalent cations does not occur until the pH is raised by 1-2 pH units. This mirrors the results seen by Tasaki and coworkers.[30] However, under these latter higher pH conditions, significant extraction of Fe(II), Ni(II), and Zn(II) is achieved. Both Ni(II) and Zn(II) follow Cu(II) in the Irving-Williams series providing a qualitative rationale for these findings. The extraction of Fe(II) was ascribed to its oxophilic nature and the fact that **1.5** provides two oxygen donor atoms.

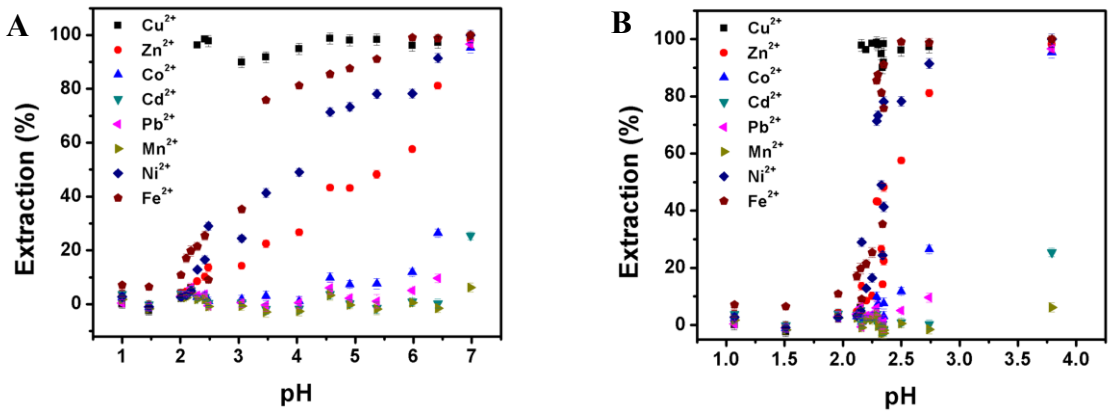


**Figure 1.15:** Liquid-liquid extraction studies with **1.5**. Organic phase: 26.7 mM **1.5** in toluene. Aqueous phase: 1 mM in the eight indicated metal salts (as $MCl_2$; total concentration of M(II) = 8 mM) in 1 M aqueous $NH_4Cl$. (A) Data shown are for the pH recorded before extraction (B) and the pH recorded at equilibrium.

Subsequent to the above predicative studies, **P1.5** was tested for its extraction ability. This polymer proved essentially insoluble in most common nonpolar solvents. Of the solvents available to us, only a mixture of methylene chloride and methanol (9:1 v/v) was immiscible with the aqueous phase, yet still dissolve **P1.5** at sufficient concentrations to

allow for study. Extraction studies were carried out with **P1.5** by adjusting the polymer concentration such that approximately 3.3 equivalents of extractant moiety (on the polymer backbone) were present in solution compared to the metal cations of interest (Figure 1.16).

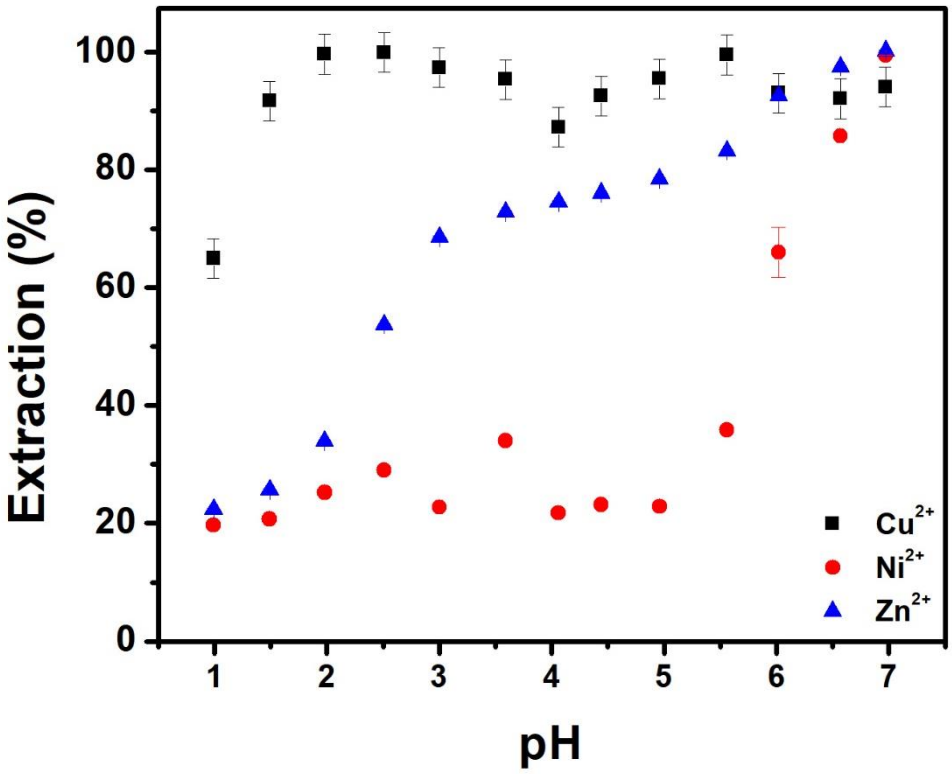


**Figure 1.16:** Liquid-liquid extraction studies with **P1.5**. Aqueous phase: 1 mM in the eight indicated metal salts (as $MCl_2$; total concentration of M(II) = 8 mM) and 1 M aqueous $NH_4Cl$. Organic phase (9:1 v/v methylene chloride:methanol): **P1.5** ($M_w$ = 23,079 D, Đ = 1.07), 3.3 equivalents of pendant extractant moiety relative to [M(II)]

While the polymer was dissolved well at the onset of extraction, notable precipitate could be seen forming within five minutes after mixing the two phases. After extraction, the biphasic mixture was filtered, and the aqueous phase tested by ICP-OES for metal ion speciation, which r that ionevealed extraction had occurred, and that Cu(II) was mostly

removed at ca. pH 2. Additionally, a decrease in specificity was seen, resulting in base extraction levels of ca. 20% of the ions that were not of interest. It is unknown whether this increased extraction at low pH is due to the increased local concentration of ligands on the polymer backbone, or if there was co-precipitation of these metal ions that occurred with the polymer during the extraction experiments. Nonetheless, the precipitation of **P1.5** during extraction was deemed problematic since it would complicate potential processing, as well as desirable metal ion stripping/recovery. Therefore, **P1.5** was tested under conditions of solid-liquid extraction. When tested in this way, **P1.5** showed pH dependent extraction features while maintaining a degree of selectivity for Cu(II) in analogy to what was found for **1.5** (Figure 1.17). Additionally, extraction was seen at a lower pH than for liquid-liquid extractions performed with **1.5** for Pb(II). While not studied in detail, this could account for why **P1.5** proved capable of extracting Pb(II) in contrast to what was seen in the case of **1.5**. When looking at the crystal structure of **1.5** with Pb(II), the organization of the ligand in the hemi-directed geometry resembles that of a cleft or pocket. It is proposed that in the solid state, the particular arrangement of ligands in more prevalent than in the case of the dissolved polymer. To the extent this is true, preorganization and the resulting reduction in the entropy penalty of complex formation may be the primary driving forces underlying the increased Pb(II) extraction achieved by solid **P1.5**.

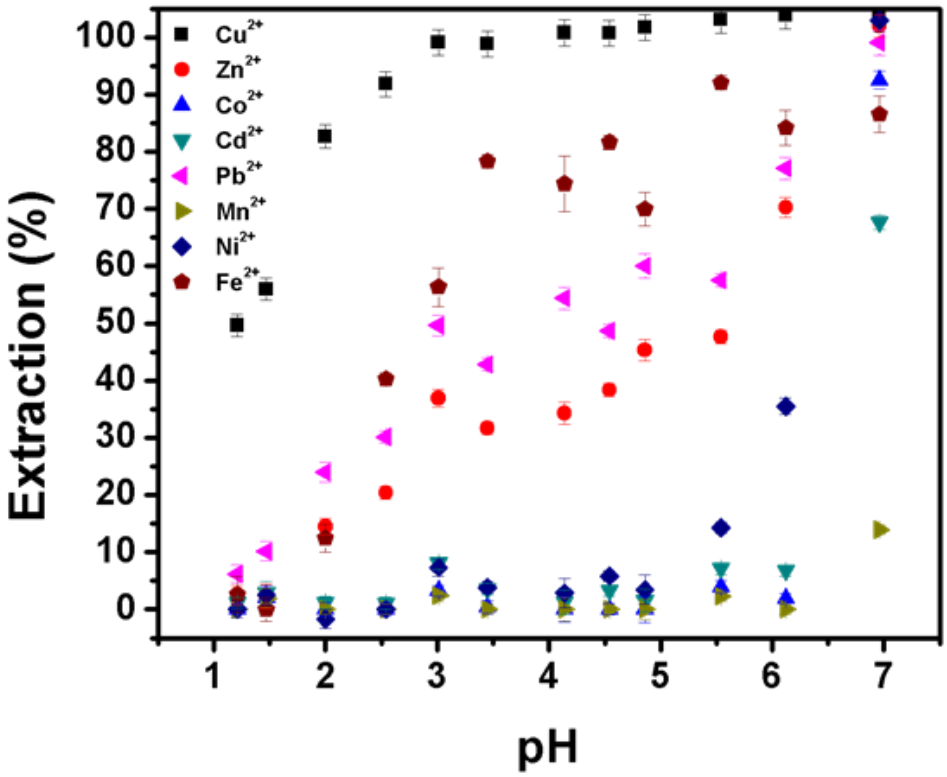


**Figure 1.17:** Solid-liquid extraction with **P1.5**. Aqueous phase: 1 mM in the eight indicated metal salts (as $MCl_2$; total concentration of M(II) = 8 mM) and 1 M aqueous $NH_4Cl$. Solid phase: **P1.5** ($M_w$ = 23,079 D, Đ = 1.07), 3.3 equivalents of pendant extractant moiety relative to [M(II)]

In order to assess the selectivity of **P1.5** for Cu(II) over other metal ions, studies were carried out using a 5-fold excess of each metal ion salt in our panel. After the putative extraction, samples of **P1.5** were digested with concentrated nitric acid and analyzed by ICP-OES to determine the nature of the extracted metal ions. Selectivity for Cu(II) was seen over a broad pH range, peaking around pH = 5 (Figure 1.18A). The pH dependence appears to be driven by competition with Fe(II) and improves in relative terms as the pH is raised. This improvement is likely due to the formation of insoluble $Fe(OH)_2$ species as the aqueous medium becomes more basic.[31]

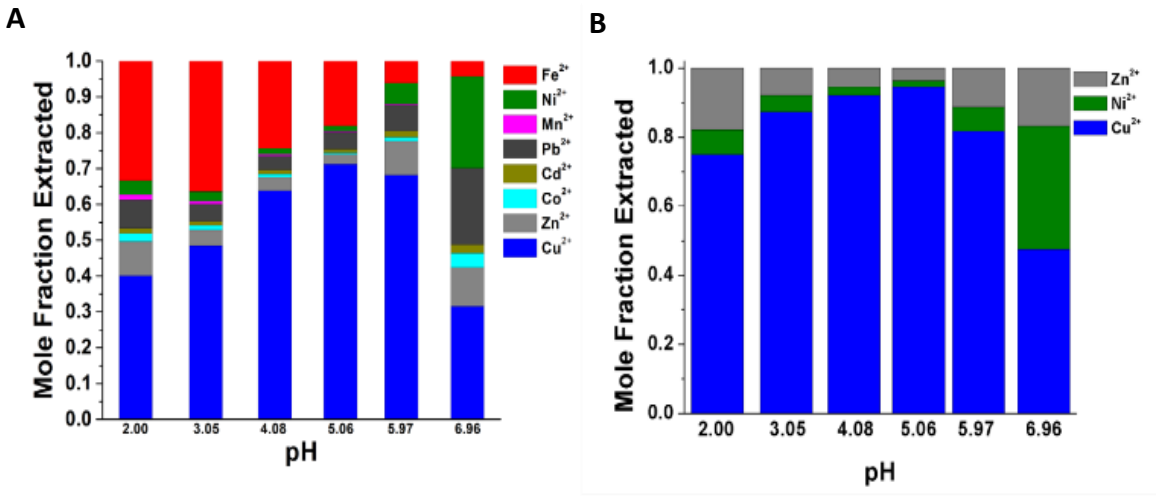


**Figure 1.18:** (A) Selectivity studies performed with **P1.5** ($M_w$ = 23,079 D, Đ = 1.07) using a 5-fold excess of each metal chloride salt relative to the picolinic acid ligand sites present on the polymer. The bars indicate the selectivity observed for each metal ion. (B) Selectivity comparison for Cu(II), Ni(II), and Zn(II)

Another key result of this study was the noted selectivity for Cu(II) over Ni(II) and Zn(II). This observation led us to believe that **P1.5** may have potential for application in the purification of Cu radioisotopes, many of which are produced from enriched Ni or Zn parent isotopes.[32] The $^{64}$Cu isotope has shown promise in the field of positron emission tomography (PET) as an attractive longer-lived ($t_{1/2}$ = 12.7 h) alternative to $^{18}$F ($t_{1/2}$ = 110 min.). The fact that $^{64}$Cu decays by both $\beta^+$ and $\beta^-$ pathways also makes it appealing for radiotherapy. The current method of preparing $^{64}$Cu involves use of a biomedical cyclotron with $^{64}$Ni as the parent isotope. Purification is then effected by ion exchange chromatography, a process which has been noted as being costly, tedious, and sometimes dangerous to the radiotechnicians preparing this isotope.[33] We hypothesized that **P1.5** could be used to purify Cu(II) away from an excess of Ni(II), as well as from Zn(II), which is a decay product for $^{64}$Cu(II).

Prior to studies with **P1.5**, its monomer was studied under biphasic extraction conditions using equimolar aqueous solutions of Cu(II), Ni(II), and Zn(II) (separate studies; 1 mM in each $MCl_2$ salt) with toluene containing **1.5** (10 mM) used as the receiving phase. Initial extraction studies under these conditions (Figure 1.19A) provided evidence that Cu(II) was extracted selectively over Ni(II) and Zn(II) at a pH of ca. 1.7. This selectivity diminished as the pH was raised and was largely absent by pH = 3.0. This finding mirrors what was seen under noncompetitive conditions.[24] Under the biphasic conditions of Figure 1.19A, the optimal Cu(II) vs. Ni(II)/Zn(II) extraction ratio for **1.5** was realized near pH 2. The effect of the concentration of **1.5** was then investigated. This was done keeping the metal ion concentration constant and varying that of **1.5**, as shown in Figure 1.19B. Good extraction efficiency and selectivity for Cu(II) over Ni(II) and Zn(II) was obtained at a 4:1 ligand:metal cation ratio. The time dependence on Cu(II) extraction was also studied, and it was found that maximum extraction efficiencies could reached within three hours, showing a linear time dependence over that time period (Figure 1.19C-D). After three hours, 88% of the Cu(II) but only 3.5% and 4.2% of Ni(II) and Zn(II), respectively, had been removed from the aqueous phase. This translates to selectivity ratios of 25:1 for Cu(II):Ni(II) and 21:1 for Cu(II):Zn(II) respectively.

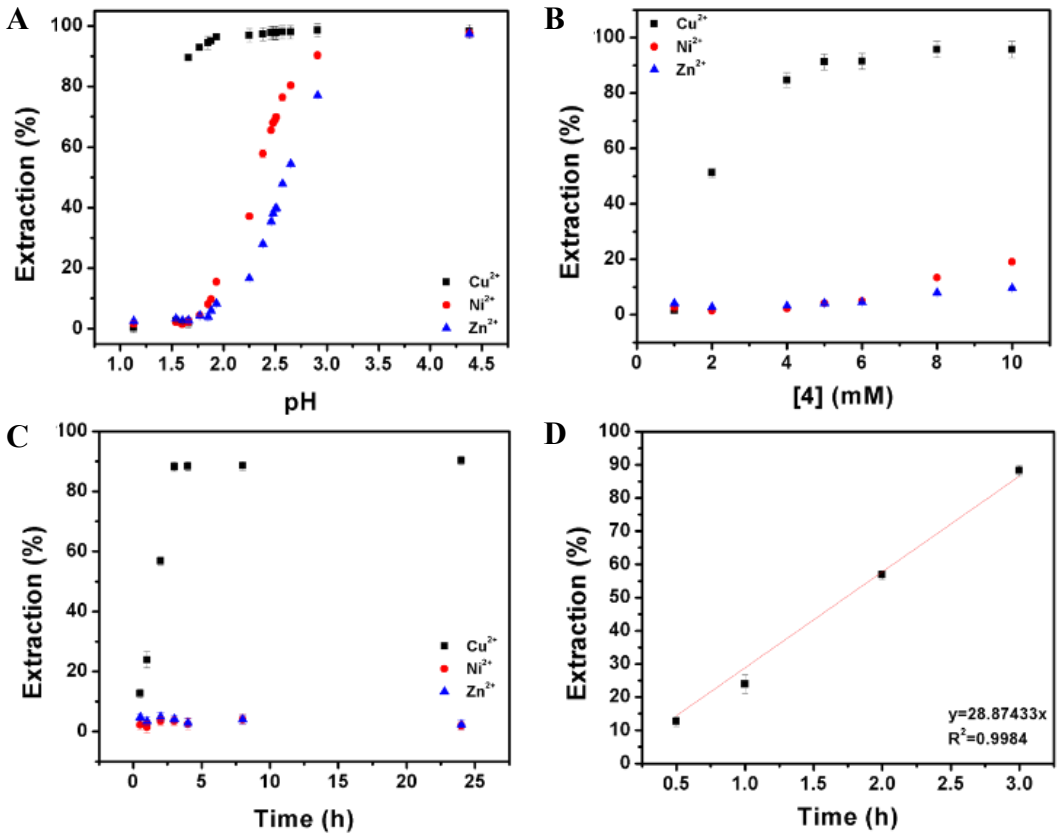


**Figure 1.19:** (A) pH-Dependent biphasic extraction studies. Organic phase: 10 mM **1.5** in toluene. Aqueous phase: 1 mM in $CuCl_2$, $NiCl_2$, and $ZnCl_2$, containing 1 M $NH_4Cl$. The data is plotted as a function of equilibrium pH. (B) Metal ion extraction at ca. pH 2, varying [**1.5**]. (C) Time-dependent extraction of metal ions (1 mM) from an aqueous phase at ca. pH 2 with **1.5** (4 mM in toluene). (D) Linear fit of the extraction of Cu(II) versus time with 4 mM **1.5** in toluene.

In the case of **P1.5**, solid-liquid extraction studies revealed that a large increase in the pH (to ca. pH = 5) was required to obtain efficient Cu(II) extractions (Figure 1.20). However, it is to be noted that the effective metal cation concentrations were lower in these studies compared to the studies with a panel of metal ions. Thus, it is difficult to assess at present the origin of the pH effect seen on moving from **1.5** to **P1.5**, but one cause may be a reduced Lewis acidic influence of metal ions on **P1.5**.

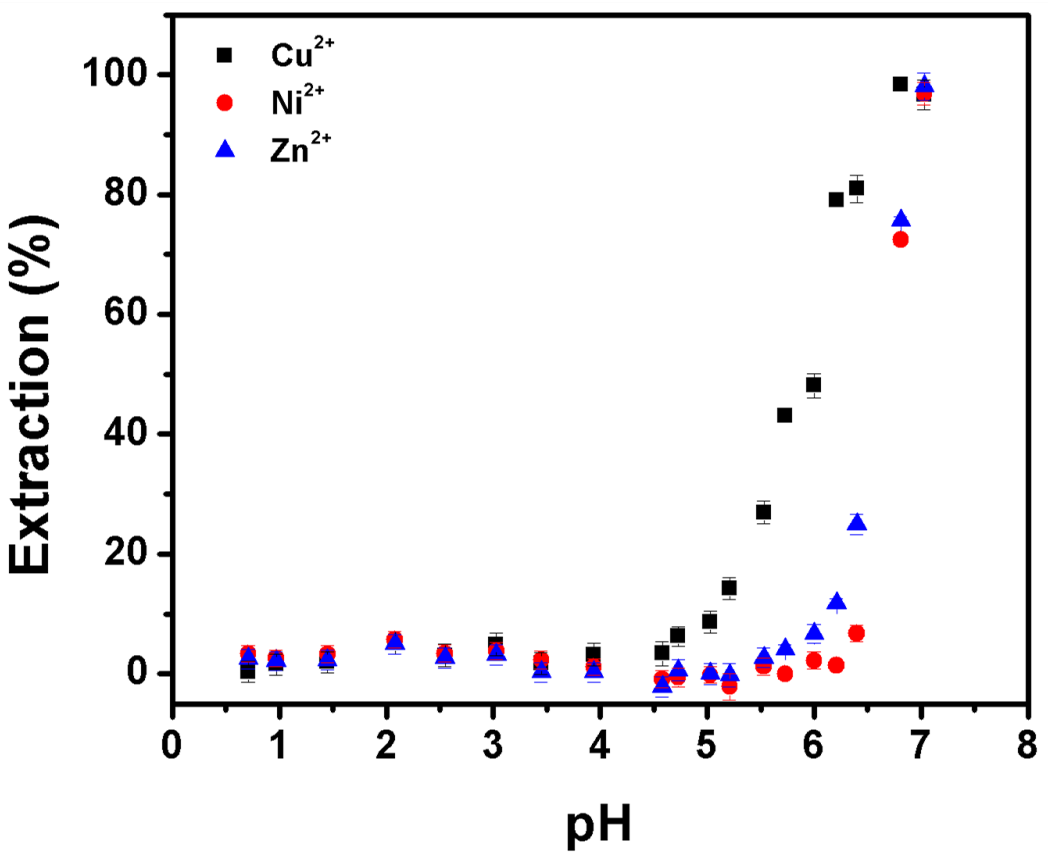


**Figure 1.20:** Solid-liquid extraction with **P1.5**. Aqueous phase: 1 mM $CuCl_2$, $NiCl_2$, and $ZnCl_2$, containing 1 M $NH_4Cl$. Solid phase: **P1.5** ($M_w$ = 23,079 D, Đ =1.07), 3.3 equivalents of pendant extractant moiety

Time-dependent extraction studies revealed a lack of linearity. Nevertheless, ca. 80% extraction was achieved with **P1.5** after 4 hours under the present solid-liquid extraction conditions (Figure 2.21). Unfortunately, lower Cu(II):Ni(II) and Cu(II):Zn(II) extraction ratios (11.6:1 and 3.3:1, respectively) were observed.

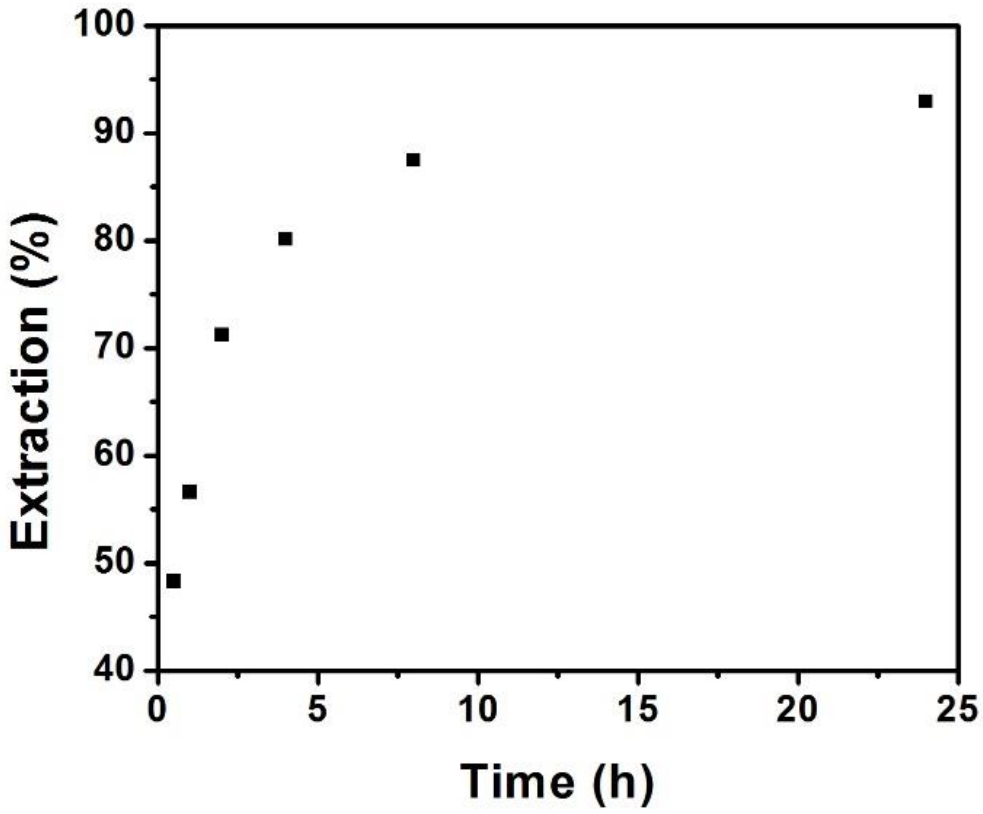


**Figure 1.21:** Time-dependent extraction of Cu(II) by **P1.5**. Aqueous phase: 1 mM $CuCl_2$, containing 1 M $NH_4Cl$. Solid phase: **P1.5** ($M_w$ = 23,079 D, Đ =1.07) bearing 3.3 equivalents of the pendant extractant moiety.

Since Ni is usually the main impurity in the production of Cu radioisotopes, the selectivity for Cu(II) over Ni(II) was further examined with **P1.5** (Figure 1.22). This was done by varying the pH to see if separation efficiencies could be improved at lower pH. Studies carried out using mixtures with 1:1, 10:1, and 100:1 Ni(II):Cu(II) ratios revealed a reasonably linear relationship between the ratio of Cu(II):Ni(II) extracted and the pH. The best results exceeded the 25:1 ratio seen in extraction studies utilizing **1.5** (Figure 1.22A).

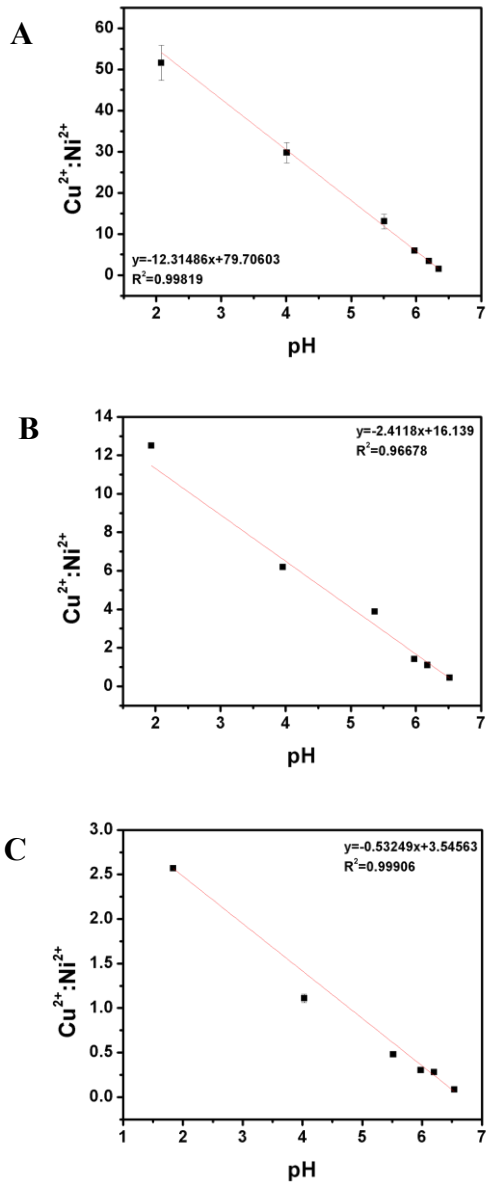


**Figure 1.22:** Solid-liquid phase selectivity studies with **P1.5** ($M_w$ = 23,079 D, Đ = 1.07). Aqueous phase: 1 mM $CuCl_2$ and 1 M $NH_4Cl$. The $NiCl_2$ concentrations were 1 mM (A), 10 mM (B), and 100 mM (C). In all cases, 0.2 equivalents of **P1.5** were used with respect to the [Cu(II)].

Another way to assess the selectivity of an extractant is by calculating the relevant separation factors ($S_{x/y}$), which are a measure of the ratio of the distribution ratios of any two analytes ("a" and "b") of interest. In accounting for the relative concentrations of each

metal ion, the separation factors at each concentration of Ni(II) show a linear dependence on pH. One exception is when [Ni(II)] = 1 mM (Figure 1.23A). In this case two independent linear regions for $S_{Cu/Ni}$ are observed. One explanation for this may be that there are two separate factors contributing to ion extraction. Increased concentrations of [$Cl^-$] may being driving complex formation by acting as an "anion swing", as described in Le Chatelier's principle. Because the [$Cl^-$] is high due to the presence of 1 M $NH_4Cl$, it may be that at lower pH, the driving force for complex formation is determined more by the ease of deprotonation of the carboxylic acids of the ligands than by [$Cl^-$] alone. Alternatively, Lewis acid influences from the metal ions present in solution may be causing the deviation from linearity at lower pH. Since in this case [M(II)] = 2 mM, selectivity driven by Lewis acid effects on ligand deprotonation may be less prevalent. Notably, in the presence of a 100-fold excess of Ni(II), separation factors as high as 290 in favor of Cu(II) were observed (Figure 1.23C). An explanation for this latter value may be found by examining the complex formation constants of Cu(II) ($\log(K_f)$ = 14.78) and Ni(II) ($\log(K_f$ = 12.44) with picolinic acid.[34] It is assumed that complex formation occurs by the reaction shown in eq. 1.3:

$$M(II) + 2\,Cl^- + 2\,L \rightarrow ML_2 + 2\,HCl \qquad (3)$$

where L corresponds to the picolinic acid ligand. Using this equation and taking the difference in the formation constants for Cu(II) and Ni(II) with picolinic acid ($\Delta\log(K_f)$ = 2.34) into account, one finds that this value is largely dependent on the ratio of Ni(II):Cu(II) in the aqueous phase. Because the ratio of Ni(II):Cu(II) in these experiments was 100:1

and $\Delta K_f \sim 220$, more Cu(II) must be extracted than Ni(II) to satisfy this equilibrium, supporting the experimental value of $S_{Cu/Ni}$.

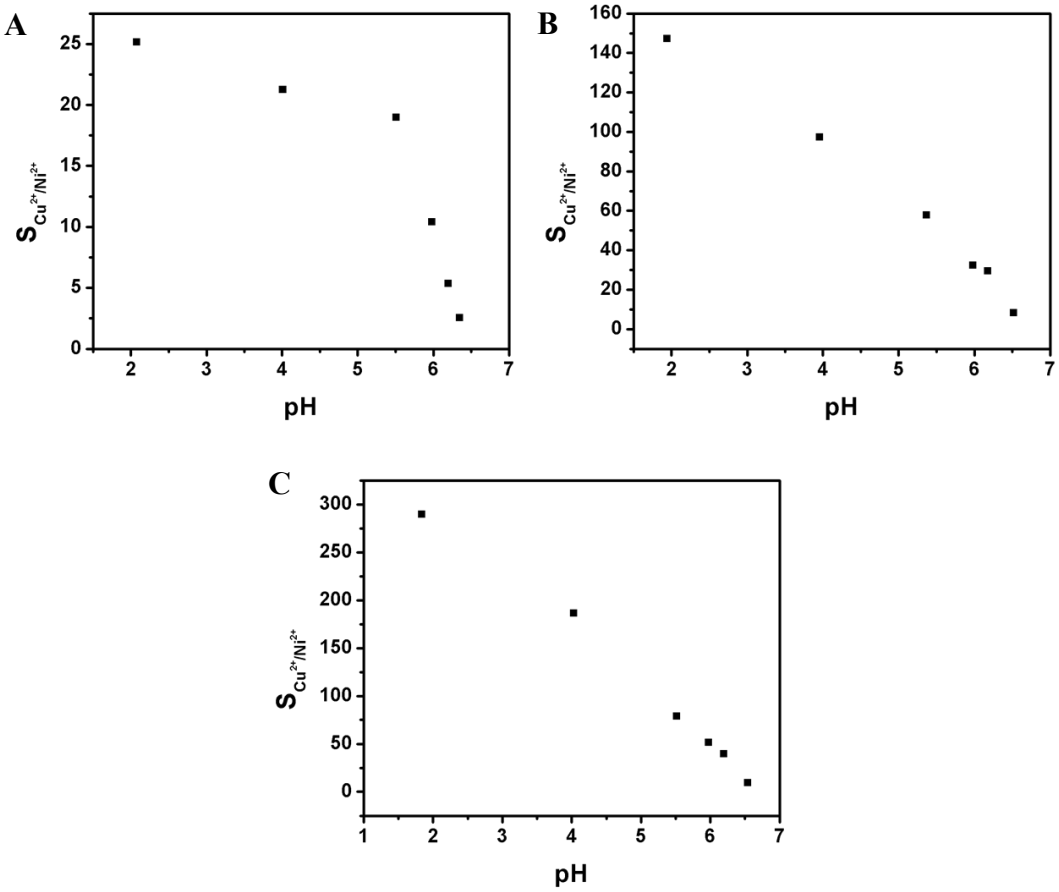


**Figure 1.23:** Plots of separation factors, carried out at varying pH from selectivity studies with **P1.5** ($M_w$ = 23,079, Đ = 1.07). Aqueous phase: 1 mM $CuCl_2$ and 1 M $NH_4Cl$. The $NiCl_2$ concentration was 1 mM (A), 10 mM (B), and 100 mM (C). In all cases 0.2 equivalents of **P1.5** were used with respect to the [Cu(II)]. Separation factors were calculated as the ratio of the distribution coefficient of Cu(II) to Ni(II), based on the concentrations in the solid polymer and in solution

To evaluate the potential of this material as a reusable extractant, **1.5** (10 mM, toluene) was first used to extract a 1mM solution of Cu(II), Ni(II), and Zn(II), buffered

with 1 M $NH_4Cl$. The organic phase and any resulting precipitate was separated from the aqueous phase, which was then taken to dryness. The resulting residue was dissolved in $CH_2Cl_2$ using minimal MeOH, and biphasic back extractions were performed using a panel of strippants. Using the initial aqueous phase and strippant solutions after extraction, the amount of metal ions stripped from **1.5** was determined by ICP- OES (Figure 1.24). These experiments showed that stripping Cu(II) bound to **1.5** was nontrivial.

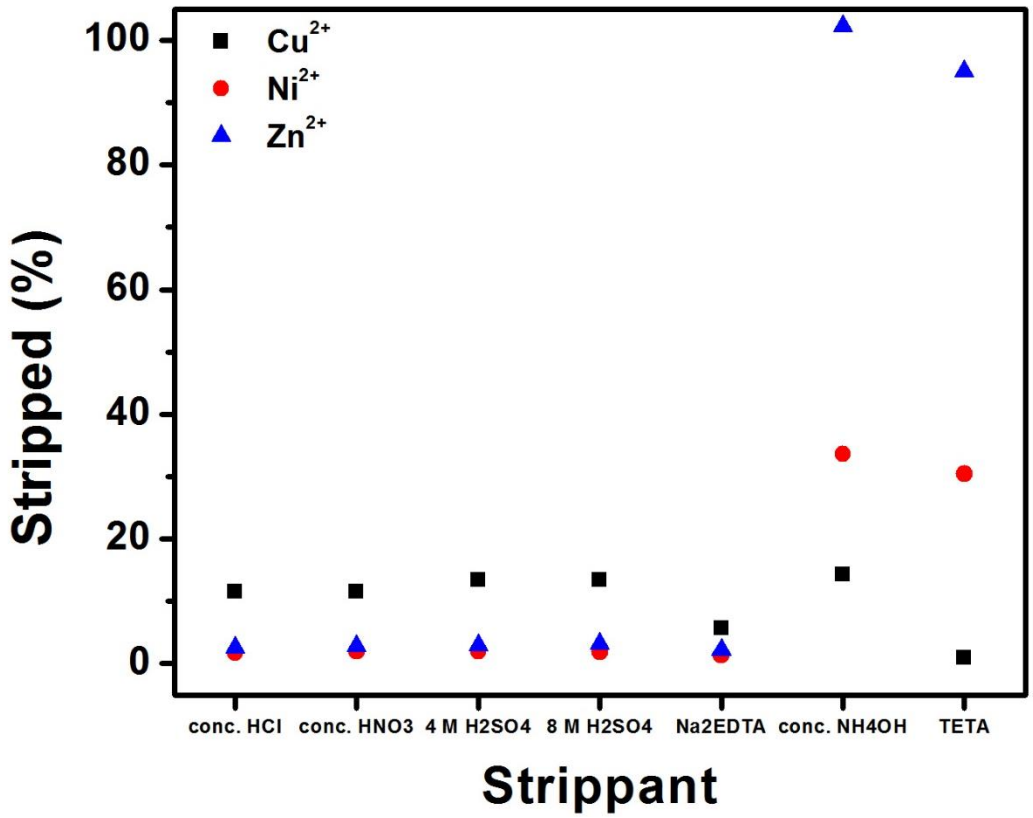


**Figure 1.24:** Stripping of Cu(II), Ni(II), and Zn(II) from **1.5** using a panel of strippant solutions consisting of the agents shown in the x-axis.

We hypothesized that the apparent stability of the Cu(II) complex of **1.5** with regard to stripping was in part due to the hydrophobicity of the norbornyl imide and hexyl chains, leading to poor interfacial contact between the organic and aqueous layers. Additionally,

entanglement of the hexyl chains around the metal complex could make it difficult for the strippant to be in close proximity to the metal center, resulting in decreased stripping efficacy. To mitigate this presumed problem, we moved to shorten the length of the alkyl chain linking the extractant and polymerizable moieties, reducing the number of carbon atoms from six to two (Scheme 1.2). When using **1.11** for extractions and subsequent stripping tests, we saw similar extraction efficiencies at ca. pH=2 as for **1.5**, but also increased stripping efficiency (Figure 1.25).

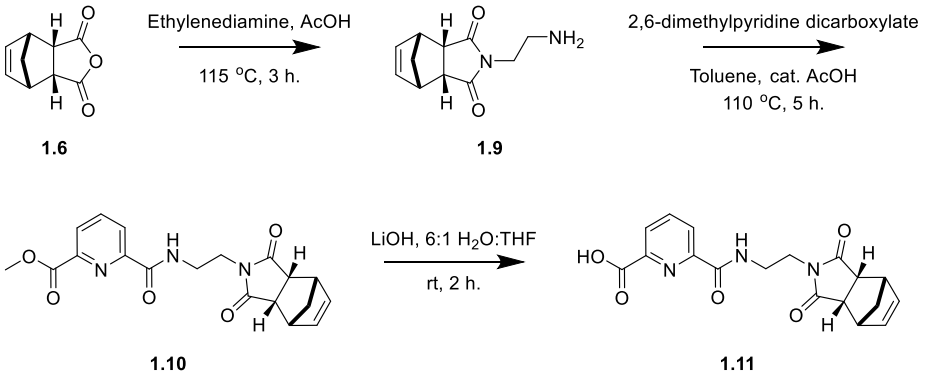


**Scheme 1.2:** Synthesis of extractant monomer containing a two-carbon atom linker

linker. Lower yields than the six-carbon atom linker may be due to an impurity in the ethylene diamine starting material. It is important to note that each strippant tested with **1.11** indiscriminately stripped about the same amount of each metal ion from the organic phase. This suggests that the release of metal ions from **1.5** is due to hydrophobic effects from the hexyl chain, rather than the inherent stability of the metal complex that is formed. While this is not advantageous for extraction with **1.5**, when going to a polymeric system, the extractant moiety should be oriented away from the hydrophobic polymer backbone, now more exposed to the aqueous strippant than as a monomeric metal complex. The release of metal ions from **P1.5** was investigated using an acid strippant, similar to studies

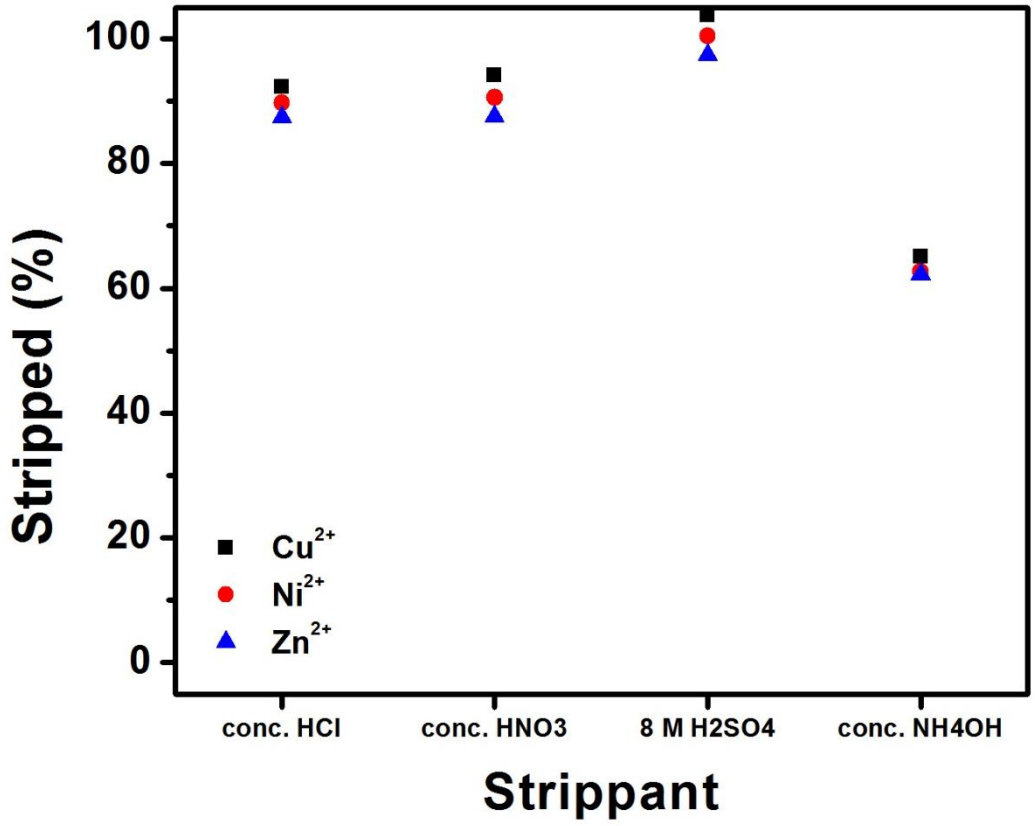


**Figure 1.25:** Stripping studies with **1.11**. Extraction of metal ions was performed at pH = 2.00

performed with **1.5** and **1.11**. Initially, several concentrated acids (HCl, $HNO_3$, $H_2SO_4$, AcOH) were chosen as strippants to test. Unfortunately, the addition of solid **P1.5** to these solutions dissolved the polymer, eventually degrading it, as evidenced by a color change from pale yellow to dark brown. Because of this, lower acid concentrations were used in the stripping tests. Initially, nitric and hydrochloric acid were tested, yielding very different results (Figure 1.26). Studies with nitric acid showed indiscriminate stripping of Cu(II) which did not seem to follow a discernable pattern or trend. Using hydrochloric acid showed better results, with up to 60% of the Cu(II) being stripped from the polymer before evidence of substantial degradation was seen. Time dependent stripping studies

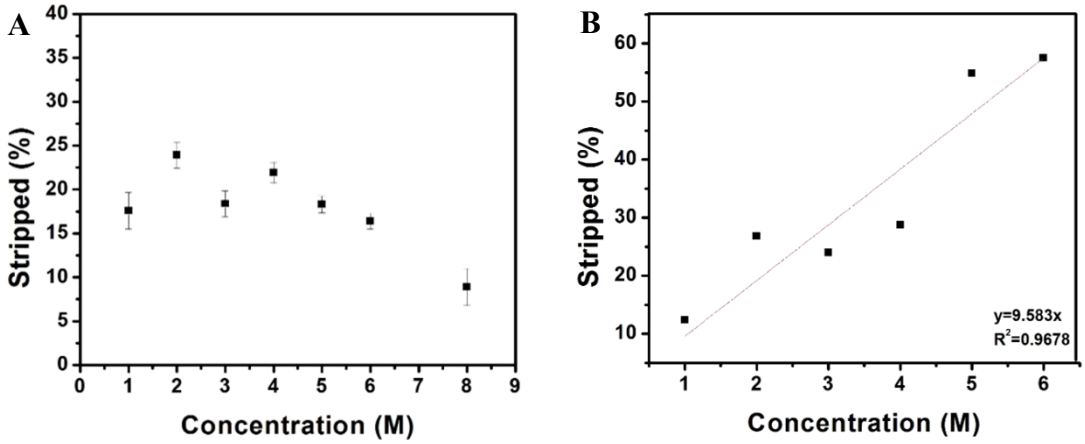


**Figure 1.26:** Stripping experiments with **P1.5** loaded with Cu(II), using (A) nitric acid and (B) hydrochloric acid

with hydrochloric acid showed maximum desorption of Cu(II) occurringwithin about 4-5 hours (Figure 1.27). A second order dependence with respect to time was seen. When comparing stripping with nitric versus hydrochloric acid, the difference in their efficacy may be ascribed to the properties of the counteranion. If we consider the hydrophobicity of the $Cl^-$ and $NO_3^-$ anions based on the Hofmeister series[35], it can be assumed that $Cl^-$ is less hydrophobic than $NO_3^-$. Due to the favorable formation of *trans* double bonds during polymerization[36], the polymer can also be viewed as having a hydrophobic polymer backbone "core", containing poly(norbornene) and the hexyl-chain tether, and a hydrophilic "surface", due to the terminal pendant picolinic acid moieites, giving the polymer an overall more hydrophilic surface with which solvent contacts. Therefore, it is expected that a hydrophilic anion would be able to more easily approach the polymer surface; in this case $Cl^-$ is more hydrophilic than $NO_3^-$, and therefore HCl can more readily strip the bound metal ions.

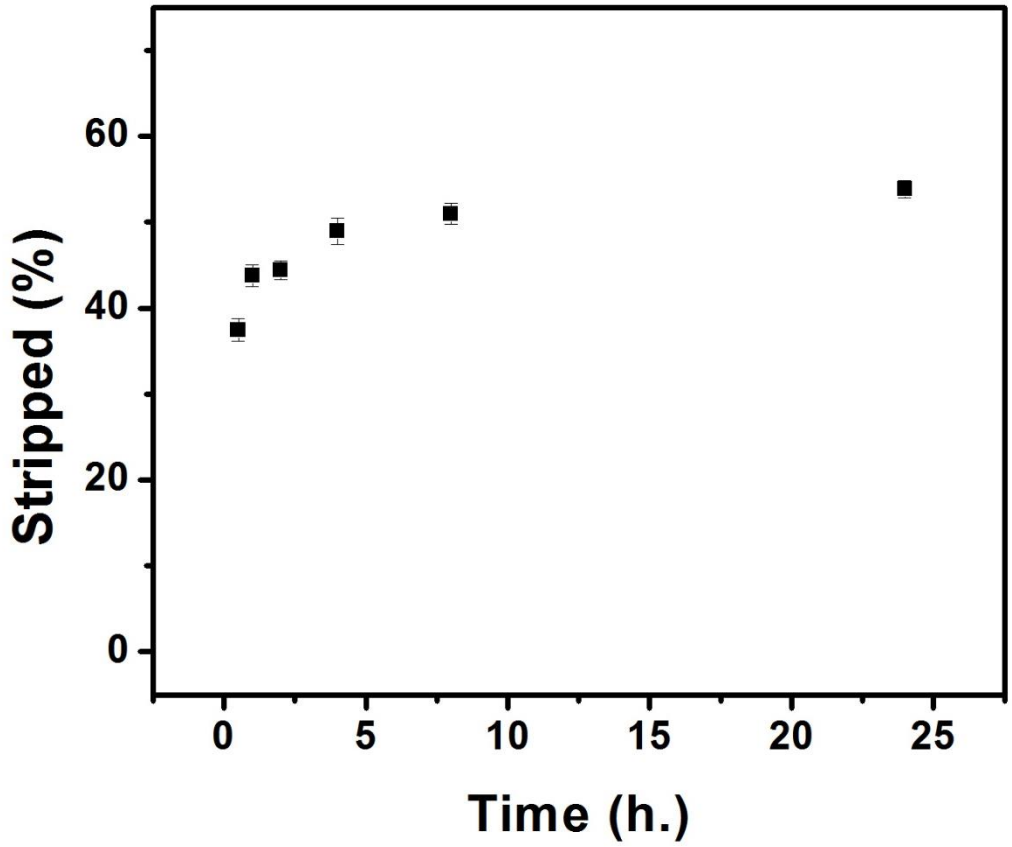


**Figure 1.27:** Time-dependent stripping of Cu(II) from **P1.5** using hydrochloric acid

**P1.5** was also tested for its ability to extract, bind, and release metal ions over several cycles. For this study, Cu(II) was loaded in the polymer and subsequently stripped with 6 M HCl over several cycles. As can be seen in Figure 1.28, diminishing returns for extraction are observed after the first cycle. Presumable this is due to the incomplete stripping of Cu(II). This results in an almost 10-fold decrease in extraction efficiency by the third extraction cycle. Future efforts to simplify the conjugate monomer by removing the amide and imide functional groups may increase acid stability. While the imide on the norbornene is a versatile attachment point, a simple *endo*-norbornene having only C-C

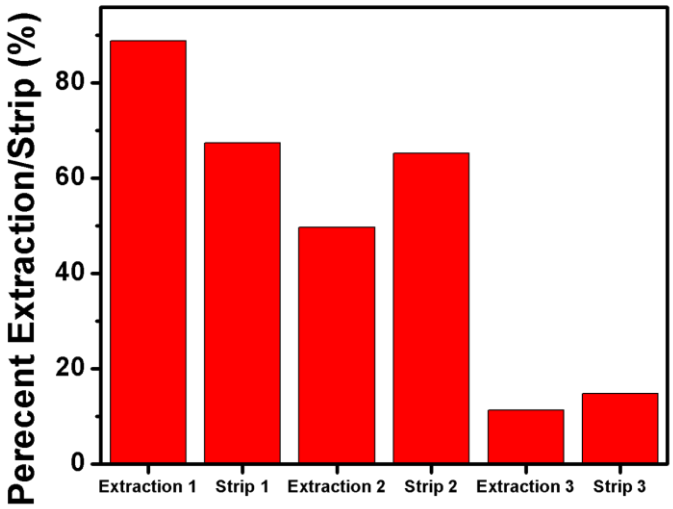


**Figure 1.28:** Recycling test with **P1.5** using 6 M HCl as the strippant

bonds to the tethered pendant group could allow for more complete stripping of the bound metal ions at higher acid concentrations.

The polymer detailed in this chapter may also show use in several other applications where removal of the bound metal ion species is not necessary or required. For example, **P1.5** could be used to remove trace metal catalysts after the production of drug targets in the pharmaceutical industry, where material purity must be highly regulated.[37] In a similar vein this material could potentially be used to scrub heavy metal ions for environmental clean-up project, as **P1.5** showed increased affinity for Pb(II) at higher pH values. It would be of interest to conduct studies using other heavy metals, such as Hg, to see if this suggestion has merit.

# CHAPTER 2: SYNTHESIS AND PERFORMANCE OF NOVEL PICOLINAMIDES BEARING HYDROPHOBIC SIDE CHAINS FOR THE SEPARATION OF AM(III) FROM EU(III)

## 2.1 Introduction

In order to utilize nuclear energy safely and effectively, each stage of the manufacturing, production, implementation, and disposal process must be carefully monitored and controlled. To limit nuclear proliferation and achieve a sustainable nuclear fuel cycle, nuclear waste and fission products (FPs) must be carefully separated, stored, and recycled wherever possible. Spent nuclear fuel consists largely of uranium (>94% by mass), with the remainder consisting mostly of fission products, such as cesium, iodine, technetium, and several minor actinides (MAs) (Figure 2.1).[38] The majority of

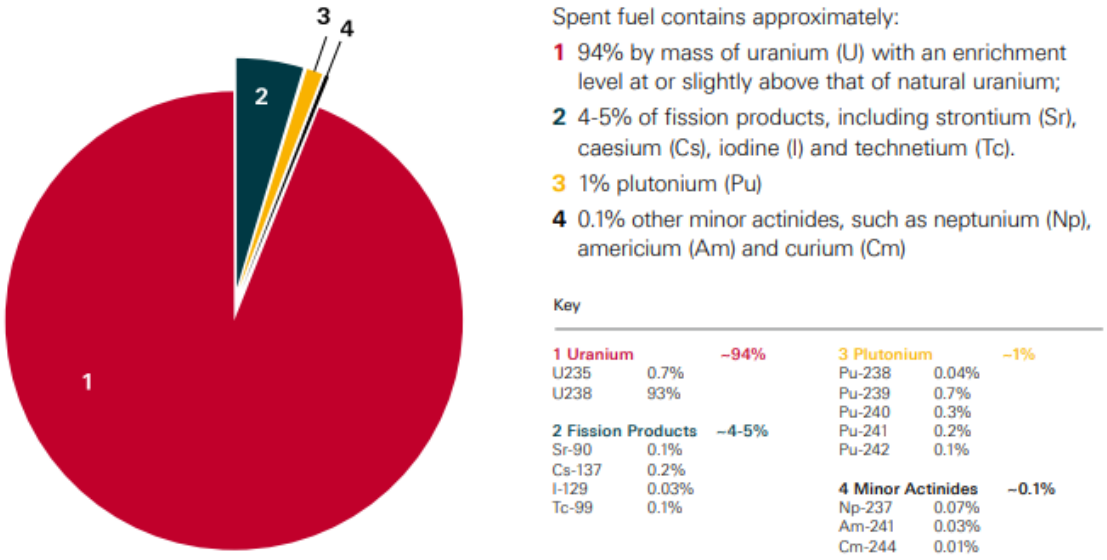


**Figure 2.1**: Makeup of nuclear fuel waste by mass[38]

uranium in the waste is recovered via the PUREX (Plutonium and Uranium Extraction) process, which significantly shortens its long-lived radiotoxicity lifetime from ca. 300,000 to 9,000 years.[39] In the remaining waste, the minor actinides (Np, Am, Cm) are responsible

for a large amount of the radiotoxicity, despite their low abundance by mass (<0.1%). In particular, $^{241}$Am represents the largest challenge in the long-term storage of spent wastes. Given the time for the fission products to decay significantly (ca. 75 years), $^{241}$Am is the predominate contributor to remaining heat from radiological decay (Figure 2.2).[40] This,

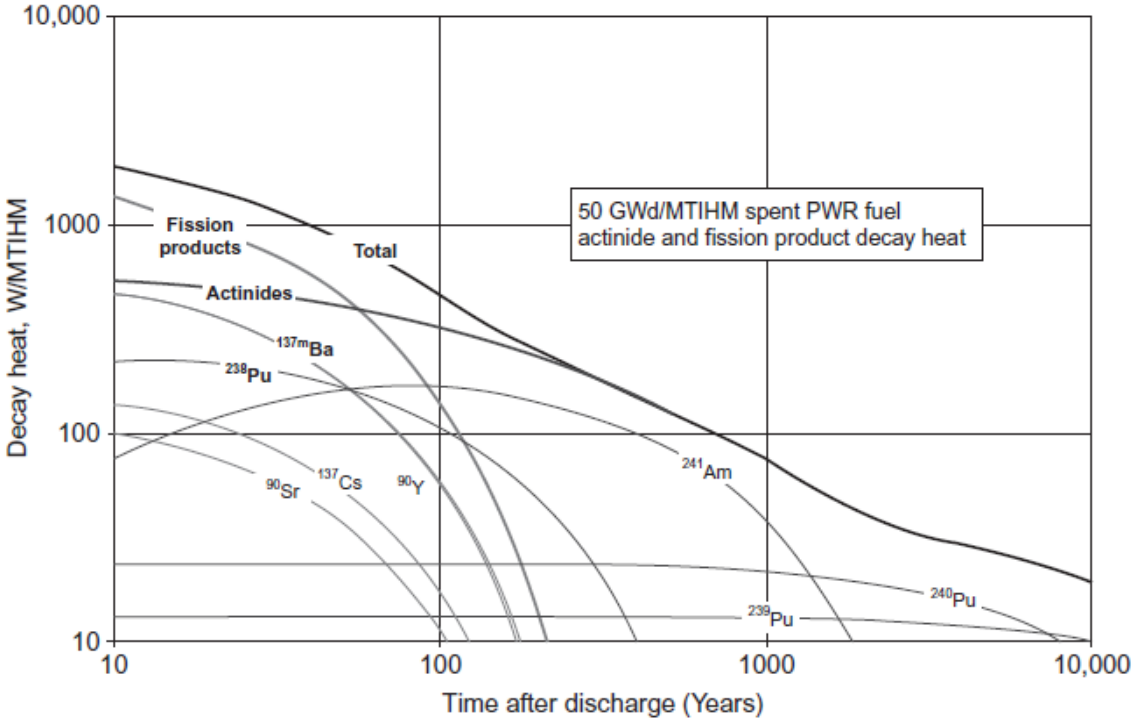


**Figure 2.2**: Decay heat of stored nuclear fuel waste on a geological repository as a function of time[40]

combined with its long half-life ($t_{1/2}$ = 433 years), makes the efficient separation of the MAs of paramount importance for the efficient and responsible storage of spent nuclear fuel waste. Several estimates of the benefits of this separation predict a several hundred-fold increase in waste storage capacity accompanied by the essentially complete (>99.9%) removal of the MAs and several other fission products. Further need for the separation of the lanthanides and actinides stems from the high neutron capture cross sections of the lanthanides. Their presemce inhibits the efficiency of the energy-producing nuclear

reactions when using recycled fuels and therefore their removal from spent wastes is also of importance.

### 2.1.1 Separation of the minor actinides

Approaches to the separation of the MAs have been two-fold: Complexation and oxidation state manipulation.[41] However, both approaches present significant challenges that must be overcome in order to perform the desired separation. The greatest challenge associated with complexation strategies is the very similar size of the trivalent lanthanides and actinides.[42] Therefore, endeavors to bind americium selectively based solely on size are not effective to perform this separation. To circumvent this problem, americium may be oxidized to higher oxidation states. However, this requires very highly oxidizing conditions, and both Am(V) and Am(VI) are unstable, being reduced to Am(III) on the order of days and minutes, respectively.[43] Additionally, the short-lived stability of these species is highly dependent on solution conditions, increasing the difficulty for this process to be achieved at scale. In light of this, strategies for the selective complexation of americium(III) have been explored more aggressively than oxidation strategies. As previously stated, discrimination of the lanthanides and actinides is difficult due to their similar size. However, the slightly softer nature of the actinides has allowed for the development of ligands that are able to effect this separation.[44] These ligands often contain soft amine donor groups, while ligands for the extraction of lanthanide ions contain harder oxygen donors, such as carboxylic or phosphoric acids. The trivalent actinide-lanthanide separations by phosphorus-reagent extraction from aqueous complexes (TALSPEAK) process, developed by Weaver and Kappelmann, utilized extraction processes in both the aqueous and organic phase to complex both lanthanide and actinide cations, partitioning them between the two phases.[45] In this separations method, diethylenetriaminepentaacetic

acid (DTPA), a ligand selective for actinide species, is introduced to a lactate buffered aqueous solution of lanthanides and actinides. Once the actinides have been coordinated, the resulting solution is contacted with an organic phase, which contains bis(2-ethylhexyl)phosphoric acid (HDEHP). This latter ligand binds the lanthanide ions in the organic phase, effectively separating the two species. The ligands in question are shown in Figure 2.3.

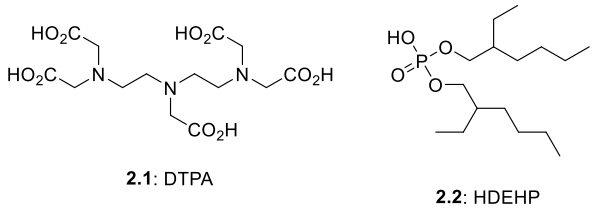


**2.1**: DTPA **2.2**: HDEHP

**Figure 2.3**: Ligands used in the TALSPEAK process

The TALSPEAK process has shown to be effective on small scale. However, it suffers at large scale due to its high sensitivity to pH. This latter problem may be mitigated by the use of high lactate buffer concentrations (Figure 2.4).[46] Unfortunately, the addition of lactate is also undesirable as it increases the amount of waste generated in the separation process. Efforts to reduce the pH sensitivity of this separation have led to the development of the so-called Advanced TALSPEAK process. In this process, DTPA is replaced by *N*-(2-Hydroxyethyl) ethylenediamine-*N,N*,*N*-triacetic acid (HEDTA), HDEHP replaced by ethylenediamine-*N*,*N*,*N*-triacetic acid (HEH[EHP]), and the lactate replaced by a citrate buffer (Figure 2.5).[47] Lanthanide extraction using HEH[EHP] now proved to be more consistent across a broader pH range than in TALSPEAK, while still exhibiting pH-dependent extraction of actinides still being observed (Figure 2.6).[48] The lower slope for the distribution ratios of americium seen in the Advanced TALSPEAK process (ca. -0.3) compared to TALSPEAK (-1.9) illustrate the increased tolerance to changes in pH for this process.

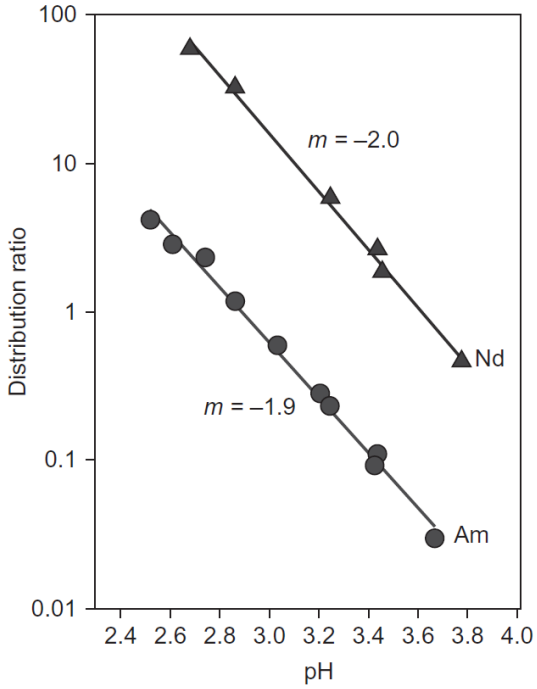


**Figure 2.4**: Distribution of Am(III) and Nd(III) species in the TALSPEAK process, using 1.5 M lactate buffer.[46]

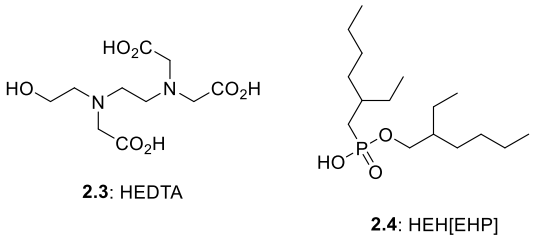


**Figure 2.5**: Ligands used in the Advanced TALSPEAK process

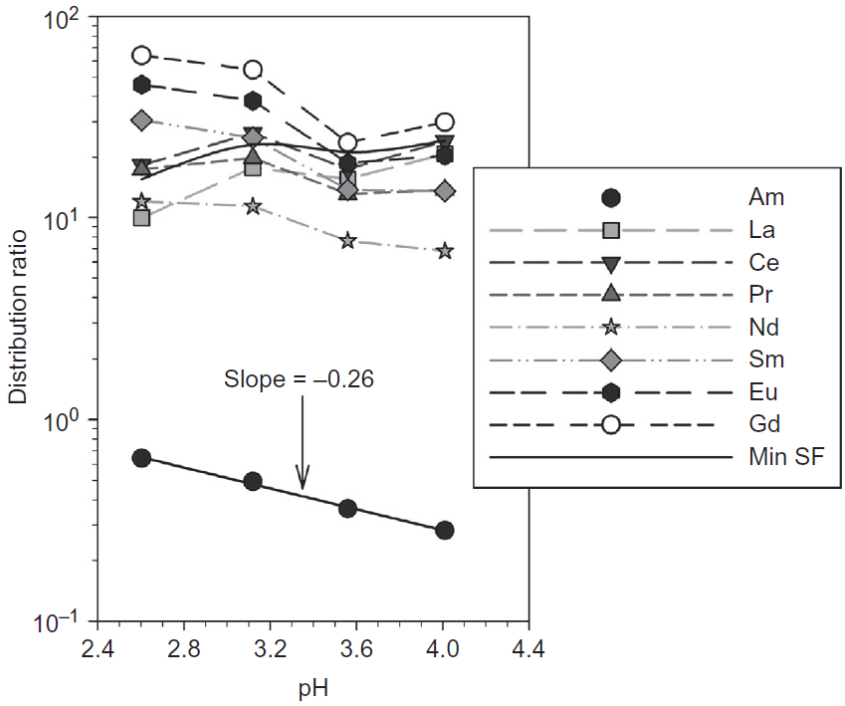


**Figure 2.6**: Distribution ratios of americium and several lanthanides performed using Advanced TALSPEAK.[48]

While effective, the Advanced TALSPEAK process still requires a separate pre-extraction event to remove wastes other than the lanthanides/actinides when performed at scale. This is because the fuel reprocessing steps produce a fair amount of additional waste that must first be dealt with. Therefore, widespread efforts to simplify the extraction process by combining various extractants into one step have been explored. These processes include variations on the PUREX procces, such as the TRUEX (TRansUranic Extraction) and DIAMEX (DIAMideEXtraction) processes. The TRUEX process was developed at Argonne National Laboratory in the 1980's and designed to be applicable under conditions seen at existing fuel reprocessing facilities.[49] That is, the separation was able to be performed under a wide range of conditions, including variations in acid, salt, and fission product concentrations. This process added a second ligand, octyl(phenyl)-

*N*,*N*-diiso-butylcarbamoylmethylphosphine oxide (CMPO), to the existing PUREX solvent, which contained tributyl phosphate (TBP) (Figure 2.7). This ligand along with

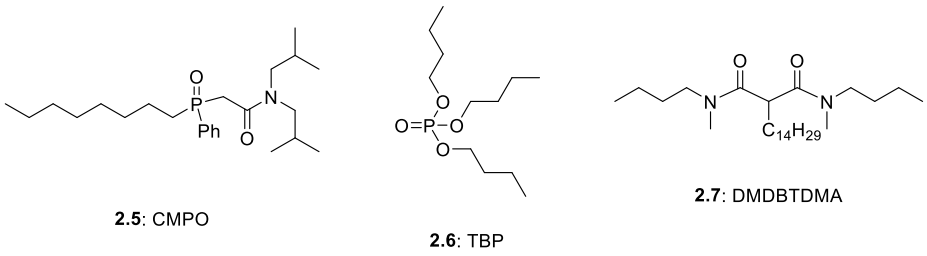


**2.5**: CMPO

**2.6**: TBP

**2.7**: DMDBTDMA

**Figure 2.7**: Examples of ligands utilized in the TRUEX and DIAMEX processes

several other derivatives were tested for their ability to extract Am(III) from PUREX raffinate solutions. Researchers saw that these CMPO derivatives extracted Am(III) selectively over the other fission products found in the PUREX waste, and operated at conditions analogous to those on process scale (Figure 2.8). CMPO has also been applied in conjunction with other extractant molecules, such as HDEHP and HEH[EHP], but has seen limited success, due to extractant-extractant interactions reducing the separation factors significantly.[50–52]

As its name suggests, the DIAMEX process utilizes diamides, specifically malondiamides for the extraction of lanthanides and actinides from PUREX raffinate. Diamides, such as dimethyl-dibutyl-tetradecyl malonamide (DMDBTDMA) have shown >99.9% recovery of MAs and lanthanides from radioactive waste streams (Figure 2.7).[53] Another process, SANEX (Selective ActiNide Extraction) is used in tandem with DIAMEX, which selectively removes the actinides from the partitioned waste resulting from DIAMEX or TRUEX processes. There is not a formal system in place for SANEX, but typical ligands utilized are selective for either lanthanides or the MAs that would be present in the TRUEX or DIAMEX waste streams. These ligands vary greatly in structure

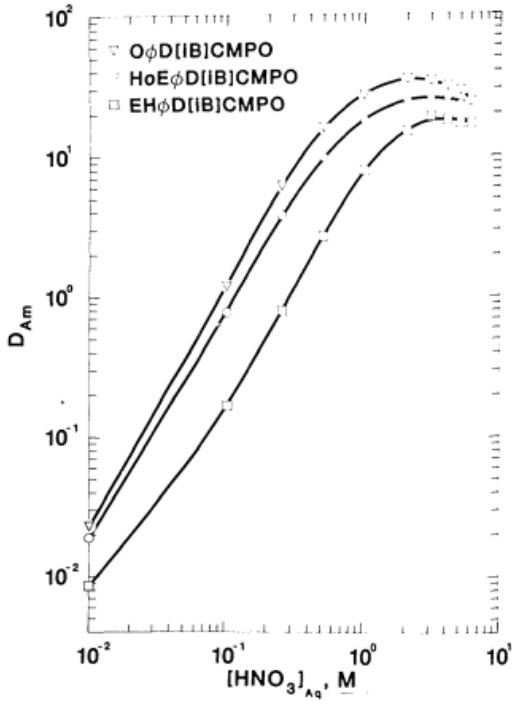


**Figure 2.8**: Extraction of Am(III) from synthetic PUREX waste solution. Results using the octyl- (top trace), 2-ethylhexoxy- (middle trace), and 2-ethylhexyl (bottom trace) derivatives are shown.[49]

and functionality, but several classes of SANEX-type ligands have been put forth and studied over the past several decades.

Diglycolamides (DGA), somewhat similar in structure to malondiamides, are one class of extractant molecules that have been heavily explored for the separation of the MAs. DGA ligands have been used in conjugation with HEH[EHP] in the ALSEP process (actinide-lanthanide separation), due to their decreased interaction with HEH[EHP] compared to that of CMPO.[54] DGA can effectively extract the MAs at molar concentrations of nitric acid, so both they and lanthanide ions are extracted in this process. Subsequent contact with aqueous solutions containing a polyaminocarboxylate, such as HEDTA, strips the MAs from the solution, separating them from the lanthanides. DGA

ligands for the ALSEP process include *N*, *N*, *N*, *N*-tetra(2-ethylhexyl)diglycolamide (T2EHDGA) and *N*, *N*, *N*, *N*-tetraethyldiglycolamide (TEDGA) (Figure 2.9). ALSEP has

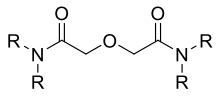

**2.8**: T2EHDGA, R=2-ethylhexyl
**2.9**: TEDGA, R=ethyl

**Figure 2.9**: DGA ligands utilized in the ALSEP process

shown extraction of americium as well as the lanthanides, at nitric acid concentrations greater than 1 M. it also shows selectivity over the lighter lanthanides, such as lanthanum (Figure 2.10).[48] Stripping with HEDTA shows lower distribution ratios for americium than that of the lanthanides. The stripping curve is characterized by a fairly low slope, indicating a fair range of pH variation would be acceptable (Figure 2.10)

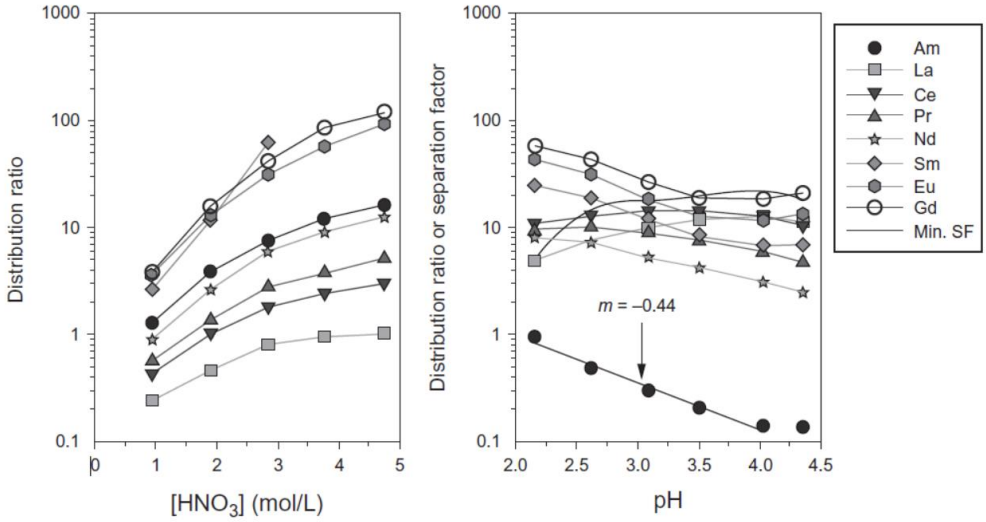


**Figure 2.10**: Extraction of americium and lanthanides using a mixture of T2EHDGA and HEH[EHP] in *n*-dodecane (left).[48]

### 2.1.2 AMERICIUM-LANTHANIDE SEPARATIONS

As previously stated, the coextraction of americium and the lanthanides, and their subsequent separation, is of great importance in developing a process which may be implemented into current fuel reprocessing infrastructures. Of interest is the separation of americium(III) and europium(III), which are in the same group in the periodic table and therefore have very similar chemical properties. Additionally, europium(III)-152/154 is a convenient radiotracer that can be used in monitoring these separations. After the development of malondiamide and diglycolylamide ligands for the coextraction of lanthanides and actinides, great effort has gone into the development of ligands that selectively extract americium from the lanthanides, with a specific focus on europium. Ligands containing soft N- and S-donors were desired, as they would have more covalent interactions with the softer americium ion lone pair electrons. Early ligands designed for this purpose included nitrogen-containing heterocycles such as 2,4,6-tri(2-pyridyl)-1,3,5-triazines (TPTZ) and terpyridines (TERPY) (Figure 2.11).[55,56] Work with these ligands showed breakthrough separation factors ($SF_{Am/Eu}$) as high as 12, which in the time period of the 1980's and 1990's was considered to be unachievable. However, intramolecular hydrogen bonding of these ligands at low pH rendered them ineffective for extraction under model field conditions.

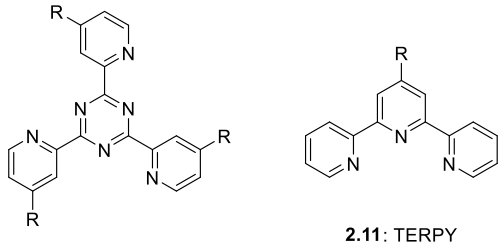


**2.10**: TPTZ

**2.11**: TERPY

**Figure 2.11**: Nitrogen heterocycle ligands for the selective extraction of americium(III) over europium(III)

Extraction studies with **2.10**-**2.12** showed the need to reduce the basicity of the N-donors. In order to achieve this, adjustments could be made to reduce the electron density of the nitrogen electron lone pair or increase the covalency of their interactions with metal cations. This was achieved by making use of the α-effect, whereby overlap of adjacent nonbonding lone pair electrons results in a more diffuse, covalent, interaction with metal cations.[57] This effect is seen in 1,2,4-triazines, and was reflected in pioneering work with (2,6-bis(1,2,4-triazin-3-yl)pyridine (BTP) systems. These latter ligands were able to extract Am(III) over Eu(III) in 1-4 M nitric acid, achieving separation factors greater than 100.[58] They also were much easier to synthesize than the previously referenced *N*-heterocycles (Scheme 2.1). Unfortunately, stripping of americium from these ligands proved difficult, and experiments

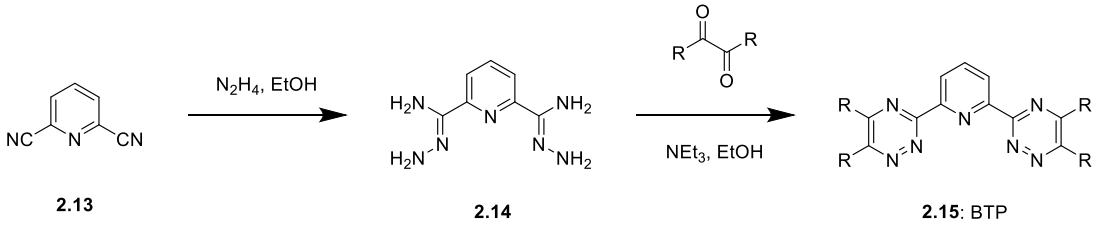


**Scheme 2.1**: Synthesis of BTP ligands

using PUREX raffinate showed that alkyl BTP derivatives were susceptible to radiological decay. The latter problem was ascribed to the presence of benzylic protons on the ligands.[59] These benzylic protons were absent in the new ligands $CyMe_4$-BTP and $BzCyMe_4$-BTP (Figure 2.12).[60] Fortuitously, these ligands outperformed their BTP predecessors, with **2.16** exhibiting high selectivity and extraction efficiency (ca. $SF_{Am/Eu} = 5{,}000$, $D_{Am} = 500$), as well as being resistant to both acid and radiation. However, stripping remained a problem with these ligands, making their implementation in SANEX-type processes virtually impossible.

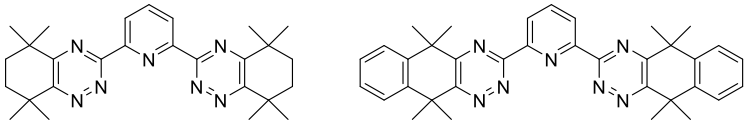

**2.16**: $CyMe_4$-BTP **2.17**: $BzCyMe_4$-BTP

**Figure 2.12**: BTP ligands containing no benzylic protons, for the extraction of Am(III) over Eu(III)

To overcome the problem of stripping the actinides from BTPs, the coordination sphere of the trivalent lanthanides and actinides was heavily investigated. Electrospray ionization mass spectrometry (ESI-MS) experiments involving complexes formed between BTPs and the trivalent lanthanides revealed a 1:3 interaction between the metal ion and BTP ligand, filling the coordination sphere of the lanthanides.[61] Crystal structures of $CyMe_4$-BTP with ytterbium (III) confirmed a 1:3 metal ion to ligand binding ratio as well.[60] It was proposed that increasing the denticity of the ligand, from tridentate to tetradentate, may weaken the ligand interactions with americium. That is, by increasing the denticity of the ligand, only two ligands would be permitted to bind americium, resulting in an overall lower stability of the resultant metal complex. A simple change from the pyridine core of BTPs to a bipyridine core was thought to be a suitable structural change to test this hypothesis. This new class of ligands, 6,6'-bis(1,2,4-triazin-3-yl)-2,2'-bipyridines (BTBPs), was prepared in a similar manner to BTPs from the condensation of a dicarbohydrazonamide and α-diketone (Scheme 2.2).[62] These ligands allowed for the

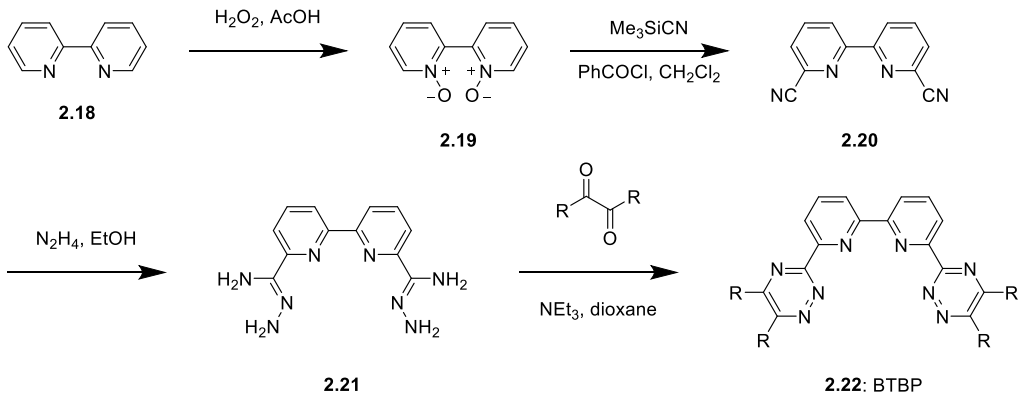


**Scheme 2.2:** Synthesis of BTBP ligands

stripping of bound americium from the ligand, and were able to be reused for further extraction processes. A large variety of BTBP derivatives have been explored to improve solubility and extraction efficiency, as well as to understand the structural factors that contribute to these properties.[63–65] However, despite achieving great success in SANEX-type applications, BTBPs suffer from slow extraction kinetics and low solubility in the nonpolar hydrocarbon solvents used in these processes. The slow extraction kinetics were ascribed to restricted rotation about the aryl-aryl bipyridine bond. Therefore, to achieve better preorganization, 2,9-bis(1,2,4-triazin-3-yl)-1,10-phenanthroline (BTPhen) ligands were proposed (Scheme 2.3). CyMe$_4$-BTPhen was prepared and studied, and gave rise to an increase in the extraction efficiency by two orders of magnitude, while maintaining similar separation efficiencies (ca. $D_{Am}$ = 1000, $SF_{Am/Eu}$ = 400).[66] The extraction time was also reduced from1 hour for CyMe$_4$-BTBP to 15 minutes for CyMe$_4$-BTPhen. Moreover, BTPhens did not require a phase transfer agent to facilitate the extraction. The only notable drawback seen with the BTPhens was that back-extraction rates were significantly lower than those for BTBPs. Solubility also remained a concern for BTPhens, and some work has gone into studying the effects of installing hydrophobic groups throughout the

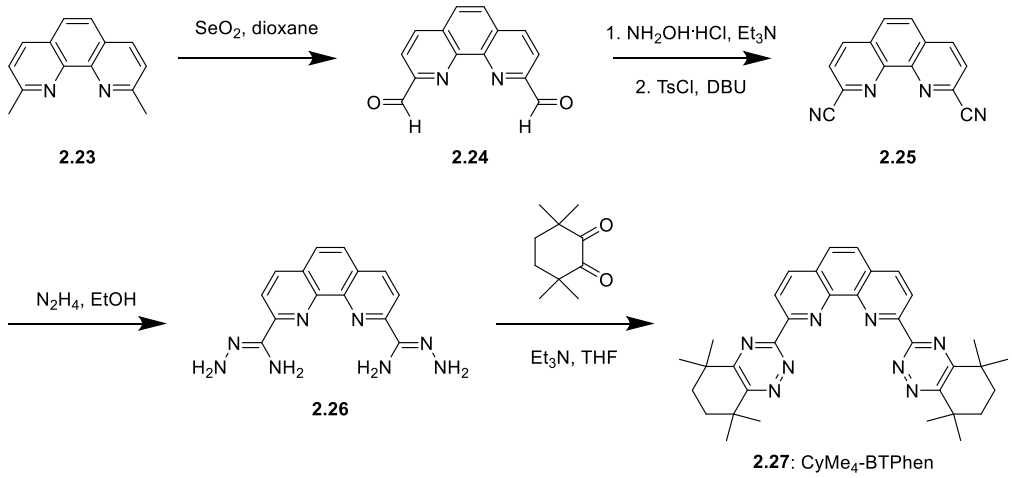


**Scheme 2.3**: Synthesis of the BTPhen derivative, $CyMe_4$-BTPhen

molecule.[67,68] Of interest are the effects of these substituents on separation efficiency, as well as interfacial activity, as $CyMe_4$-BTPhen seems to lie in a "sweet-spot" between these competing needs. Several research groups have also investigated the immobilization of these ligands onto solid supports, in order to remove the use of organic solvents in the separation process.[69,70] Additional work with BTPhens has been in the form of water soluble ligands. Lewis and coworkers have developed a tetrasulfonated BTPhen, which selectivity binds Am(III) over Eu(III) in aqueous solutions (Figure 2.13).[71] By introducing an organic phase containing the nonspecific N, N, N',N'-tetraoctyldiglycolamide(TODGA) coextractant, they were able to study the separation efficiencies of **2.28**. These experiments revealed a four-fold increase in separation efficiency for TS-BTPhen-2 compared to $CyMe_4$-BTPhen. This presents an alternative strategy for the separation of the MAs.

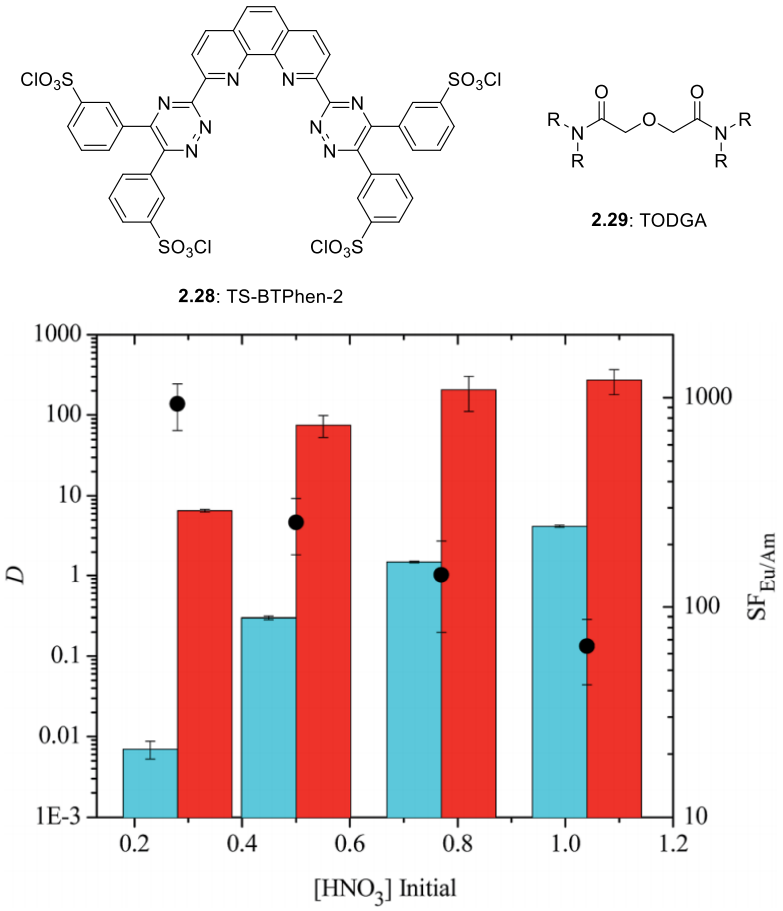


**Figure 2.13**: Tetrasulfonated BTPhen and nonspecific TODGA ligands (Top). Extraction of Am (III) from Eu (III) using **2.28**; blue bars: $D_{Am}$, red bars: $D_{Eu}$, solid bullet: $SF_{Eu/Am}$ (Bottom).[71]

Further investigations into the BTPhen ligand scaffold have focused on increasing ligand preorganization, as the triazine functional groups still contain two degrees of rotational freedom. By reducing rotation, extraction kinetics may be improved further still. Xiao and coworkers have reported a new phenanthroline-based diamide ligand, which was thought to have diminished rotation due to the presence of amide groups on the phenanthroline core (Figure 2.14).[72] Additionally, they sought to install considerable steric bulk on their ligand in order to promote a 1:1 complexation. Extraction experiments using several actinides (Th(IV), U(VI), Am(III)) and Eu(III) showed favorable extraction of

actinides, with very minimal extraction of the test lanthanide cation, Eu(III). Crystal structural studies of **2.30** with U(VI) (Figure 2.14) and Th(IV) (not shown) provided support for the contention that a 1:1 complex was formed. Computational methods also supported the proposed 1:1 complex stoichiometry for the Am(III) complex of **2.30**. These calculations led to suggestions that this ligand binds Am(III) more strongly than Eu(III).

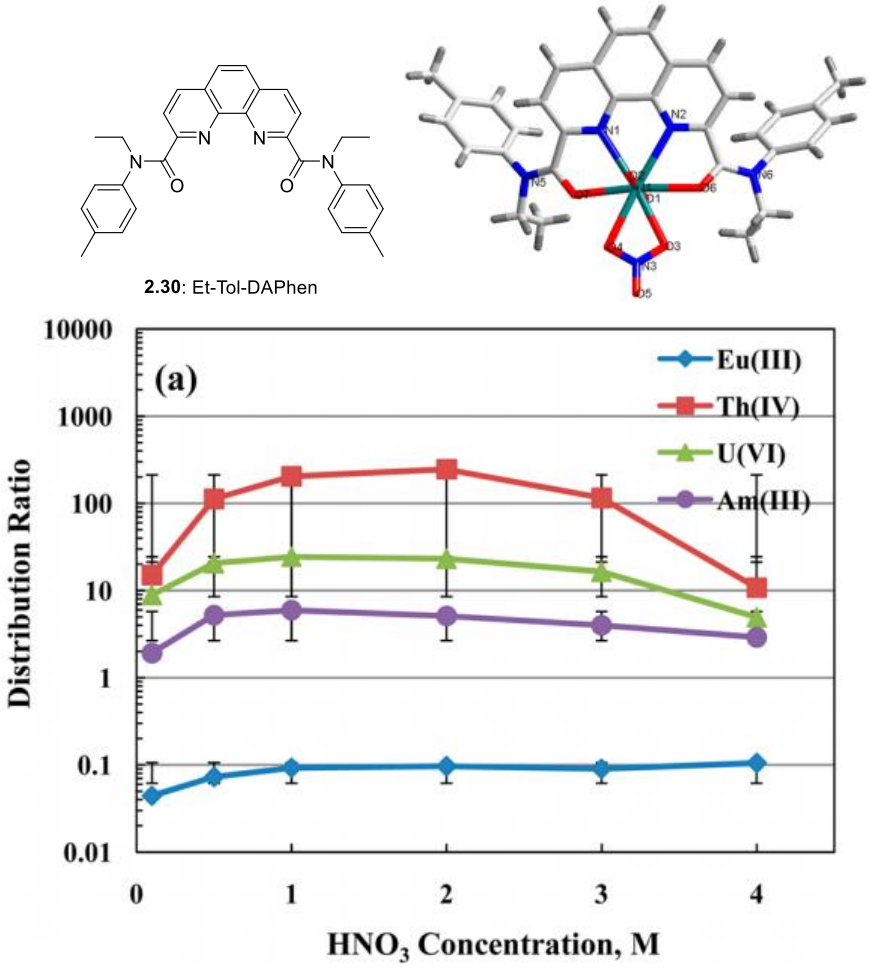


**Figure 2.14**: Et-Tol-DAPhen ligand **2.30** and its crystal structure with $UO_2^{2+}$ bound (Top). Extraction data for lanthanide and actinide ions using Et-Tol-DAPhen as an extractant (Bottom).[72]

While only one lanthanide was studied in this work, the researchers' efforts showed that their ligand was in fact capable of complexing a wide range of actinides.

Complete preorganization of a phenanthroline-based ligand was achieved by Jansone-Popova and coworkers at The Oak Ridge National Laboratory.[73] For this work, new 2,9-bis-lactam-1,10-phenathroline (BLPhen) ligands were synthesized, in which the lactam rings were thought to restrict amide bond rotation (Figure 2.15). A crystal structure

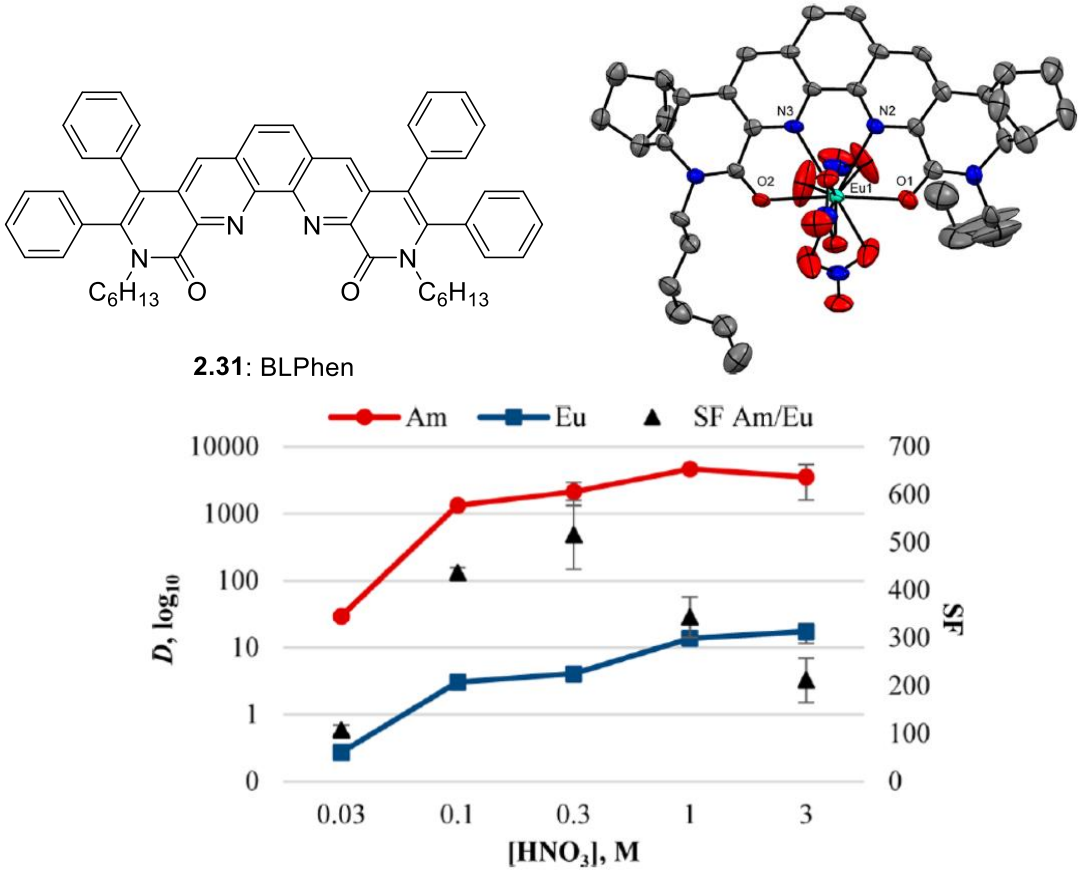


**Figure 2.15**: BLPhen ligand developed for the selective extraction of Am(III) over Eu(III) (Top). Nitric acid dependence on metal ion extraction and selectivity (Bottom).[73]

of BLPhen coordinated to Eu(III) revealed a 1:1 binding stoichiometry, and correspondingly extraction equilibrium was reached after 1 hour. Extractions with Am(III) and Eu(III) showed excellent efficiency and selectivity for Am(III), with a low affinity being seen for Eu(III) ($D_{Am}$ = 3525, $SF_{Am/Eu}$ = 211). Extractions were performed in 1,2-dichloroethane (DCE). This means additional solubilizing groups will be required if this ligand is to be used in current fuel reprocessing systems.

### 2.1.3 PICOLINAMIDE EXTRACTANTS

*N*-Alkyl picolinamides are another class of ligands that have garnered interest in the selective extraction of the MAs. Initial work by Berthon and coworkers investigated the extraction of Am(III) from Eu(III) using several picolinamides and their analogs (Figure 2.16).[74] In the presence of molar concentrations of $LiNO_3$, derivatives of **2.32** showed modest selectivity for americium ($SF_{Am/Eu} \leq 8$), while **2.33** showed essentially no selectivity. These ligands were weak extractants ($D_{Am} \leq 4$), which may reflect the unrestricted rotation of the amide group. Picolinamides have also been incorporated

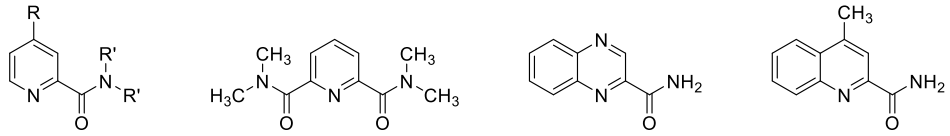


**2.32** **2.33** **2.34** **2.35**

**Figure 2.16**: Picolinamide ligands and its analogs for the separation of Am (III) and Eu (III)

into macromolecular systems. Presumably, this was done in an attempt to circumvent this very problem. As picolinamides have a slight preference for americium(III) over the lanthanides, increasing the local concentration of these groups by preorganizing them onto a scaffold may increase extraction efficiency and potentially selectivity. Several research

groups have used calix[n]arenes as a macrocyclic scaffold for this separation (Figure 2.17).[75–77] Despite increased ligand preorganization, these compounds also suffered from poor extraction efficiency and modest selectivities ($SF_{Am/Eu} \leq 4$). Unfortunately, any optimization of these ligands to increase extraction efficiency resulted in a complete loss in selectivity. These results point further towards the impact of amide bond rotation on the efficiency of metal ion extraction.

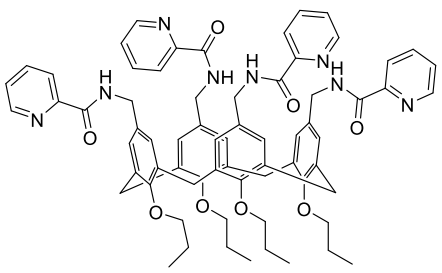

**2.36**

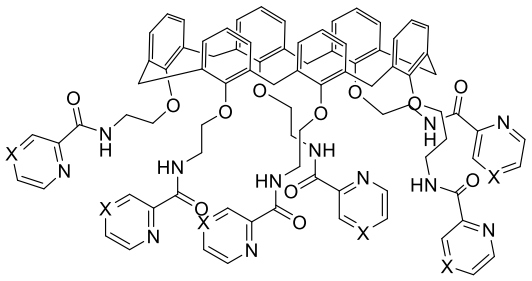

**2.37**: X = N
**2.38**: X = C-Cl

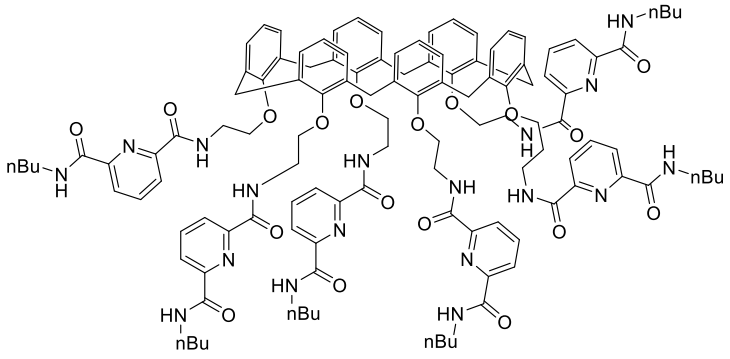

**2.38**

**Figure 2.17**: Picolinamide functionalized calix[n]arenes for the separation of Am (III) and Eu (III)

Picolinamides have also been incorporated into phenanthroline and triazine systems. Work by Bisson and coworkers installed *N*, *N*-dialkyl picolinamides off of phenanthroline and triazine cores, respectively, in an attempt to improve synergistic extraction (Figure 2.18).[78]

These ligands were not particularly efficient extractants for Am(III). However, they did display improved selectivity compared to the previous picolinamide ligands. Phenanthroline ligands, **2.39** and **2.40** showed the greatest selectivity ($SF_{Am/Eu} \leq 27$). The triazine ligands **2.41** and **2.42** were also more selective than previously mentioned picolinamide ligands ($SF_{Am/Eu} = 12$). These ligands were also able to operate at molar acid concentrations, increasing their viability if used in current fuel reprocessing systems.

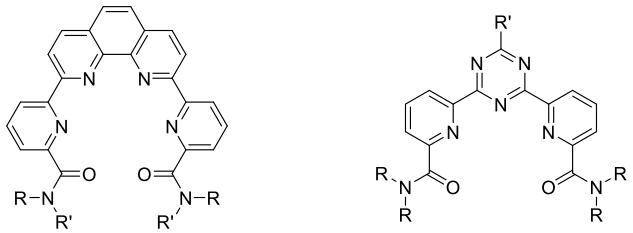

**2.39**: R = R' = $C_8H_{17}$
**2.40**: R = $C_6H_{13}$, R' = $C_6H_5$

**2.41**: R = $C_8H_{17}$, R' = $NH_2$
**2.42**: R = $C_8H_{17}$, R' = $C_6H_5$

**Figure 2.18**: Phenanthroline and triazine ligands containing picolinamide functional groups

Previous work by the Chemical Separations Group at The Oak Ridge National Laboratory explored *N*-alkyl dihydroisoquinolin-1-ones, as conformationally locked picolinamide ligands for Am(III) separations (Figure 2.19). It was believed that by restricting rotation about the amide bond, the extraction efficiency, as well as the selectivity could be improved. Extraction experiments with **2.43** and **2.44** in the presence of 7 M $LiNO_3$ showed a clear improvement in extraction efficiency for both Am(III) and Eu(III) using the rigidified picolinamide. Selectivity for Am(III) also improved, by approximately an order of magnitude ($SF_{Am/Eu} \leq 17$). However, these extractions were performed at $[HNO_3] = 10^{-4}$ M, due to significant third phase formation at higher acid concentrations. Additionally, the solubility of **2.43** limited its use to DCE, which is a solvent incompatible

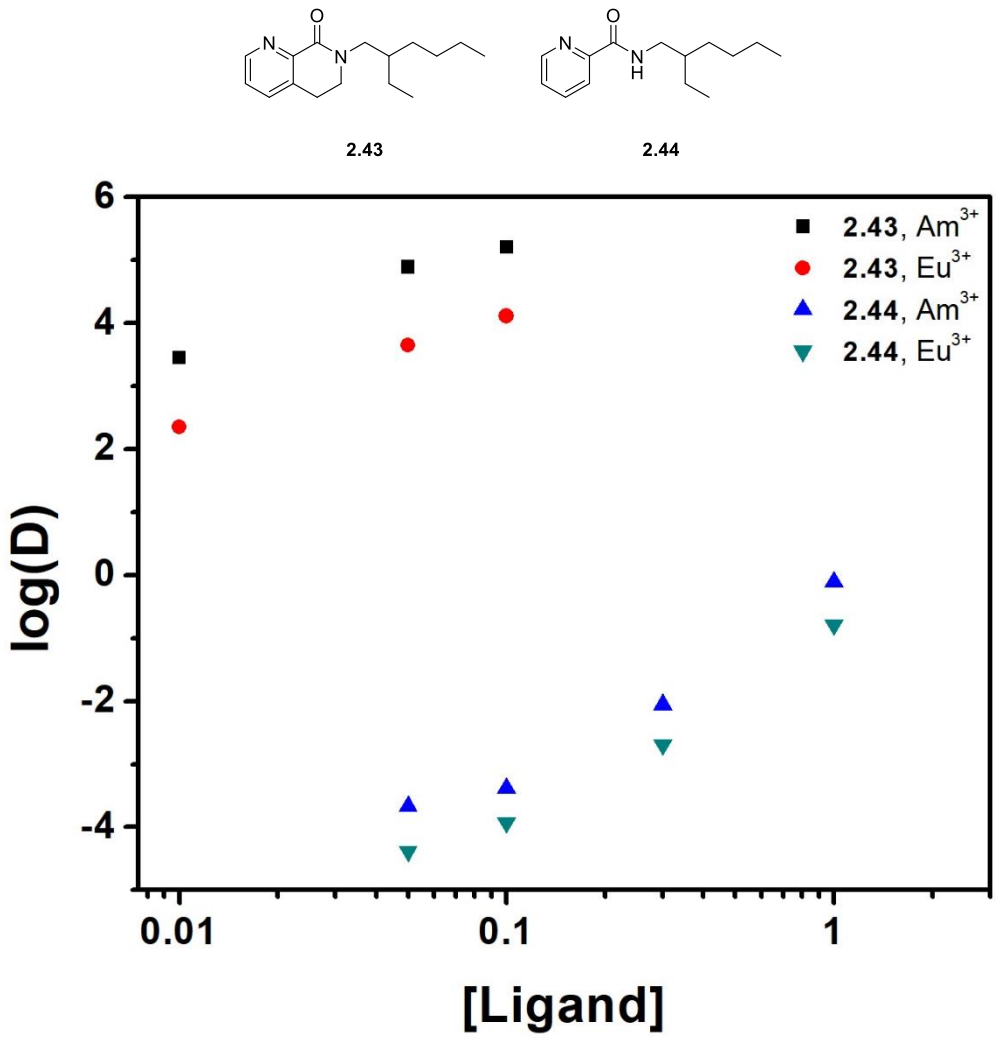


**Figure 2.19**: Extraction of Am(III) and Eu(III) using dihydroisoquinilin-1-one and picolinamide extractants

with current fuel reprocessing systems. However, given these promising results, it is hoped that similar ligands with more desirable solubility and tolerance to higher acid concentrations would prove effective. This inspired our own synthetic efforts. We believed that increasing the lipophilicity of the alkyl group on the dihydroisoquilin-1-one core would serve to improve both solubility and reduce third phase formation. We were

also interested in exploring the effects of increasing the conjugation of our ligand by preparing the isoquinolin-1-one as well.

## 2.2 Results and Discussion

### 2.2.1 Extractant Synthesis

The synthesis of the dihydroisoquinolin-1-one **2.47** is shown in Scheme 2.4. The dihydroisoquinolin-1-one **2.45** was reacted with the alkyl bromide **2.46** and sodium hydride to give the desired *N*-alkyl dihydroisoquinolin-1-one **2.47** in 81% yield. Initially, this reaction gave **2.47** in very poor yields (<30%). However, by increasing the amount of sodium hydride from one to three equivalents, higher yields were achieved. The 9-heptadecyl alkyl group was chosen because it provided exceptional solubility for **2.47** in Isopar-L Fluid, a high-boiling isoparaffinic hydrocarbon solvent used in hydrometallurgical solvent extraction. A 3,7-dimethyloctyl group was also considered. However, it did not provide enough solubility to the ligand.

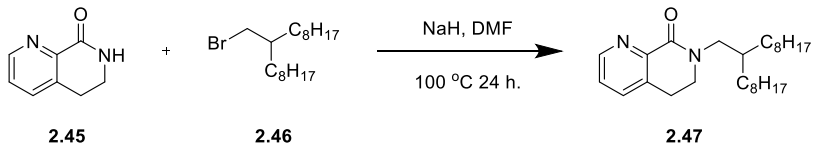


**2.45** **2.46** **2.47**

**Scheme 2.4**: Synthesis of new dihydroisoquinolin-1-one ligand for Am(III) extractions

Scheme 2.5 outlines the synthesis of the isoquinolin-8-one ligand. First, 1,7-naphthyridin-8-amine was deaminated by heating at reflux in sulfuric acid. This gave the requisite isoquinolin-8-one **2.49** in 80% yield. Subsequent alkylation with conditions analogous to those employed in the synthesis of **2.47** gave the desired ligand in 73% yield. An analogous picolinic acid ligand was also synthesized for comparison. This synthetic work is summarized in Scheme 2.6. The corresponding amine **2.53** was synthesized from

**2.46** in 75% yield over two steps via a Gabriel synthesis. Amide condensation of **2.53** and methyl picolinate in the presence of a catalytic amount of acid gave the desired picolinamide **2.55** in 76% yield.

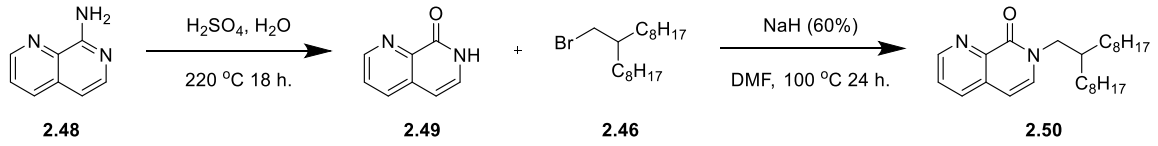


2.48 2.49 2.46 2.50

**Scheme 2.5**: Synthesis of new isoquinolin-8-one ligand for Am (III) extractions

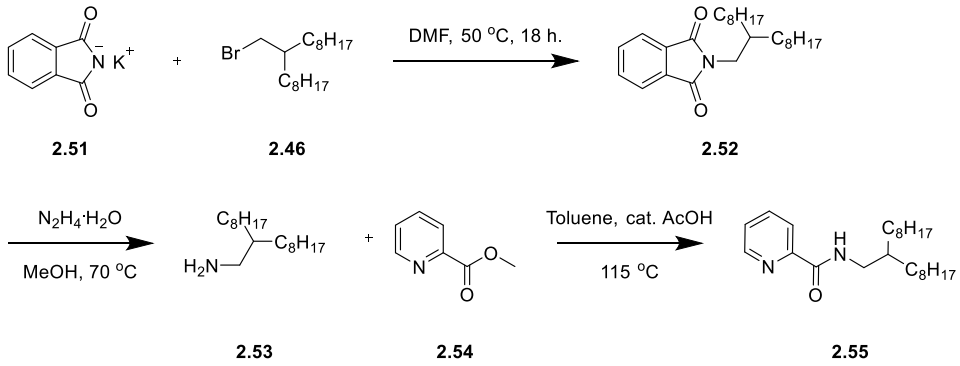


2.51 2.46 2.52

2.53 2.54 2.55

**Scheme 2.6**: Synthesis of picolinamide with analogous alkyl group for Am (III) extractions

### 2.2.2 EXTRACTION STUDIES

With our new ligands in hand, we sought to evaluate their ability to extract Am(III) and Eu(III). All extractions were performed at 25 °C using a 1:1 ratio of organic and aqueous phases. We began with **2.47**, using conditions similar to the previous work with **2.43**. However, we omitted the use of $LiNO_3$ from these experiments. Instead, we increased the ligand concentration to 25 mM. This provided data suitable for analysis. Initial studies, using DCE as the diluent, varied [$HNO_3$] to observe the effect of acid concentration on extraction efficiency and selectivity (Figure 2.20). The extraction efficiency for both Am(III) and Eu(III) increased linearly until around [$HNO_3$] = 0.3 M.

Selectivity was seen to decrease as the acid concentration was increased as well, with a dramatic drop off above [$HNO_3$] = 1 M. This decrease in extraction and selectivity at higher acid concentrations may have been due to extraction of nitric acid into the organic phase. To test this latter hypothesis, we determined the amount of nitric acid extracted into the organic phase by **2.47** in the absence of any metal ions (Figure 2.21).

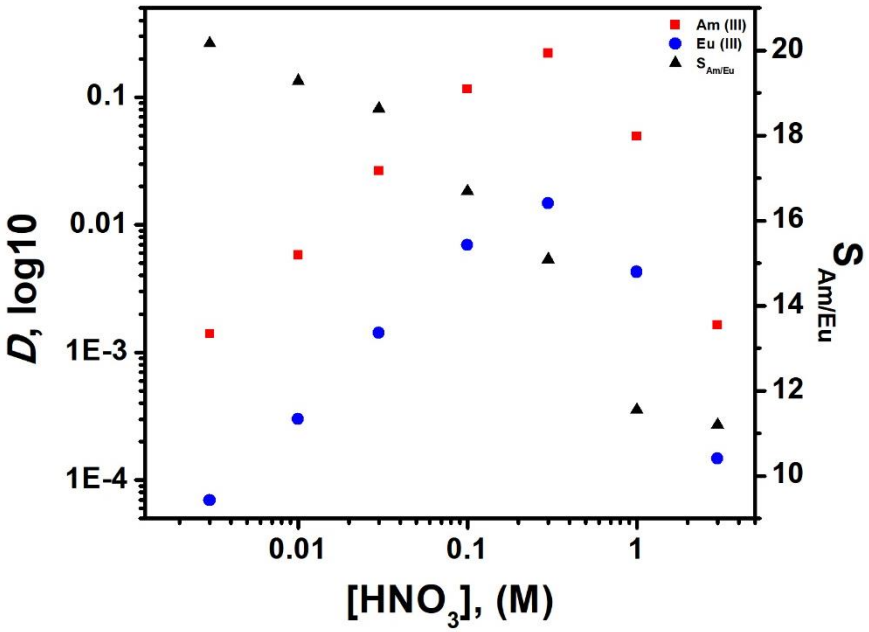


**Figure 2.20**: Extraction of Am(III) and Eu(III) using 25 mM **2.47** in 1,2-dichloroethane, and an aqueous phase containing a 10 µL spike of 1.85 x $10^3$ kBq $^{241}$Am(III) and $^{152/154}$Eu(III) tracer and $10^{-4}$ M $Eu(NO_3)_3$, plotted against the initial [$HNO_3$]

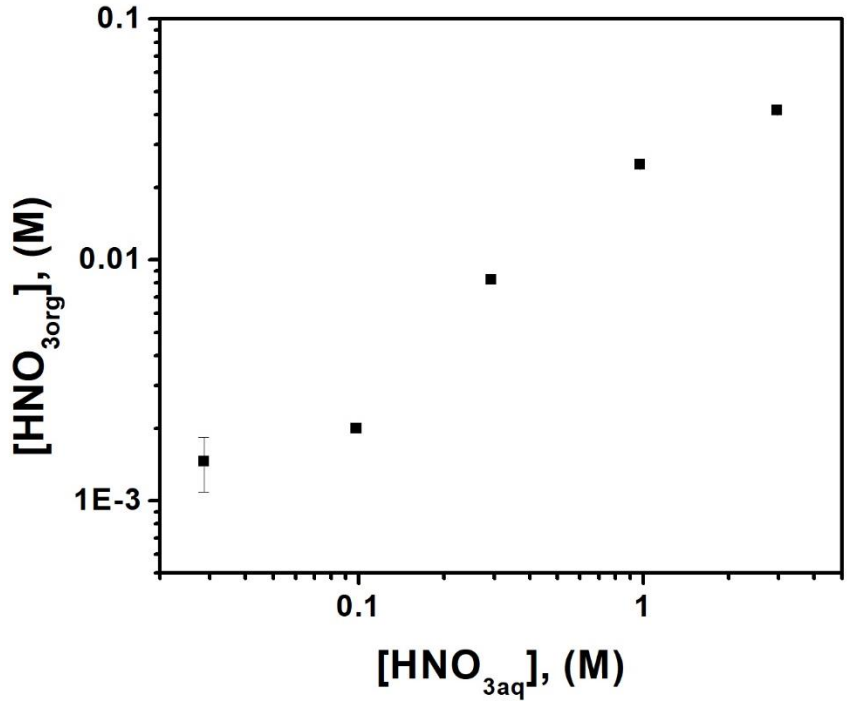


**Figure 2.21**: Extraction of nitric acid by **2.47** (25 mM) into 1,2-dichloroethane, as a function of the aqueous phase nitric acid concentration

This study revealed that when 1 M nitric acid was used, ca. 25 mM of acid was extracted into the organic phase. This finding meant that almost all of **2.47** was protonated in solution under these conditions. This served to explain the large decrease in extraction efficiency seen for both Am(III) and Eu(III) at higher acid concentrations since the protonated ligand was expected to be much to be much less effective. Stoichiometric slope analyses were then performed to assess further the complexation characteristics of **2.47** (Figure 2.22). Slope analysis with both Am(III) and Eu(III) present together in solution, as well as with Am(III) alone revealed a non-integer slope of ca. 2.3 ligands per metal ion in both cases. This finding may reflect the fact that several metal complex species are present concurrently in solution. However, slope analysis is not the most effective way to

characterize binding stoichiometry, and techniques such as X-ray crystallography could provide a more precise description of the metal ion complexes and their composition.

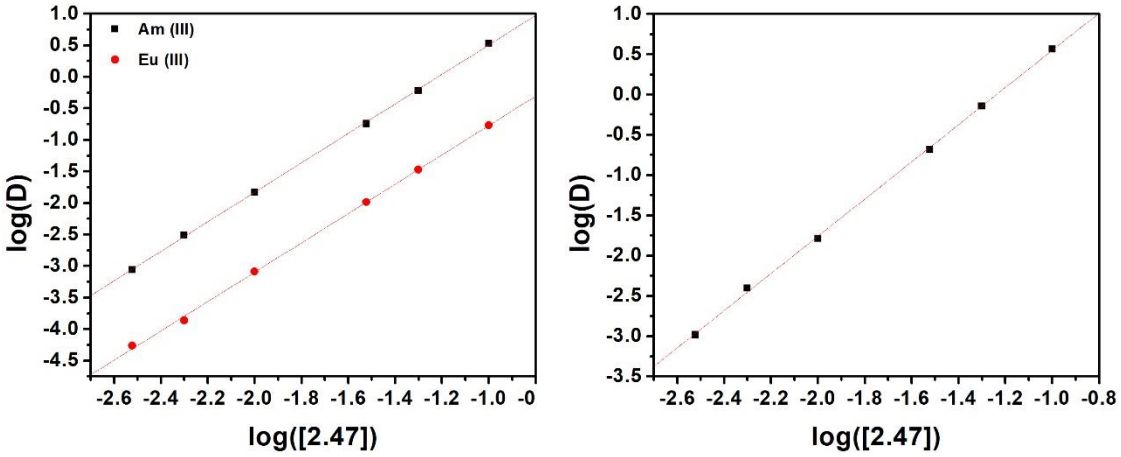


**Figure 2.22**: Slope analyses for the interaction of **2.47** (25 mM) in 1,2-dichloroethane with a 10 µL spike of 1.85 x $10^3$ kBq $^{241}$Am(III) and $^{152/154}$Eu(III) tracer (Left), and a 10 µL spike of 1.85 x $10^3$ kBq $^{241}$Am(III) alone (Right). [$HNO_3$] = 0.1 M.

Similar experiments were performed using **2.50**, to examine the effects of increased conjugation on extraction and selectivity (Figure 2.23). We believed that the additional degree of unsaturation in **2.50** would decrease the basicity of the heterocyclic nitrogen atom, allowing for extraction to occur at higher acid concentrations. Studies with **2.50** in DCE showed that the extraction efficiency did not decrease until above [$HNO_3$] = 1 M. This represents an increase in operating range of about an order of magnitude relative to **2.47**. This improvement was further evidenced from the acid extraction data, which revealed only ca. 20 mM of acid was extracted by **2.50** at [$HNO_3$] = 1 M (Figure 2.24). However, **2.50** performed similarly to **2.47** when considering maximum extraction efficiencies and selectivity. In results almost mirroring those for **2.47**, slope analysis of **2.50** gave a non-integer slope in the range of 2.1-2.2. Again, this value left the binding

stoichiometry of this class of ligand relatively unknown (Figure 2.25). To date, no known metal complexes of this ligand class or similar ligands have been reported.

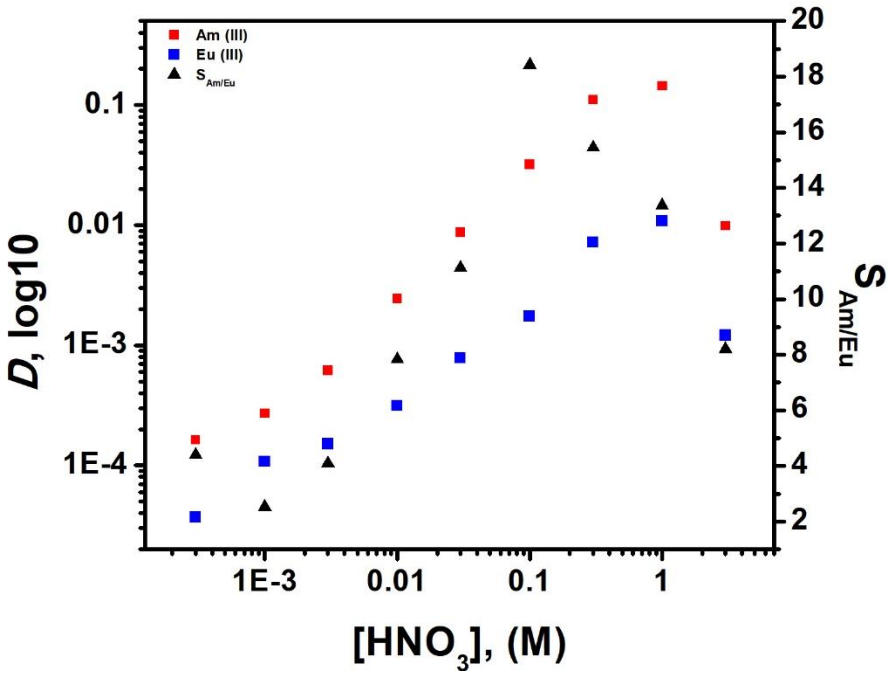


**Figure 2.23**: Extraction of Am(III) and Eu(III) using 25 mM **2.50** in 1,2-dichloroethane, and an aqueous phase containing a 10 µL spike of 1.85 x $10^3$ kBq $^{241}$Am(III) and $^{152/154}$Eu(III) tracer and $10^{-4}$ M $Eu(NO_3)_3$, plotted against the initial $[HNO_3]$

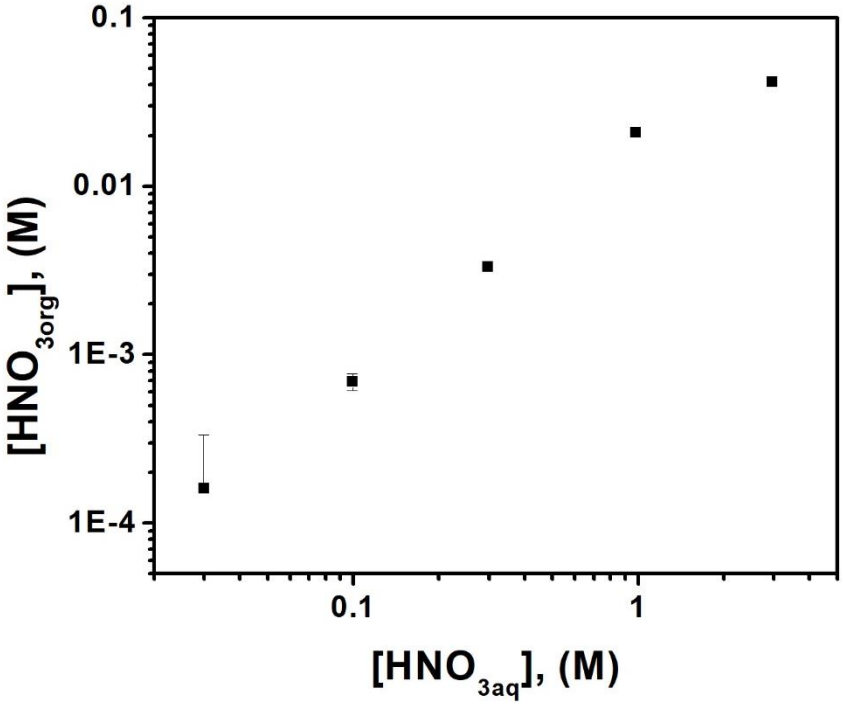


**Figure 2.24**: Extraction of nitric acid by **2.50** (25 mM) into 1,2-dichloroethane, as a function of the aqueous phase nitric acid concentration

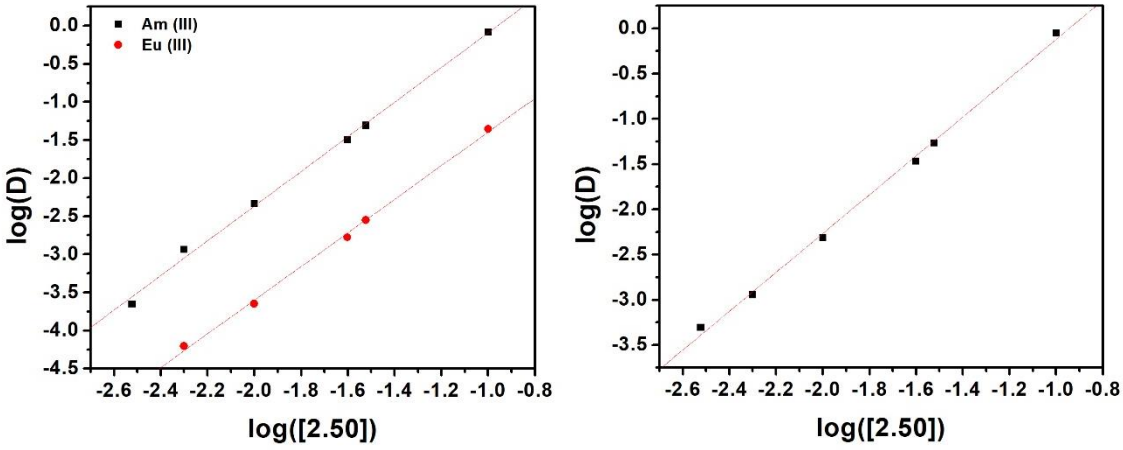


**Figure 2.25**: Slope analyses for the interaction of **2.50** (25 mM) in 1,2-dichloroethane with a 10 µL spike of 1.85 x $10^3$ kBq $^{241}$Am(III) and $^{152/154}$Eu(III) tracer (Left), and a 10 µL spike of 1.85 x $10^3$ kBq $^{241}$Am(III) alone (Right)

We also sought to test whether our new ligands could be effective under solvent extraction conditions more similar to those used in current fuel reprocessing systems. Therefore, we performed extraction studies with **2.47** and **2.50** in Isopar L Fluid. Initial studies with **2.47** resulted in large emulsions after contacting with aqueous nitric acid solutions. Therefore, the organic phase was adjusted to contain 3% Exxal 13, a branched mixture of 13-carbon alcohols. With this new mixture, nearly all the emulsions were eliminated. Extraction of Am(III) and Eu(III) using **2.47** is shown in Figure 2.26. Several notable differences

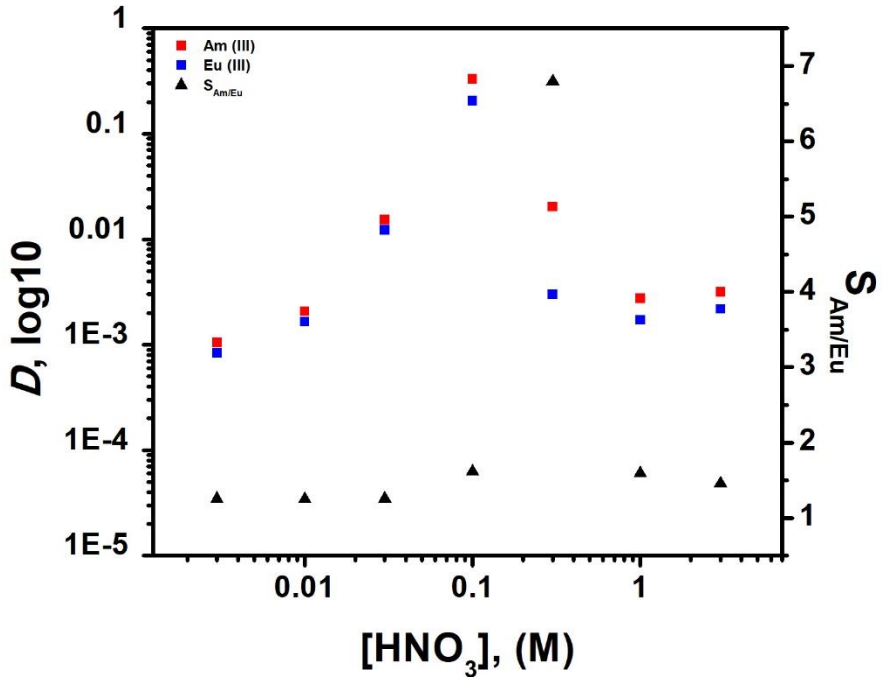


**Figure 2.26**: Extraction of Am(III) and Eu(III) using 25 mM **2.47** in 97:3 Isopar:Exxal 13, and an aqueous phase containing a 10 µL spike of 1.85 x $10^3$ kBq $^{241}$Am(III) and $^{152/154}$Eu(III) tracer and $10^{-4}$ M $Eu(NO_3)_3$, plotted against the initial [$HNO_3$]

between extractions in DCE and the Isopar mixture can be seen. In Isopar, **2.47** appears to have increased sensitivity to acid, as extraction begins diminishing at nitric acid concentrations above 0.1 M, whereas in DCE, this was seen above 0.3 M. Titrations to

determine the amount of nitric acid extracted into the organic phase provided quantitative evidence of this difference (Figure 2.27). Despite this increased sensitivity, the extraction efficiency of **2.47** in Isopar was comparable to that for DCE. However, selectivity was essentially nonexistent, and may have been a result of the use of Exxal 13. The additional OH-groups in solution could occupy any open coordination sites around the Am(III) or Eu(III) cations,

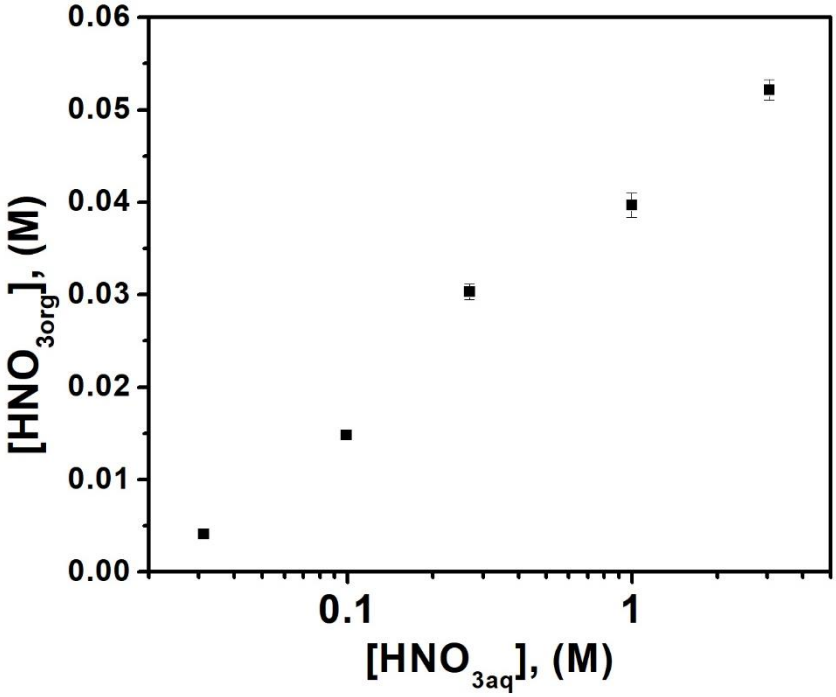


**Figure 2.27**: Extraction of nitric acid by **2.47** (25 mM) into 97:3 Isopar:Exxal 13, as a function of the aqueous phase nitric acid concentration

potentially reducing the selectivity of the system. Slope analysis for **2.47** in Isopar gave inconclusive results, yielding a 4:1 ligand:metal ion binding stoichiometry for Am(III), but no meaningful data for Eu(III) (Figure 2.28). While a 4:1 binding ratio was suspiciously high, the exceptionally hydrophobic nature of Isopar could promote increased exclusion of

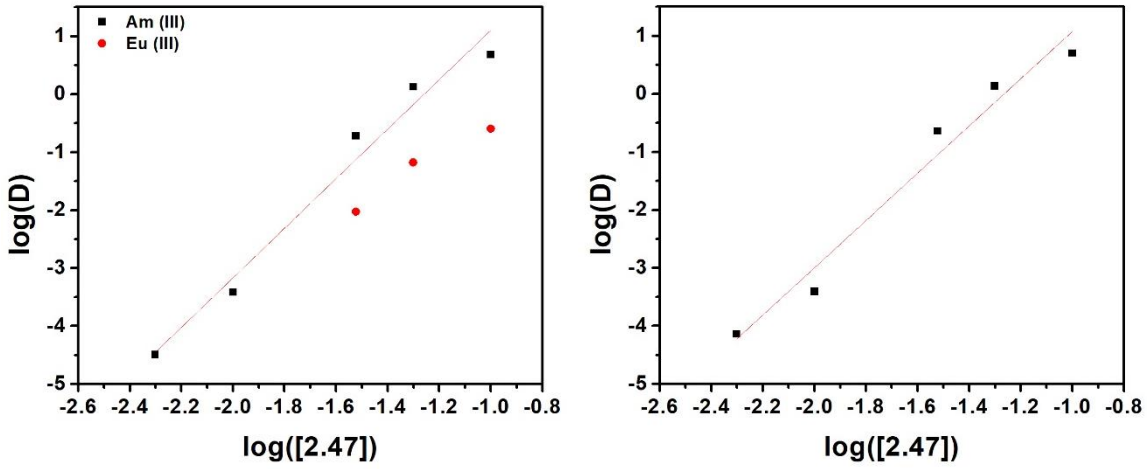


**Figure 2.28**: Slope analyses for the interaction of **2.47** (25 mM) in 97:3 Isopar:Exxal 13 with a 10 µL spike of 1.85 x $10^3$ kBq $^{241}$Am(III) and $^{152/154}$Eu(III) tracer (Left), and a 10 µL spike of 1.85 x $10^3$ kBq $^{241}$Am(III) alone (Right)

the metal cations from the solvent. Extractions performed using **2.50** showed a higher tolerance towards nitric acid, as was seen when using DCE as the solvent (Figure 2.29). Noticeably, the use of **2.50** did not lead to a drastic decrease in selectivity, as was seen with **2.47**. The selectivity of **2.50** for Am(III) tracked nicely with nitric acid concentration, and this system showed the highest selectivity thus far ($S_{Am/Eu} \leq 21$). Ligand **2.50** also extracted more acid in Isopar than it did in DCE (Figure 2.30). Slope analysis of this compound in Isopar gave different results than for **2.47**. Specifically, slopes of 3.00 and 2.63 were recorded for Am(III) and Eu(III), respectively (Figure 2.31). These numbers are closer to what one would expect for metal ion complexes formed from a ligand such as **2.50**. Unfortunately, a slight deviation from linearity at higher ligand concentrations was also observed. This latter finding could reflect high concentration effects, such as ligand-ligand interactions. To compare the effects of imparting rigidity to the structures of **2.47** and **2.50**, **2.55** was studied under similar extraction conditions in DCE. Unfortunately, this latter system proved ineffective. Notably, even at higher concentrations of $HNO_3$, there was not

sufficient extraction of either Am(III) or Eu(III) into the organic phase to allow distribution coefficients to be calculated.

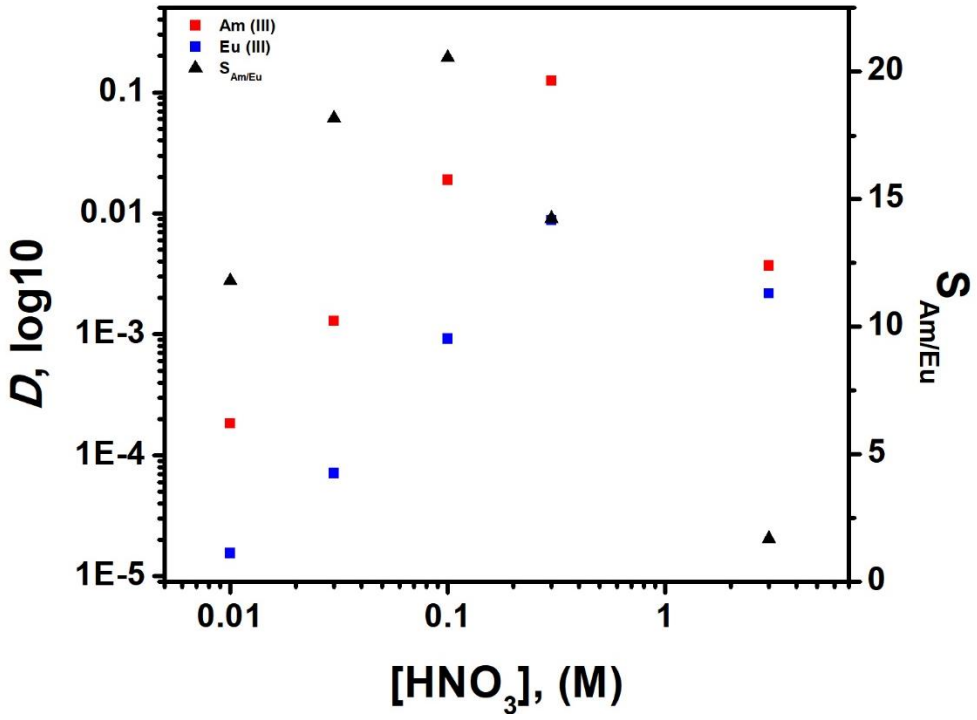


**Figure 2.29**: Extraction of Am(III) and Eu(III) using 25 mM **2.50** in 97:3 Isopar:Exxal 13, and an aqueous phase containing a 10 µL spike of 1.85 x $10^3$ kBq $^{241}$Am(III) and $^{152/154}$Eu(III) tracer and $10^{-4}$ M $Eu(NO_3)_3$, plotted against the initial $[HNO_3]$

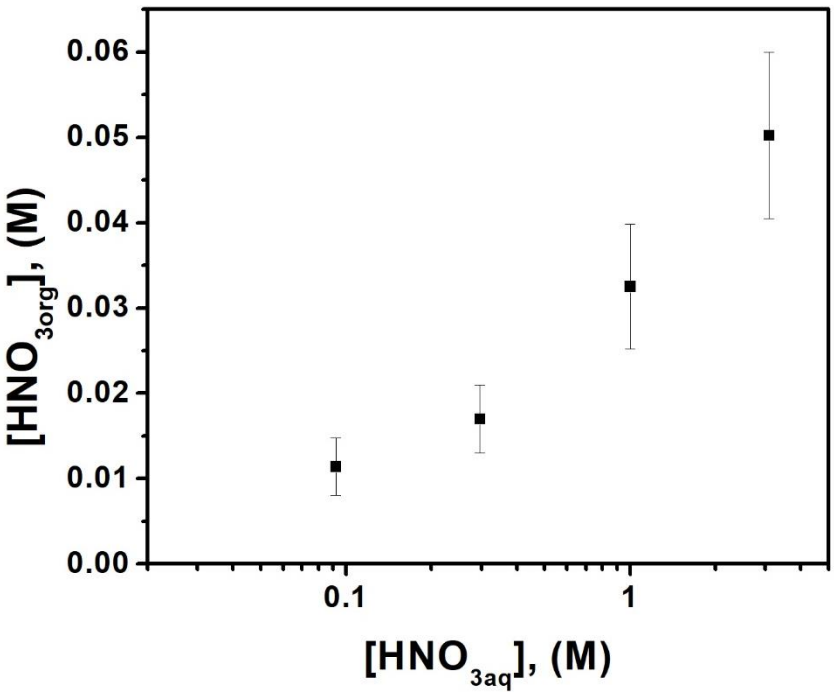


**Figure 2.30**: Extraction of nitric acid by **2.50** (25 mM) into 97:3 Isopar:Exxal 13, as a function of the aqueous phase nitric acid concentration

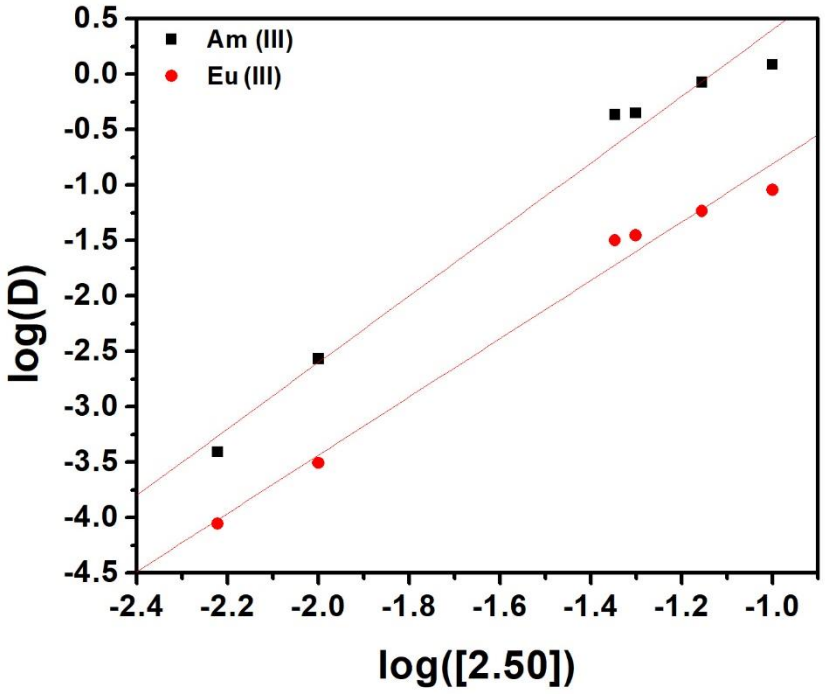


**Figure 2.31**: Slope analyses for the interaction of **2.50** (25 mM) in 97:3 Isopar:Exxal 13 with a 10 µL spike of 1.85 x $10^3$ kBq $^{241}$Am(III) and $^{152/154}$Eu(III) tracer

In an effort to compare the performance of **2.47** and **2.50** to **2.43**,extraction studies of these two ligands in the presence of $LiNO_3$, up to 10 M, were carried out. We chose a nitric acid concentration that produced the most efficient extraction, namely 0.1 M, in performing these experiments. Extraction studies with **2.47** in DCE revealed a fairly linear relationship between [$NO_3^-$] and extraction efficiency. The distribution coefficients were increased by 2-3 orders of magnitude for both Am(III) and Eu(III) when the [$LiNO_3$] was 10 M (Figure 2.32). However, as [$LiNO_3^-$] was increased, selectivity for Am(III) decreased steadily, from approximately 20 to 5, going from 0 M $LiNO_3$ to 10 M. A similar result was seen when examining **2.50** in DCE (Figure 2.33). Extraction of Am(III) and Eu(III) increased by approximately three orders of magnitude, achieving a distribution coefficient

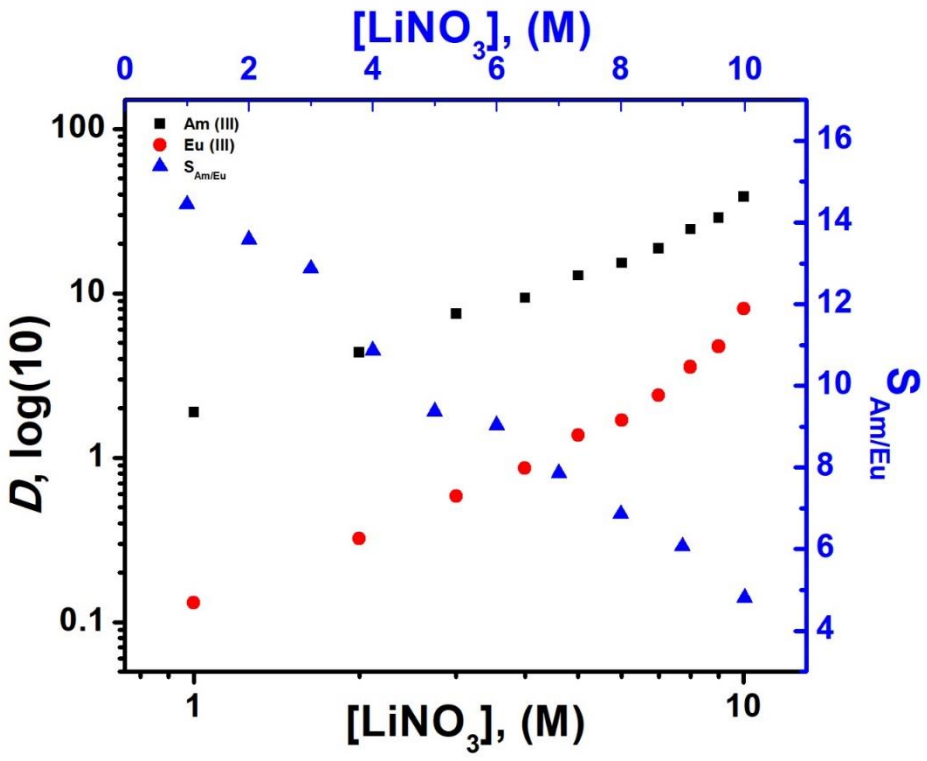


**Figure 2.32**: Extraction efficiencies for Am(III) and Eu(III) with 25 mM **2.47** in 1,2-dichloromethane, as a function of the [$LiNO_3$] in the aqueous phase, containing a 10 µL spike of 1.85 x $10^3$ kBq $^{241}$Am(III) and $^{152/154}$Eu(III) tracer and $10^{-4}$ M $Eu(NO_3)_3$

of 165 for Am(III). Selectivity decreased by about the same amount as was seen for **2.47**. These findings reduce the appeal of increasing [$NO_3^-$] to achieve higher extraction efficiency. Interestingly, changing the solvent from DCE to Isopar led to a reduction in extraction efficiency in the case of **2.47** (Figure 2.34). The addition of $LiNO_3$ appeared to have little to no effect on the extraction of either metal ion at higher concentrations, while at lower concentrations extraction efficiency was increased by ca. two orders of magnitude. Selectivity was fairly low across all concentrations of $LiNO_3$ as well. Such a drastic change in extraction behavior upon changing the solvent from DCE to Isopar was unexpected, and

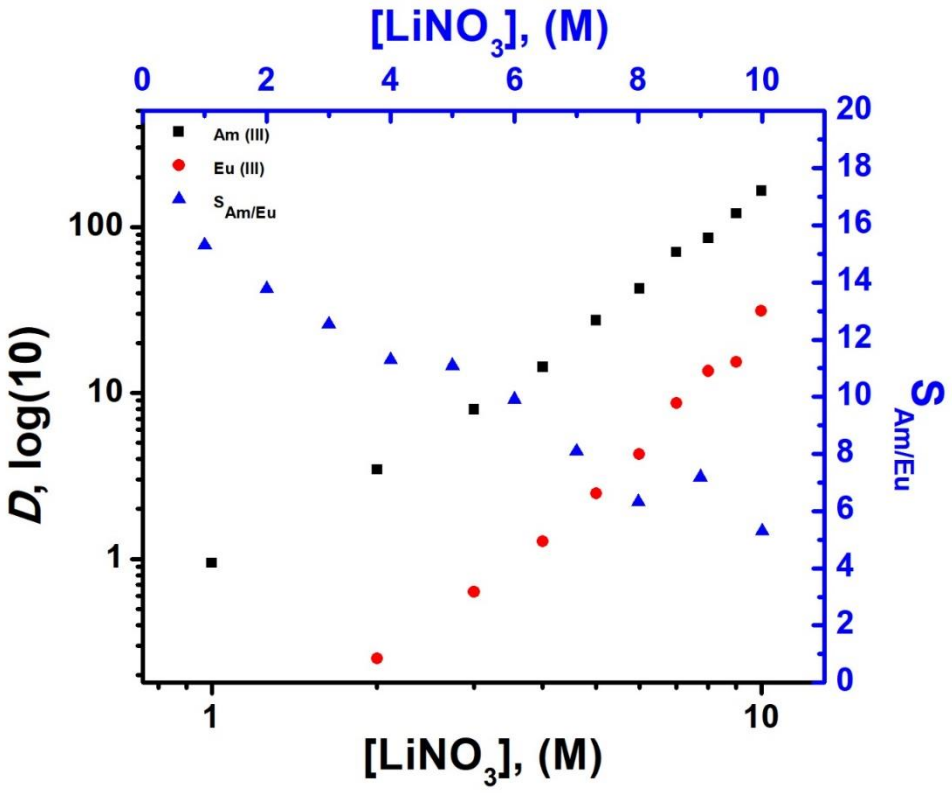


**Figure 2.33**: Extraction efficiencies for Am(III) and Eu(III) with 25 mM **2.50** in 1,2-dichloromethane, as a function of the [$LiNO_3$] in the aqueous phase, containing a 10 µL spike of 1.85 x $10^3$ kBq $^{241}$Am(III) and $^{152/154}$Eu(III) tracer and $10^{-4}$ M $Eu(NO_3)_3$

it is unclear exactly what is the cause of this change. Extraction was further reduced when $LiNO_3$ was used in conjunction with **2.50** in Isopar (Figure 2.35). Extraction efficiency was decreased to such an extent that there was not enough sample extracted at lower concentrations of $LiNO_3$ ([$LiNO_3$ < 5 M) to calculate distribution coefficients for either metal ion species. Overall, distribution coefficients were reduced by at least 1-2 orders of magnitude when $LiNO_3$ was present in the system, and selectivity was reduced significantly as well. From these experiments, we infer that the solvent plays a substantial role in modulating the efficiency of \ **2.47** and **2.50** in the presence of $LiNO_3$.

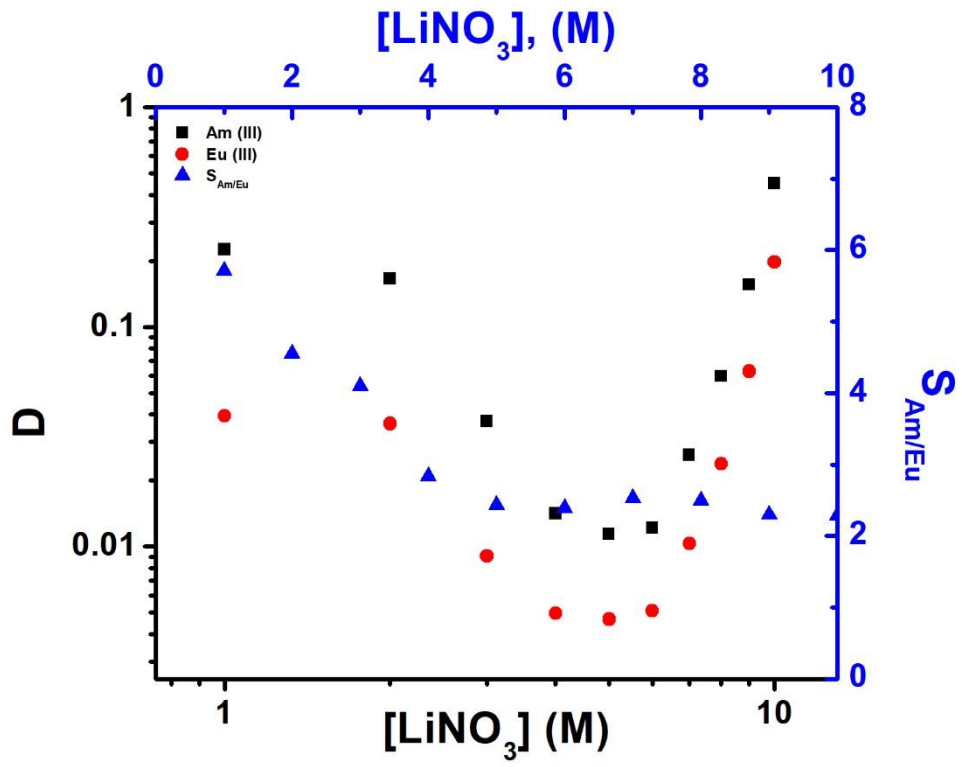


**Figure 2.34**: Extraction efficiencies for Am(III) and Eu(III) with 25 mM **2.47** in 97:3 Isopar:Exxal 13, as a function of the [$LiNO_3$] in the aqueous phase, containing a 10 µL spike of 1.85 x $10^3$ kBq $^{241}$Am(III) and $^{152/154}$Eu(III) tracer and $10^{-4}$ M $Eu(NO_3)_3$

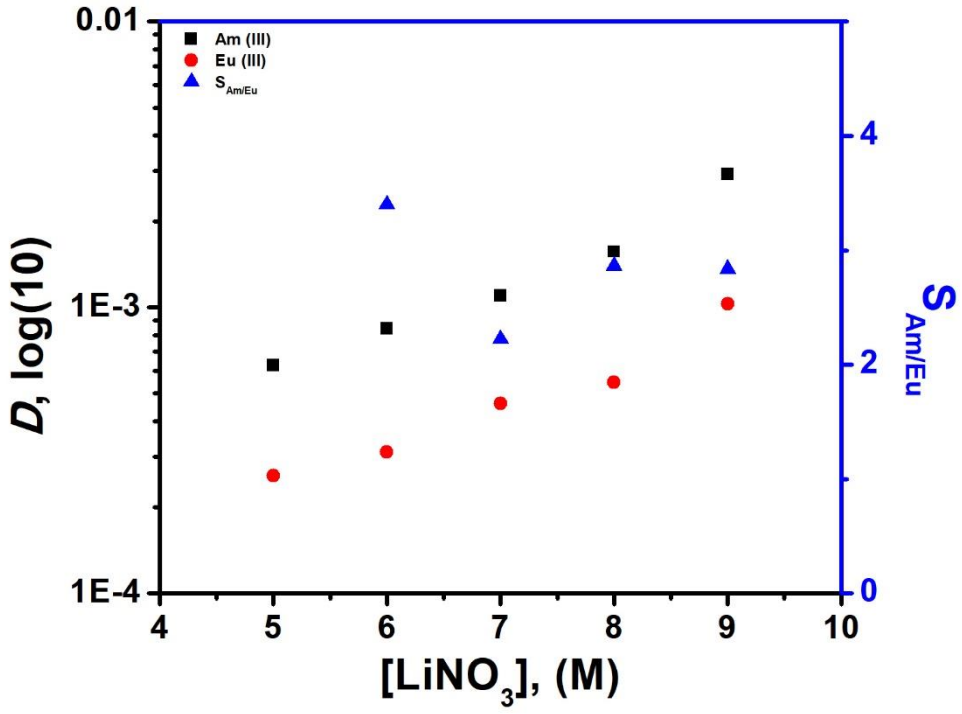


**Figure 2.35**: Extraction efficiencies for Am(III) and Eu(III) with 25 mM **2.50** in 97:3 Isopar:Exxal 13, as a function of the [$LiNO_3$] in the aqueous phase, containing a 10 µL spike of 1.85 x $10^3$ kBq $^{241}$Am(III) and $^{152/154}$Eu(III) tracer and $10^{-4}$ M $Eu(NO_3)_3$

### LIGAND STABILITY

We next sought to test the stability of our ligands under extraction conditions. For these studies, we monitored the stability of our compounds by NMR spectroscopy, varying the nitric acid concentration and observing any changes in the spectrum that occurred over a one week period. After one week, the respective organic phases were washed with distilled water, so as to remove, theoretically, any nitric acid that had been co-extracted. The results

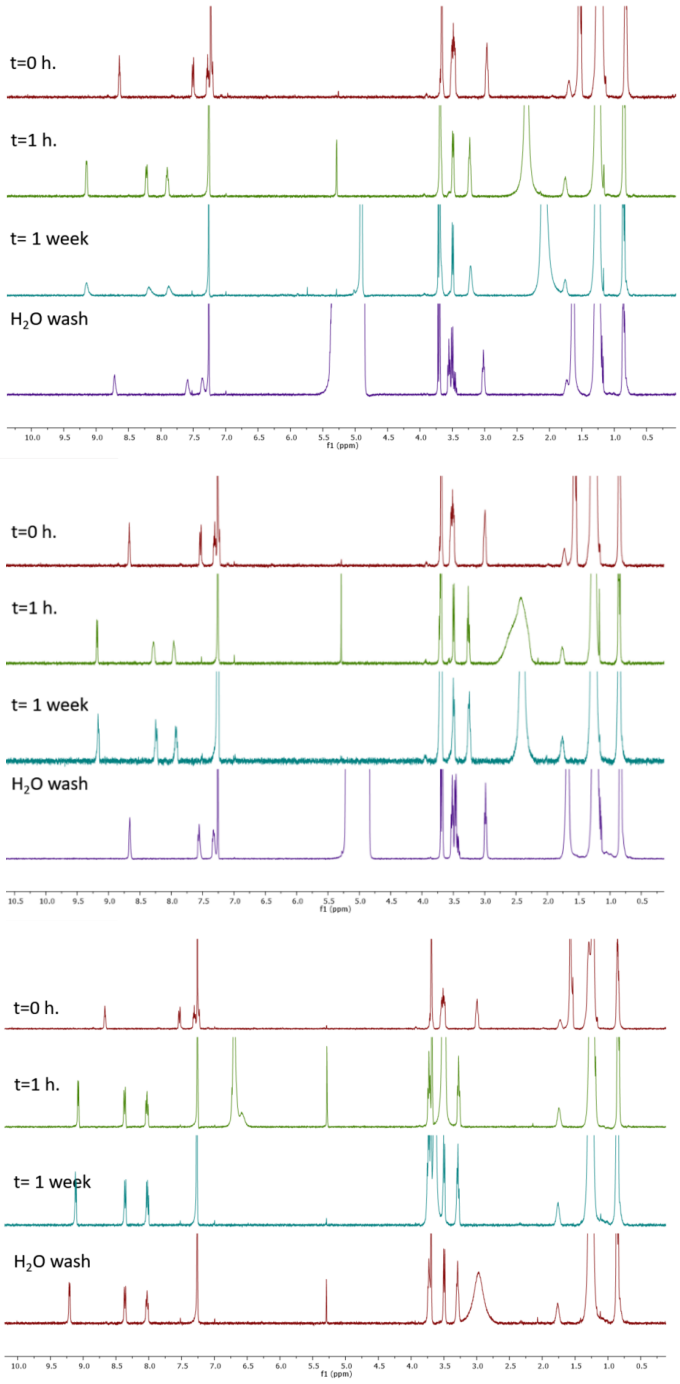


**Figure 2.36**: Stability of **2.47** (25 mM) in 1,2-dichloroethane-$d_4$ contacted with 0.1 M (Top), 1 M (Middle), and 5 M (Bottom) aqueous nitric acid solutions, as monitored by $^1$H NMR spectroscopy over a period of one week, followed by contact with distilled water

for **2.47** are shown in Figure 2.36. After contact with nitric acid solutions of all three concentrations, downfield shifts of the ligand resonances (ca. 9.0, 8.0, 7.5, 7.1, and 6.4 ppm) were observed. This was thought to be due to the protonation of the ligand, which would withdraw electron density and cause a downfield shift in proton resonances. After one hour, an equilibrium appears to have been reached, as no further changes were seen in the NMR spectra for each concentration of nitric acid after one day or one week. After contacting **2.47** with distilled water, resonances for samples contacted with 0.1 M and 1 M nitric acid solutions appear to shift upfield and return to their initial frequencies. However, the sample contacted with 5 M nitric acid sees little to no shift in the peak resonances after washing with distilled water. This may have been due to an insufficient number of washes to remove all of the nitric acid that was extracted. We do not believe that this difference was due to degradation of the material, as the magnitude of the peak shifts after contact with each nitric acid solution were relatively the same. An additional experiment with multiple water washes would most likely reveal that **2.47** was also stable to contact with 5 M nitric acid.

Similar experiments performed with **2.50** revealed somewhat different behavior than what was seen for **2.47** (Figure 2.37). After contact in solutions of **2.50** with aqueous nitric acid for one hour, two sets of new peaks, shifted downfield, were seen in the NMR spectrum of each sample. The area ratios of the two sets of peaks were found to vary as a function of the nitric acid concentration. This ratio did not appear to follow any trend with relation to the amount of nitric acid present in the contacting solution. After washing with water, not much change was seen in the NMR spectra of the sample contacted with 0.1 M nitric acid. In contrast, the sample contacted with 1 M nitric acid showed upfield peak shifts in the NMR spectrum after washing with water, but two sets of peaks were still present. The most surprising finding was that the sample contacted with 5 M nitric acid

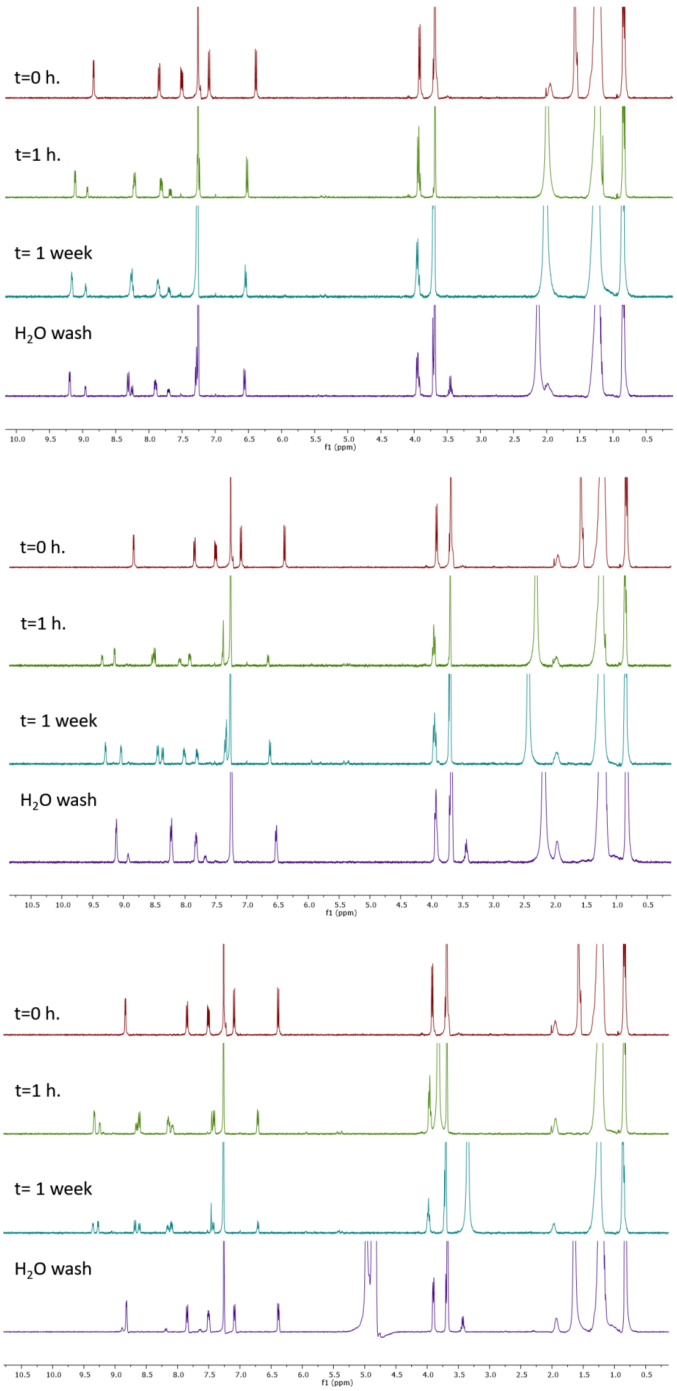


**Figure 2.37**: Stability of **2.50** (25 mM) in 1,2-dichloroethane-$d_4$ contacted with 0.1 M (Top), 1 M (Middle), and 5 M (Bottom) aqueous nitric acid solutions, as monitored by $^1$H NMR spectroscopy over a period of one week, followed by contact with distilled water

showed an almost complete reversion in the peak shifts after washing with water. This compound, **2.50**, was thus deemed stable under these seemingly harsh conditions. There were still two sets of peaks seen in the NMR spectrum after the water wash. However, the major set of peaks corresponded to ca. >95% of the peak area, and had very similar chemical shifts as the starting material before this treatment. This led us to believe that in this case some degradation of the material was occurring, albeit at the <5% level. For the samples contacted with 0.1 M and 1 M nitric acid, the two new sets of peaks that were seen and persisted after the water wash. These peaks could potentially be ascribed to the presence of varying proportions of the protonated and unprotonated ligand. This could have been seen with **2.50** and not **2.47**, since acid extraction titrations showed that **2.47** is more basic than **2.50** and would be more likely to be completely protonated in solution. Additionally, the acid protonation equilibrium could simply be faster for **2.47** than for **2.50**. To the extent this is true, one would only see one set of peaks. Another possibility is that the two acid-base equilibria structures for the protonated form of **2.50** correspond to the two sets of peaks seen in the NMR spectrum (Figure 2.38). This would provide another nitrogen atom that could be protonated and could explain the varied chemical shifts seen in the NMR spectra. This could also explain why the water washes did not return the same chemical shifts as seen in the starting material.

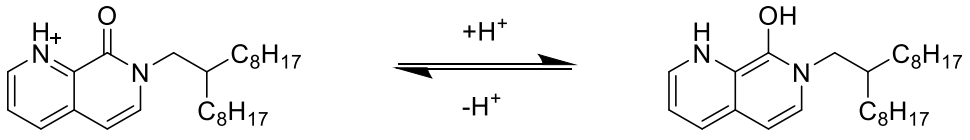


**2.56** **2.57**

**Figure 2.38**: Potential acid-base equilibria for protonated **2.50**

In summary, we have prepared two new ligands, **2.47** and **2.50**, and a control ligand, **2.55** in order to study their extraction properties towards Am (III) over Eu (III) for applications in nuclear fuel waste reprocessing. Studies were performed in DCE and a mixture of Isopar/Exxal 13, so as to test the effects of nitrate concentration, in the form of nitric acid and lithium nitrate, on extraction efficiency and selectivity. Distribution coefficients below 1.0 were observed for both **2.47** and **2.50** over a range of nitric acid concentrations in DCE and Isopar. On the other hand, selectivities as high was 20 were observed. These latter values eclipse those recorded by previous researchers using **2.43**. We were also able to quantify the concentration of nitric acid extracted into the organic phase by ligands **2.47** and **2.50**. The quantitative values reflected the resultant decrease in extraction efficiency seen at higher concentrations of nitric acid. We also observed a stark contrast between the effect of [$LiNO_3$] on extraction when performed in DCE versus what was seen in Isopar. In DCE, increasing the $LiNO_3$ concentration served to increase the distribution coefficients by several orders of magnitude. In contrast, in Isopar these values were either unaffected or diminished by at least 2-3 orders of magnitude. Further work will be needed to explore and rationalize these findings. The stability of the ligands was tested as well, with **2.47** showing good stability to nitric acid. The stability of **2.50** requires further examination, as several sets of new peaks appeared in the NMR spectrum after it was contacted with nitric acid. These new peaks persisted after washing with water. Whether these new peaks represent degradation products or are simply different protonation states of the ligand remains to be determined.

# CHAPTER 3: SYNTHESIS OF NORBORNENE-TYPE MONOMERS CONTAINING IMIDAZOLIUM FUNCTIONALITIES FOR POLYMERIZATION BY RING-OPENING METATHESIS POLYMERIZATION, SEQUESTRATION OF RADIOIODINE BY SILVER IMPREGNATED POLYMERS

## 3.1 Introduction

In order to facilitate the growth and expansion of nuclear energy, the safe, long-term storage of spent nuclear fuel must be examined, in the form of waste reprocessing. However, these processes release several volatile radionuclides whose environmental exposure must be well-controlled. One element of concern present in these waste streams is iodine. While nominally present in the form of $I^-$, the high concentrations of nitric acid used to dissolve fuel rods in the for reprocessing leads it its oxidation to $I_2$, which is volatile and present in off-gas streams.[79] Several isotopes of iodine are present in this off-gas, including stable $^{127}I$ and some unstable isotopes ($^{129}I$, $^{131}I$ to $^{135}I$).[80] Many of these possess short half-lives with the exception of $^{129}I$, which is on the order of $10^7$ years. While short-lived radionuclides other than $^{129}I$ will be present in higher concentrations during fuel reprocessing, after 1 year $^{129}I$ is the most prominent remaining source of radioiodine from these wastes.[81] Because of this, the Environmental Protection Agency (EPA) has set required decontamination factors (DF) between $10^4$-$10^5$ for $^{129}I$, which correspond to greater than 99% capture.[82] In addition to $I_2$, iodine has been found to be present in these off-gas systems in the form of HI, ICN, and alkyl iodides, predominantly methyl iodide but up to octyl iodide.

### 3.1.1 Liquid Scrubbing Processes

Given the need to fix volatile radioiodine from the air and environment, several wet scrubbing and sequestration strategies have been developed and implemented. One relatively simple method involves is the use of an alkaline solution (e.g. NaOH) to scrub iodine from off-gas streams. Under these basic conditions, disproportionation of $I_2$ occurs according to eq. 3.1:

$$3\ I_2 + 6\ OH^- \leftrightarrow 5\ I^- + IO_3^- + 3\ H_2O \quad (3.1)$$

In which the aqueous iodine salts can then be precipitated as the corresponding barium salts.[83] Decontamination factors for this process are in the range of $10^1$-$10^2$, due to the presence of organic iodine species which have a much lower propensity to be removed compared to elemental iodine. Another method, which removes both elemental and organic sources of iodine, is the Mercurex process. This process utilizes mercuric nitrate in a nitric acid solution to scrub elemental iodine (eq. 3.2):

$$6\ I_2 + 6\ Hg(NO_3)_2 + 6\ H_2O \leftrightarrow 5\ HgI_2 + Hg(IO_3)_2 + 12\ HNO_3 \quad (3.2)$$

and organic iodide (eq. 3.3):

$$2\ CH_3I + Hg(NO_3)_2 \leftrightarrow HgI_2 + 2\ CH_3NO_3 \quad (3.3)$$

Decontamination factors on the order of $10^4$ have been reported for this process, but typically more modest numbers in the range of 10-150 have been observed at scale.[80,84] The use of mercury is also a limitation, as environmental regulations limit the scale in using this toxic metal.

Eliminating the use of mercury, the Iodox process uses hyperazeotropic nitric acid (20-30 M) and can also scrub and solubilize elemental and organic iodine. Volatile iodine is fixed in solution through several oxidation reactions, shown below (eqs. 3.4-3.6):

$$2\ CH_3I + 4\ HNO_3 \leftrightarrow 2\ CH_3NO_3 + I_2 + N_2O_4 + 2\ H_2O \quad (3.4)$$

$$I_2 + 4\ H_2O + 2\ HNO_3 \leftrightarrow 2\ I^+ + N_2O_4 + 2\ H_2O + 2\ H^+ \quad (3.5)$$

$$I^+ + 3\ HNO_3 + NO_3^- \leftrightarrow IO_3^- + H^+ + 2\ N_2O_4 + H_2O \quad (3.6)$$

This process has reported decontamination factors on the order of $10^4$ but suffers in practical terms due to the use of hyperazeotropic nitric acid, which is both scarce and especially corrosive. Additionally, its use may lead to high concentrations of organic nitrates, which limit the scope and scale of its application.[85] Investigation into reducing the concentration of nitric acid required for these scrub solutions has led to the study of electrolytic scrubbing techniques. One such method utilizes Co(III) as an oxidant, which is regenerated electrochemically throughout the process. Work performed on a laboratory scale has reported decontamination factors as high as 600 for elemental iodine, and 100 for organic iodide, but the system suffers from acute sensitivity to the presence of $NO_2$, which competes with $I_2$ and $I^-$ in the oxidation reaction with Co(III). A reduction in the decontamination factor by an order of magnitude can be seen with as little as 1% $NO_2$ present in the system.[86] Additional work involving wet scrubbing solutions for the solubilization of iodine has focused on the use of fluorocarbons, polysiloxanes, and molten salts. Unfortunately these methods have not been applied at scales larger than that of a laboratory setting or small pilot plant.[87]

### 3.1.2 SOLID ADSORBENTS

An alternative strategy for fixing volatile iodine species is the use of solid adsorbents. These systems have several advantages over liquid scrubbing techniques, as the use of corrosive solutions is minimized, and the captured iodine does not need to be further transformed for storage, as it is already incorporated onto a solid material. These systems also require less infrastructure for application and can be processed much more easily than liquid scrub solutions. Several traditional adsorbents have been examined, such as activated carbon and Amberlite, but were not considered to be suitably efficient for radioiodine capture.[88,89] Primarily, adsorbents containing silver have been studied for application due to the known propensity of silver and iodine to form solid silver iodide/iodate species.[90] These materials, which include zeolites, mordenites, as well as silica and alumina-based adsorbents, are exchanged or impregnated with silver cations. Advantages of using these types of adsorbents are their high loading capacities and stability, as well as their strong ability to retain both organic and elemental iodine. Initial work with solid adsorbents utilized silver nitrate on amorphous silica, which reacted with elemental iodine (eqs. 3.7-3.8):

$$AgNO_3 + I_2 \rightarrow AgI + INO_3 \quad (3.7)$$

$$4\ INO_3 + 2\ AgNO_3 \rightarrow 2\ AgIO_3 + 6\ NO_2 + I_2 \quad (3.8)$$

And alkyl iodides (eq. 3.9):

$$AgNO_3 + RI \rightarrow RNO_3 + AgI \quad (3.9)$$

which irreversibly fixed the iodine species within the solid matrix. These materials tolerated the higher temperatures (>150 °C) required to facilitate the reaction of silver with

alkyl iodides, and were able to remove iodine from air at the >99.99% level in a laboratory setting, and >99% when performed at scale.[91,92] Additional work has been performed using silver-impregnated alumina as well, achieving similar iodine removal at scale as silica materials.[93]

Silver-exchanged zeolites, such as faujasite (AgX) and mordenite (AgZ), are another class of material for radioiodine capture. In fact, they have been one of the most studied systems in the United States towards this purpose. These types of materials contain labile sodium counterions within the porous matrix, which may be exchanged for silver cations with relative ease. Zeolites are attractive in that they are commercially available and can be selected based on the desired physical properties, which include acid stability and porosity (i.e. the availability of sodium ions for exchange). It is believed that iodine sorption occurs via a redox reaction with silver (I) oxides within the zeolite (eq. 3.10):

$$2\ Ag_2O + 2\ I_2 \leftrightarrow 4\ AgI + O_2 \qquad (3.10)$$

however a formal mechanism has yet to be accepted.[92] Work with AgX and AgZ sorbents has shown decontamination factors on the order of $10^3$-$10^5$ for both elemental and organic iodine species with the materials containing approximately 15% silver by weight.[94] Of note, Chapman and coworkers discovered that silver-exchanged mordenites produced differing results depending on the oxidation state of silver within the material.[95] Commercial NaZ was exchanged with silver and then reduced under a hydrogen gas stream, yielding $Ag^+Z$ and $Ag^0Z$ sorbents. Upon iodine capture, crystallographic analysis of these two materials showed the formation of subnanoscale AgI within the zeolites, as well as nanocrystalline AgI on the zeolite surface in the case of $Ag^0Z$ (Figure 3.1). This

implied that migration of $Ag^0$ was occurring during iodine capture with $Ag^0Z$, while $Ag^+$ was confined to the zeolite pores in $Ag^+Z$. This has led to concerns with using $Ag^0Z$ for iodine capture applications, as pore-confined AgI represents a lower risk for iodine leakage than surface-bound AgI. However, in an effort to reduce the cost of these materials, methods for their regeneration using hydrogen gas have been developed, using a PbX adsorbent bed as a cheaper alternative for long term storage.[96] Pretreated $Ag^0Z$ systems have also shown improved uptake of organic iodide compared to $Ag^+Z$, and the optimization of these materials for implementation at scale is currently ongoing.[97]

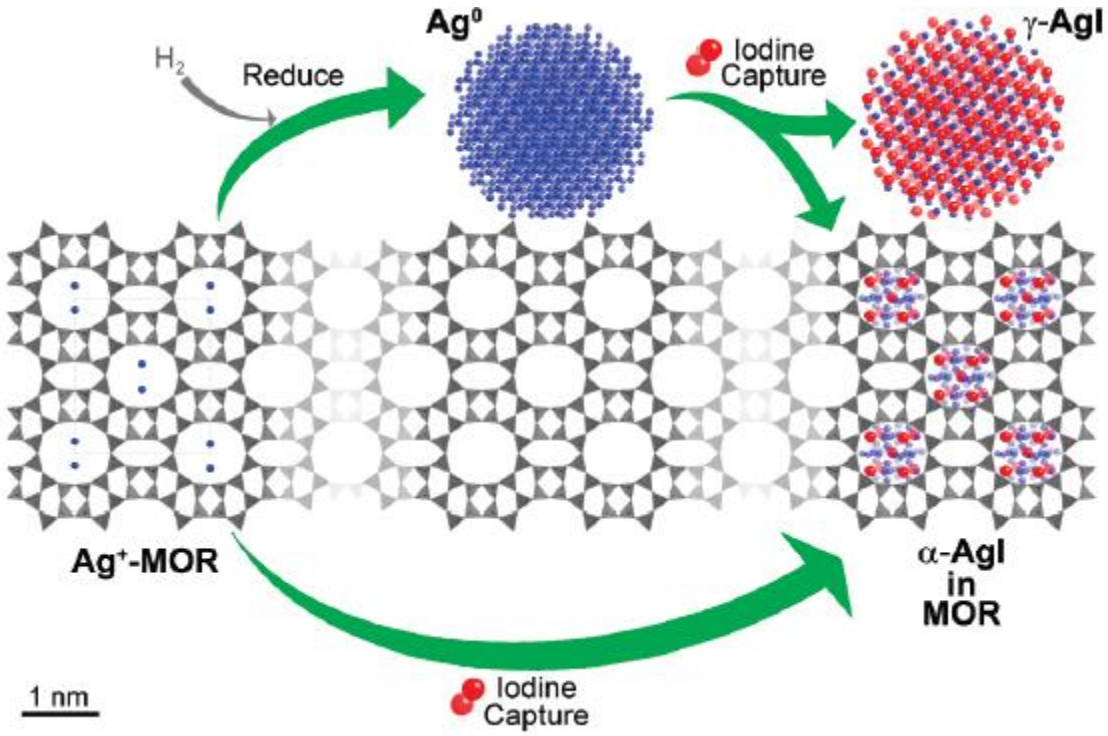


**Figure 3.1**: Iodine capture performed using silver-exchanged mordenite and reduced silver-exchanged mordenite.[95]

Over the last decade, aerogels have shown promise as materials with significantly higher iodine uptake than zeolite materials. Aerogels are a class of materials that have extremely low densities, due to approximately 95% of the material being porous space; they are also highly robust and temperature stable, making them ideal adsorbents for iodine capture and storage.[98] These materials are prepared first by synthesizing and casting the gels; for silica aerogels, they are prepared by the acid-catalyzed gelation of a siloxane. The gels are then aged in the mother liquor to ensure that the entire material is saturated, and then the gels are dried, removing the solvent from within the material. This is typically done using supercritical $CO_2$, yielding the desired aerogel material.[99] Silica aerogels have been used as iodine capture materials through their functionalization and incorporation of silver; within the pores and on the surface of the aerogel are free hydroxyl moieties, which can be further reacted with silanes to install various functional handles. Researchers at Pacific Northwest National Laboratory (PNNL) were able to functionalize silica aerogels with thiol groups and subsequently bind silver(I). Reduction of this material gave an $Ag^0$-functionalized silica aerogel ($Ag^0$-aero) capable of iodine capture and storage (Figure 3.2). In experiments using simulated iodine carrier gas feeds, $Ag^0$-aero outperformed $Ag^0Z$ materials, with a mass increase of near 40%, as opposed to 10% $Ag^0Z$ (Figure 3.3). Additionally, after six months of aging the materials, $Ag^0$-aero only showed a 22% loss in iodine uptake performance, while $Ag^0Z$ showed a loss of 40%. $Ag^0$-aero also showed no discernable change in the aerogel structure or silver nanoparticle size over that time, while

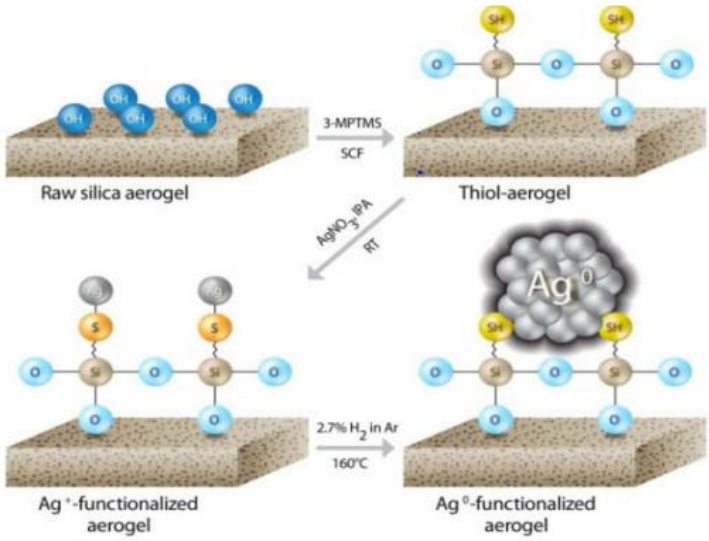


**Figure 3.2**: Functionalization of raw silica aerogels to bind silver, for iodine capture experiments.[100]

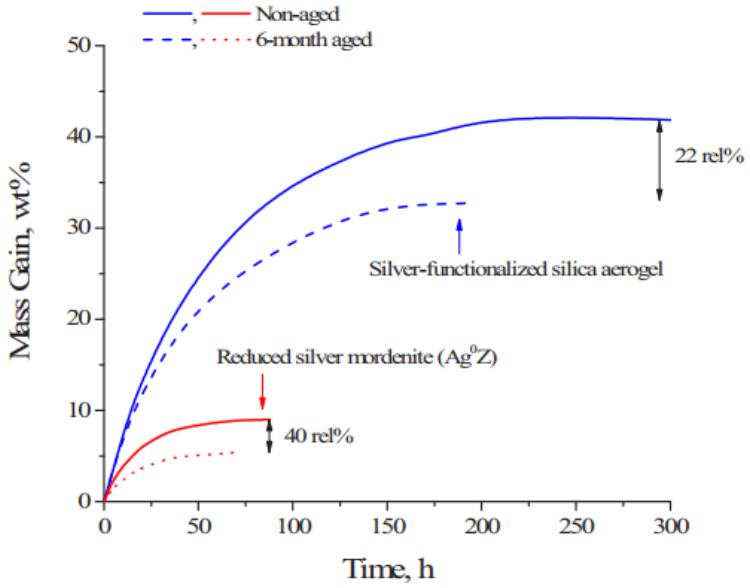


**Figure 3.3**: Iodine capture performance by as-synthesized (solid lines) six-month aged (dashed lines) $Ag^0$-aero and $Ag^0Z$[100]

$Ag^0Z$ is known to be air-sensitive and degrade over time.[100] Another class of aerogels are chalcogels, which are made up of a network of chalcogens (S, Se, and Te) and various interlinking metals. One advantage of chalcogels compared to silica aerogels is that they do not require functionalization, as they already contain chalcogen anions instead of oxygen.[101] They also have a wider range of precursors (Cd, Zn, Pb, Ge), which has allowed for their physical and chemical properties to be tuned as desired (e.g. surface area, chemical affinity).[102,103] Work performed by researchers at PNNL with several chalcogels containing differing metal ions saw very high capture efficiences, greater than 99%, with the SnS chalcogel performing sufficiently well as to satisfy the EPA standards for iodine capture and breakthrough (Figure 3.4).[104,105] Chalcogels have also shown high iodine retention at

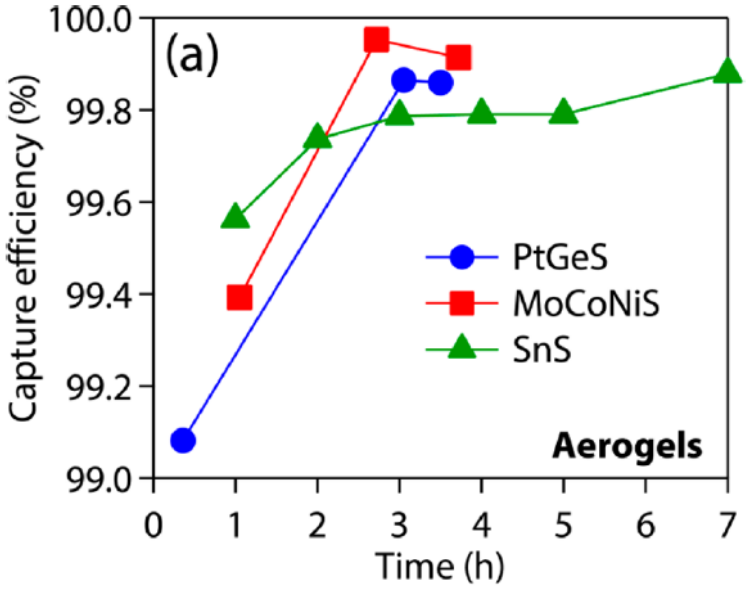


**Figure 3.4**: Plot of iodine capture performed with several chalcogels containing varying interlinking metal ions.[105]

temperatures up to 600 °C, further supporting their use as a long term storage option for captured radioiodine.[106]

While these solid sorbent materials are effective, they are not able to be regulated; each system relies on nonspecific interactions of silver and the material upon loading, which may be irregular. Therefore, the fabrication of each material cannot be truly replicated, as there is no formal ordering in place. In light of these deficiencies, discrete systems for iodine capture have been investigated. One such system relies on the use of cyclodextrins, which are known to form inclusion complexes with iodine. Various methylated α-, β-, and γ-cyclodextrins were shown to have strong affinities for iodine and were used in a wet solution scrub to capture airborne iodine. Once crosslinked, these cyclodextrin derivatives were used as solid adsorbents, and showed efficient iodine capture and retention at elevated temperatures.[107] Work by Sessler and coworkers has shown the ability of calix[3]bipyrrole (Figure 3.5) to bind iodide anions with affinity on the order of the aforementioned cyclodextrins.[108] The Sessler group has also demonstrated the use of poly(methyl methacrylates) containing pendant calix[4]pyrroles in the extraction of halides in a biphasic extraction system. This approach has the advantage of allowing discrete control over the number of calix[4]pyrrole repeat units on the polymer backbone.[14]

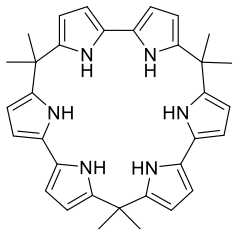


3.1

**Figure 3.5**: Calix[3]bipyrrole, a receptor capable of binding iodide anions in organic media

The development of a well-controlled, selective material for iodine capture based on the success of these receptors could lead to the development of new sorbents. We have proposed the use of organic polymers fabricated via ring-opening metathesis polymerization (ROMP). ROMP allows for the systematic chain growth of polymers from discrete, well-characterized monomers. The Grubbs catalyst utilized for ROMP also has a broad scope of reactivity and a large functional group tolerance.[18] In designing our ligands, we sought a functional group that would have a discrete interaction with silver, and contain a point of attachment for installing a norbornyl moiety for polymerization. We proposed an *N*-heterocyclic carbene (NHC) as the silver complexing entity. This ligand class is well known to form monomeric or dimeric complexes and is fairly simple to characterize by standard NMR spectroscopic methods.[109] In order to generate an NHC, we planned on starting from an imidazolium precursor, which could be functionalized as desired off both nitrogen atoms (Figure 3.6).

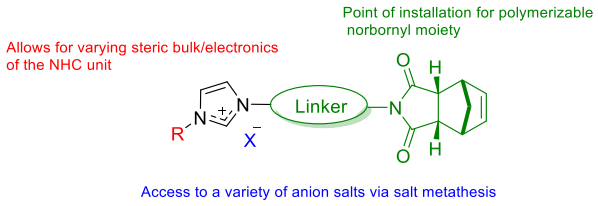


**Figure 3.6:** Imidazolium precursor for NHC monomer designed to bind silver, with key functional areas highlighted

One nitrogen atom of the imidazolium would serve as an attachment point for our tether and norbornyl moiety, while the other could serve as a point of diversification, varying the steric bulk or electronics. In changing the size of the substituent, we sought to be able to favor the formation of *mono*-carbene species over *bis*-carbenes, a level of tuning that, in turn, was expected to allow control over the silver loading capacities. Additionally, anion metathesis could allow for a variety of salts to be prepared. This would allow us to investigate their effects on iodine capture and loading. A proposed general imidazolium monomer is shown in Figure 3.7.

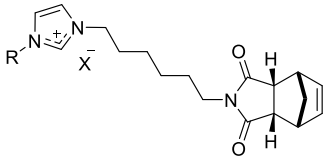

**Figure 3.7**: Proposed general imidazolium monomer structure

## 3.2 Results and Discussion

### 3.2.1 Monomer and Polymer Synthesis

The general synthetic scheme for synthesizing imidazolium monomers is shown in Scheme 3.1. Imidazole derivatives **3.2-3.5** were prepared using a known literature procedure from the corresponding aniline.[110] Separately, the alkyl halide, **3.7**, was prepared

by substitution of the norbornyl imide **3.6** with 1,6-dibromohexane, in 83% yield. Heating this compound neat with **3.2-3.5** gave the imidazolium bromide salts **3.8-3.11** in modest to good yields.

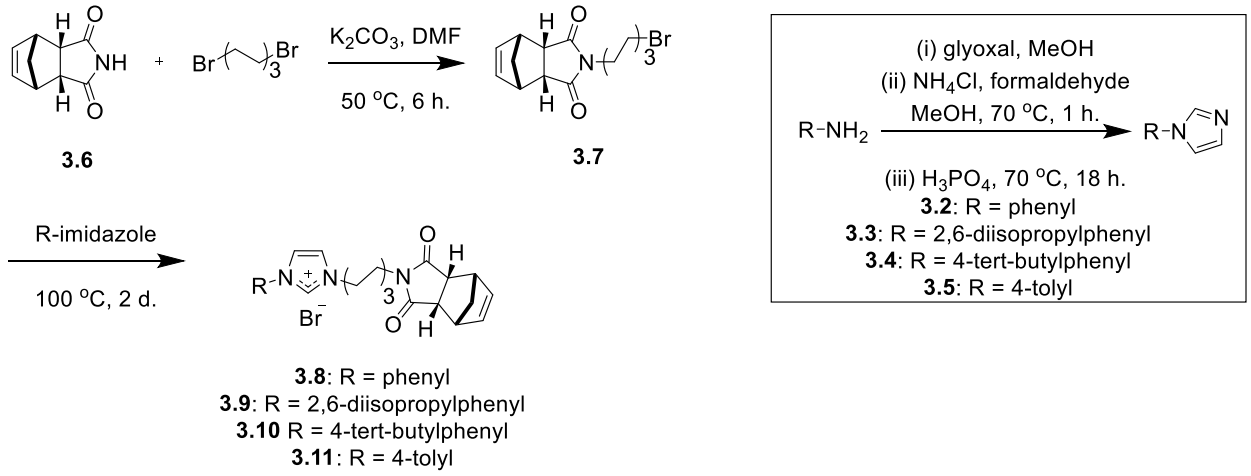


**Scheme 3.1**: Synthesis of imidazolium bromide monomers

To assess the binding mode of our imidazolium monomers with silver, precursor **3.8** was reacted with silver(I) oxide under ambient conditions to give the silver carbene complex **3.12** in 59% yield (Scheme 3.2). The progress of this reaction was monitored by NMR spectroscopy and completion was evidenced by the disappearance of the resonance of the C2 proton at ca. 9 ppm. Unfortunately, attempts to obtain crystals of this complex suitable for X-ray diffraction analysis proved unsuccessful, possibly due to the "greasy" carbon chains and the presence of the somewhat hydrophobic bromide anion. Therefore, further efforts to synthesize *N*-heterocyclic carbene-silver complexes of these monomers were focused on exchanging the counterion for a hexafluorophosphate ion ($PF_6^-$). The $PF_6^-$

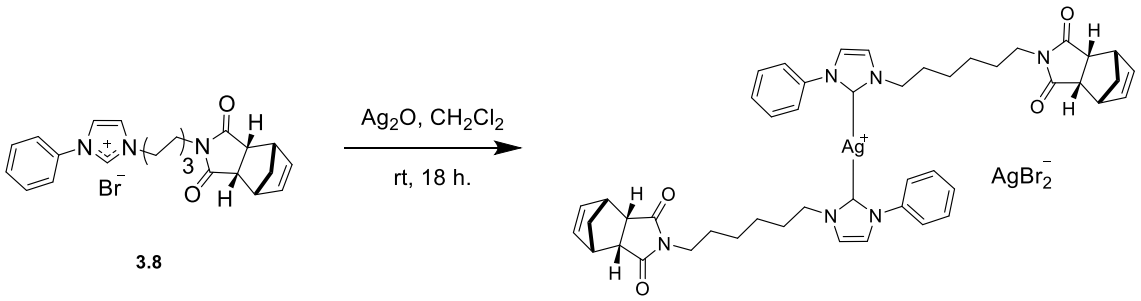


**Scheme 3.2**: Synthesis of the *N*-heterocyclic carbene-silver complex **3.12**

ion is significantly more hydrophobic and may help the complex in forming a crystalline material.[111] The synthesis of these salts and their corresponding *N*-heterocyclic carbene-silver complexes is shown in Scheme 3.3. Salt metathesis using excess potassium hexafluorophosphate gave the imidiazolium hexafluorophosphate salts **3.13-3.16** in good yields. The corresponding *N*-heterocyclic carbene-silver complexes were prepared by stirring with silve(I) oxide in the presence of base, with the reaction being monitored by

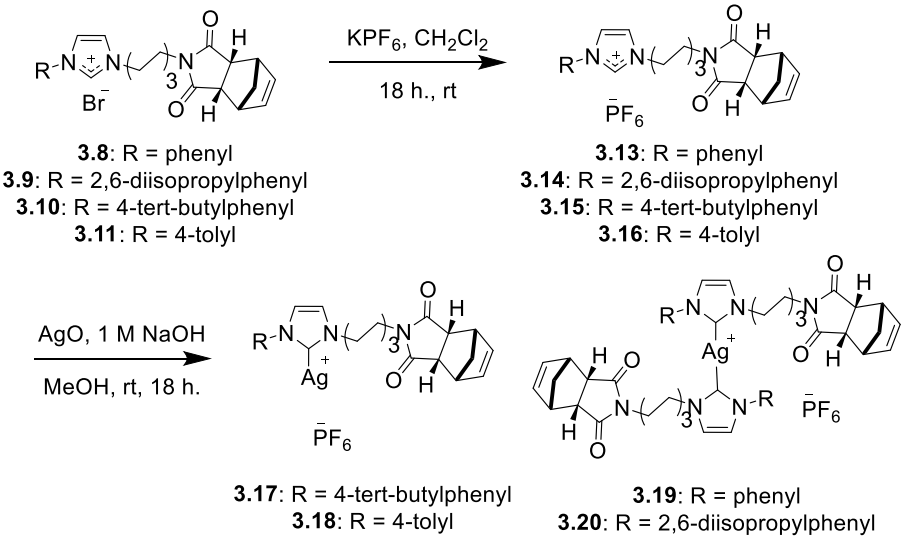


**Scheme 3.3**. Synthesis of *N*-heterocyclic carbene-silver complexes from hexafluorphosphate salt precursors

NMR spectroscopy. Upon complete disappearance of the C2 proton resonance at ca. 9 ppm, the reaction was deemed complete. The complexes were then isolated in good yields. Fortunately, we were able to obtain crystals suitable for X-ray diffraction analysis in the case of **3.8** and **3.19** (Figure 3.8-3.9). Of note, **3.19** is a *bis*- carbene silver complex, a result that we had hoped to see. Due to the inability to obtain crystal structures for **3.17**, **3.18**, and **3.20**, we sought to characterize the nature of the complexes by another method. High-resolution mass spectrometry (HRMS) of these complexes allowed us to determine whether *mono*- or *bis*-carbene species had been formed with these ligands (Figure 3.10). From these results, we saw that **3.17** and **3.18** formed *bis*-carbenes with silver, while **3.19** and **3.20** formed *mono*-carbenes. From this small sample size, we inferred that substitution at the 4-position of the aryl ring off the heterocycle was a potential determining factor for *mono*- or *bis*-carbene formation. Substitution with isopropyl groups at the 2,6-positions led to *bis*-carbene formation, as in the case of **3.20**. This was ascribed to orthogonal

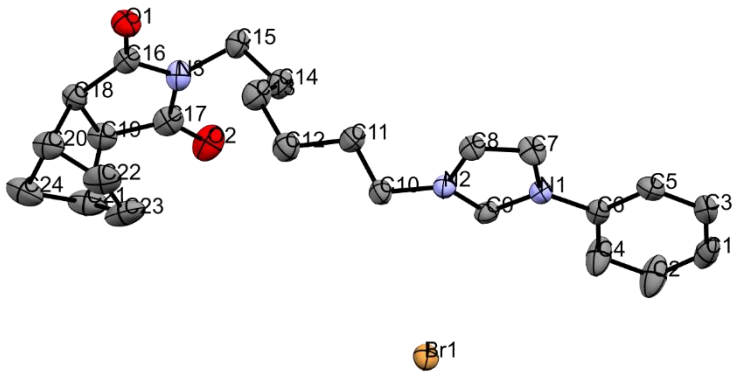


**Figure 3.8**: Molecular structure of **3.8**. The atom labeling scheme is shown. Displacement ellipsoids are shown at the 50% probability level.

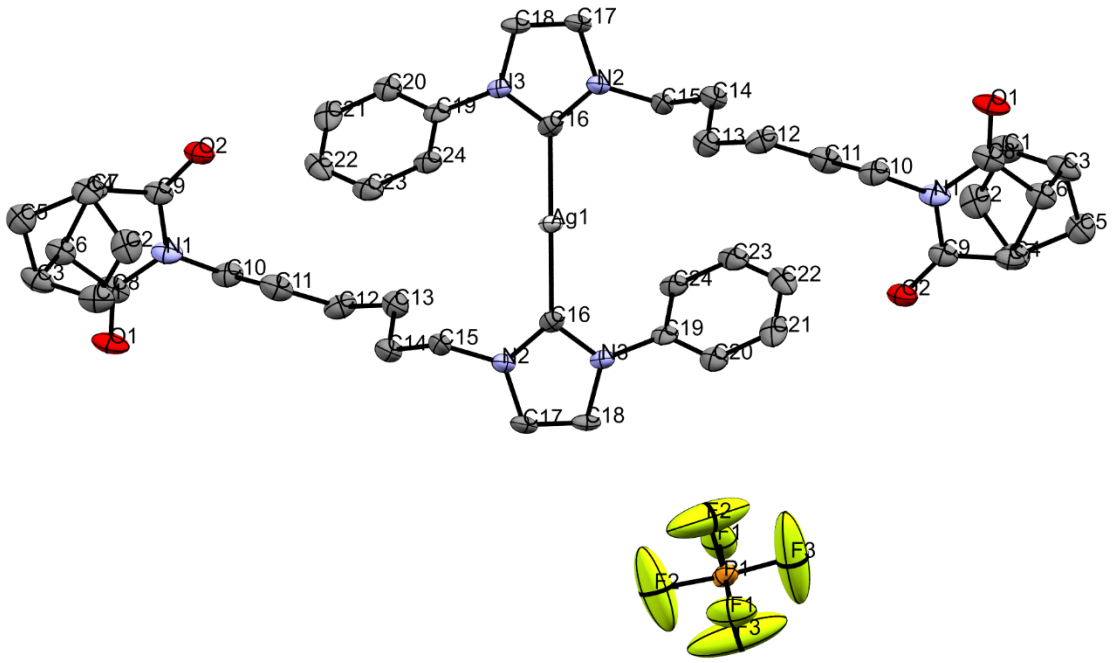


**Figure 3.9**: Molecular structure of **3.19**. The atom labeling scheme is shown. Displacement ellipsoids are shown at the 50% probability level.

rotation of the aryl group away from the ligation site, resulting in reduced steric crowding. This is not seen in the case of **3.8**, where in the solid state the phenyl ring was co-planar to the imidazolium ring; this may be due to increased π-overlap between the p-orbitals of the two aromatic rings. However, upon complex formation, the C2 carbon becomes a σ-donor with an empty p-orbital, disrupting aromatic character across the heterocycle and promoting rotation about the N-Ar bond.

Ring-opening metathesis polymerization experiments involving these monomers were carried out using the Grubbs 3$^{rd}$ generation catalyst. Efforts to polymerize the

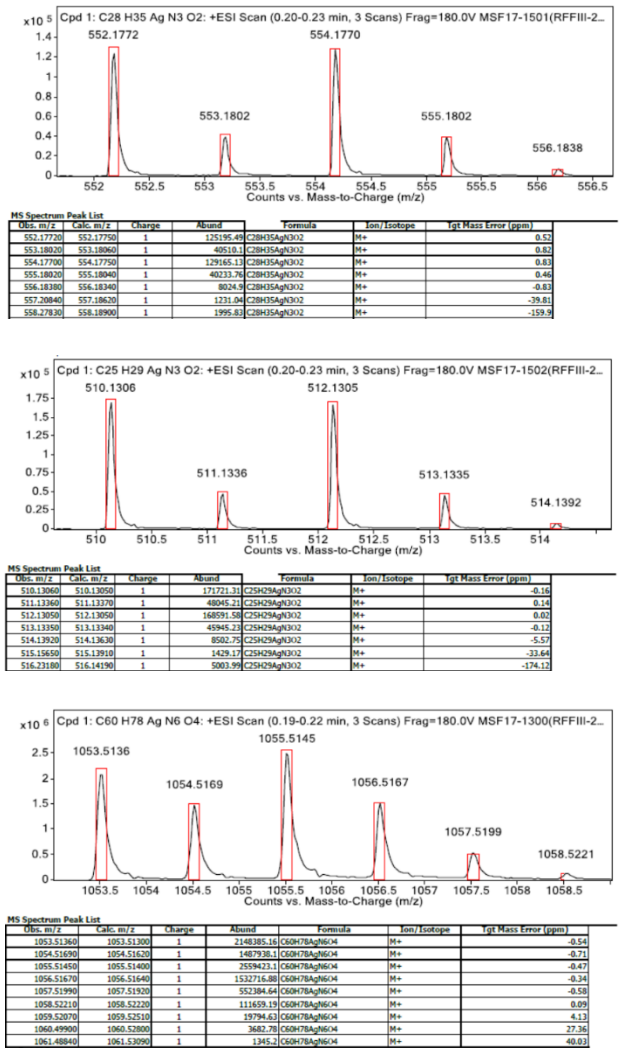


**Figure 3.10**: HRMS traces of **3.17** (top), **3.18** (middle), and **3.20** (bottom) used to identify the formation of *mono*- or *bis*-carbene species

imidazolium bromides **3.8-3.11** in methylene chloride yielded polymers of unusually high molecular weights, as determined by NMR spectroscopy. However, upon changing the polymerization solvent to DMF, polymers of expected molecular weights were obtained, up to ca. 60 repeat units ($M_n$ = 28,225 D). Efforts to produce polymers with higher molecular weights resulted in incomplete conversion of monomer to polymer, stalling

around 60 repeat units. This result lead us to surmise that the buildup of charge on the growing polymer chain may contribute to the undesirable loss of control seen in using methylene chloride as our solvent. The higher polarity of DMF may have been able to support growing chains more effectively, but only up to a certain number of repeat units. Polymerization of the hexafluorphosphate salts **3.13-3.16** in DMF also gave polymers with good control over the molecular weight. Interestingly, when polymerizations were carried out in methylene chloride, the resultant polymers precipitated out of solution after polymerization was complete. These polymers were found to be of the desired molecular weight as inferred from both NMR spectroscopy and GPC analyses. An experimental molecular weight of 26,003 D was determined for one sample of **P3.13**, as compared to the the desired weight of 26,774 D. The dispersity of this sample was 1.122, which is fairly low and points towards a living polymerization character. However, further polymerization experiments will need to be carried out to confirm this latter mechanistic assumption. We also did not see a limit to the molecular weight of these polymers, as was seen when the bromide salts were employed. We believed that one explanation for this latter result is the lower solubility of the hexafluorophosphate salt in methylene chloride. It may be that during polymerization the growing end of the polymer chain is solubilized, while the bulk polymer chain containing the hexafluorophosphate salts is precipitated from solution. It is unclear why the bromide salts undergo polymerization in a manner that leads to a loss of control of molecular weight. Attempts to metallate **P3.8-P3.11** using silver (I) oxide were unfortunately unsuccessful. Several silver precursors were screened, without any notable formation of silver complexes off the polymer backbone. We

attributed this putative problem to the fact that silver halide species form secondary structures, supported by μ-halide bridges between silver atoms.[112] This may allow for some metallation to occur, but could inhibit further complex formation throughout the entire polymer. Metallation of **P3.17-P3.20** did not suffer from this problem, and polymers with bound silver, **AgP3.17-AgP3.20**, were prepared using silver(I/III) oxide in acetonitrile with moderate heating. Similar to experiments with the monomeric species, reaction progression was monitored by NMR spectroscopy. Notably, a larger increase in mass was seen after metallation of **P3.17** and **P3.18** (14% and 27%, respectively) than for **P3.19** and **P3.20**. Since **3.17** and **3.18** are expected to form *mono*-carbene species, it comes as no surprise that more silver could be bound to their corresponding polymers than for **3.19** and **3.20**. This latter finding provided support for the use of bulkier substituents at 4-position of the *N*-aryl ring on our monomers, in order to maximize the amount of silver than can be bound by each polymer chain. Similar to work done with silver-exchanged zeolites, we then sought to reduce the silver bound to our polymers to study its effects on iodine capture. The silver-bound polymer, **AgP3.19** was subjected to a 5% $H_2$ gas stream under $N_2$ atmosphere at 150 °C for 24 hours to reduce the silver bound within the polymer to its elemental state. After this treatment, the solid polymer was characterized by a lustrous sheen, and showed no loss of mass. NMR spectroscopic studies of this material (DMSO-$d_6$) showed a return of the C2 proton resonance at ca. 9 ppm, as well as no change in the olefinic peaks on the polymer backbone at ca. 5.75-5.25 ppm (Figure 3.11). The fact that the bound silver underwent reduction was further evidenced by the fact that the lustrous

material was insoluble and could not be dissolved. This insolulibty was ascribed to the presence of elemental silver.

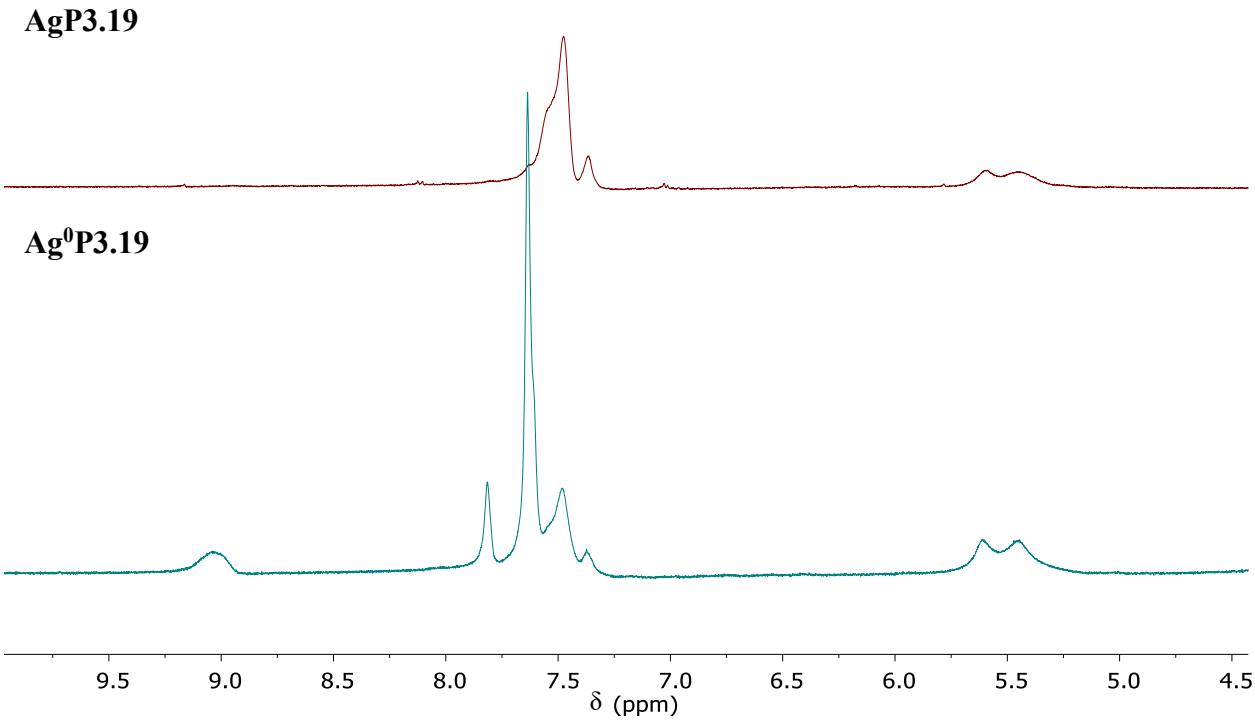


**Figure 3.11**: Overlaid NMR spectra (DMSO-$d_6$) of **AgP3.19** and **Ag$^0$P3.19**

In conclusion, we have synthesized several monomers containing imidazolium functionalities with substituents of varying steric bulk. *N*-heterocyclic carbene silver complexes of these monomers were prepared, in order to characterize the binding nature of the complex, which was confirmed by X-ray crystallography or HRMS. These monomers were then subject to polymerization, and suitable conditions were found when monomers containined hexafluorophosphate as the counteranion. Initial characterization of these polymers provided evidence for potential living character, despite the polymer precipitating over the course of the polymerization reaction. Further experiments will,

however, be required to determine if this inference holds for all monomers of this class. We were able to metallate each polymer, and observed an increase in mass gained for polymer containing functional groups believed to form *mono*-carbene species. Further characterization of the silver content by ICP-OES will be required to support this hypothesis. We also demonstrated the ability to reduce the silver cations within one of these polymers. This reduction should allow us to determine if there are any differences in iodine capture between the two silver species. Future efforts will be focused on determining the maximum iodine uptake of each polymer, as well as the iodine breakthrough time under simulated off-gas conditions. It may also be of interest to see if similar AgI nanostructures are formed within these polymers, as were seen when similar experiments were performed using silver-exchanged zeolites.

# CHAPTER 4: EXPERIMENTAL METHODS

## GENERAL METHODS

All reactions were carried out under a dry $N_2$ atmosphere in flame dried glassware using standard Schlenk techniques unless otherwise specified. Ground glass joints were greased with Dow Corning High Vacuum Grease®. Dry solvents were collected in solvent bulbs from an Innovative Technologies Pure-Solve 400 solvent purification system and stored over 3 Å molecular sieves. All chemicals were used as received from commercial suppliers unless otherwise specified. Samples of $^{241}$Am were obtained from the Reactor Engineering Design Center (REDC) at The Oak Ridge National Laboratory. Samples of $^{152}$Eu were purchased from Isotope Product Laboratories. Thin layer chromatography (TLC) was performed using Silicycle silica gel 60 $F_{254}$ pre-coated aluminum sheets. Column chromatography was performed using Silicycle Silica Flash® F60 silical gel or using a Teledyne ISCO Combiflash system. NMR spectra were recorded with a Varian DirectDrive 400 MHz spectrometer at ambient temperature and were referenced internally to the residual solvent peaks. All chemical shifts are given in ppm and coupling constants are given in Hertz (Hz). Mass spectrometry was performed with a Micromass Autospec Ultima HRMS (for $CI^+$) or an Agilent 6530 QTOF system (for $ESI^+$). Determination of elemental composition from extraction studies was performed using a Varian 720 ES Inductively-Coupled Plasma Optical Emission Spectrophotometer (ICP-OES). The following emission wavelengths (nm) were used by for the ICP-OES analysis of each of the following elements: Cu 224.700, Zn 206.200, Co 230.786, Cd 214.439, Pb 220.353, Mn 293.931, Ni 227.021, Fe 261.187.

## EXTRACTION STUDIES

*Extractions performed with **1.5**, **1.11**, and **P1.5**:*

Extractions were performed using a Fisher Scientific™ Multi-Purpose Tube Rotator, set to 40 rpm. Extractions were performed in Falcon™ Conical Centrifuge Tubes, and all studies were performed over a 24 hour period unless otherwise stated. Aqueous solutions were analyzed using a Varian 720 ES Inductively-Coupled Plasma Optical Emission Spectrophotometer (ICP-OES) after extraction, and the percent extraction of each metal ion was determined from the mass balance of the initial solution of metal ions before extraction. Liquid-liquid extractions were performed using water and toluene, with the aqueous phase containing the divalent cation in question (as the corresponding chloride salt) at an initial concentration of 1 mM along with 1 M NH4Cl. The concentration of **1.5/1.11** in toluene was adjusted to 3.3 equivalents of the total metal ion concentration, unless otherwise stated. Solid-liquid extractions with **P1.5** were performed using aqueous solutions that were initially 1 mM in the divalent metal chloride salt and 1 M in $NH_4Cl$. The amount of polymer was adjusted such that approximately 3.3 equivalents of extractant on the polymer backbone were present relative to the total metal ion concentration. Selectivity studies were performed using 5 equivalents of each metal ion (each at 1 mM) in relation to the total amount of extractant moieties on the polymer. After extraction, the polymer was separated from the aqueous phase, washed with excess water, and dried in vacuo. The polymer was then digested in concentrated nitric acid and analyzed by ICP-OES to determine the metal speciation.

*Extractions performed with **2.47**, **2.50**, and **2.55**:*

Extractions were performed using a conventional rotating wheel, set to 60 rpm in an air box set to 2.5 ± 0.5 °C. Samples consisted of a 600 µL aqueous phase of varying $[HNO_3]$ containing 10 µL of 1.85 x $10^3$ kBq of $^{241}Am$ and $^{152}Eu$, and $10^{-4}$ M $Eu(NO_3)_3$, as

specified, and a 600 μL organic phase containing **2.47**, **2.50**, or **2.55** in DCE or Isopar-L fluid. The two phases were contacted in 1.8 mL capacity snap-top Eppendorf tubes for one hour, and contacts were performed in duplicate. After contact, samples were subject to centrifugation at 3000 rpm for five minutes, at 25 °C to separate the phases. The phases were then subsampled into polypropylene tubes, taking 300 μL aliquots of each phase. Samples were counted using a Canberra Gamma Analyst Integrated Gamma Spectrometer. The counting time was varied such that a sufficient signal-to-noise ratio was achieved, using the integration of the peak at 59.5 keV for americium, and 121.8 keV for europium. Counting values on the order of $10^4$ were obtained for each measurement where possible to minimize potential errors. The areas of each peak were used in determining distribution ratios and separation factors. Extractions were performed in duplicate and measurements were in agreement of each other within 5%.

### X-RAY CRYSTALLOGRAPHY

Metal complexes of **1.5** and a panel of divalent transition metal cations (Mn, Fe, Co, Cu, Ni, Zn, Cd, Pb) were synthesized by stirring a $H_2O$-EtOH (1:3 v/v) solution of **1.5** with NaOH and the corresponding metal dichloride salt. These solutions were filtered and allowed to evaporate at room temperature over several days, yielding crystals of metal complexes of **1.5** and Cu(II), Ni(II), Zn(II), and Pb(II) suitable for X-ray diffraction. Data were collected for these complexes at 100 K on an Agilent Technologies SuperNova Dual Source diffractometer equipped with an AtlasS2 CCD detector using a μ-focus Cu Kα radiation source (λ = 1.5418 Å) and an Oxford 700 Cryostream system. Data collection, unit cell refinement, and data reduction of **1.5** and the metal complexes were performed using Agilent Technologies CrysAlisPro software, and performed by Dr. Leander Cinninger and Dr. Vincent Lynch.[113] The structures were solved by direct methods using

the SIR2014 program and refined by full-matrix least-squares on F2 with anisotropic displacement parameters for all non-H atoms using SHELXL-2014.[114,115] The structural analyses were performed using the PLATON98 and WinGX programs.[116,117] The hydrogen atoms were placed in fixed, calculated positions with isotropic displacement parameters set to 1.2 x Ueq with respect to the attached atom. Crystallographic images were created using the Cambridge Crystallographic Data Centre's Mercury software and rendered using POV-ray.[118] All bond angles, torsion angles, and intermolecular interactions were calculated using the Cambridge Crystallographic Data Centre's Mercury software. Intermolecular interactions were calculated by the Mercury software by looking for atoms within close contact of each other based on their Van der Waal radii +0.15 Å.

**TITRATION STUDIES**

pH titrations were performed using a Mettler Toledo DL77 Titrator. Titrant solutions of aqueous NaOH were standardized in triplicate using potassium hydrogen phthalate from Acros Organics. Samples for analysis were prepared by contacting either **2.47** or **2.50** dissolved in either DCE or Isopar™ L Fluid at 25 mM with the corresponding nitric acid solution for one hour. Analyte solutions were separated from the organic phase and diluted with ca. 20 mL ethanol for each titration. Titrations were performed in triplicate using the LabX® software suite. Stir speed was set to 60 rpm for all experiments. The pH electrode was standardized using pH 4.01, 7.00, and 10.01 buffer solutions from Thermo Fisher Scientific. Before each recording each reading, adequate time was allowed for the electrode to stabilize, up to five minutes for more dilute solutions. Titration end points were determined using second derivative analysis of each titration. For each ligand and diluent, a blank containing no ligand concentration was taken to measure the amount of nitric acid extracted by the solvent.

**SYNTHESIS**

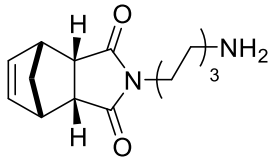

**(3a*R*,4*S*,7*R*,7a*S*)-2-(6-Aminohexyl)-3a,4,7,7a-tetrahydro-1*H*-4,7-methanoisoindole-1,3(2*H*)-dione (1.7) RFFII-98**

A solution of **1.6** (10.0265 g, 61.08 mmol) and 1,6-diaminohexane (21.2934 g, 183.32 mmol) in 300 mL of glacial acetic acid was heated at reflux for 3 hours. The solution was allowed to cool to room temperature and 500 mL water was added. The resulting mixture was extracted with $CH_2Cl_2$ (3x, 500 mL), and the organic layers collected and washed with water (3x, 250 mL). The aqueous layers were combined and neutralized to pH 9 using 1 M NaOH, and extracted with excess $CH_2Cl_2$ (3x, 1.5 L). The organic layers were collected and dried over $Na_2SO_4$. The volatiles were evaporated off under reduced pressure and the residue purified by column chromatography using $CH_2Cl_2$:MeOH:MeCN:TEA (94:2:2:2) as the eluent to give the product as a pale yellow oil (14.258 g, 89%). $^1$H NMR (400 MHz, $CDCl_3$): δ 1.18-1.46 (m, 8H) 1.52 (d, *J* = 8.8, 1H), 1.71 (dt, *J* = 8.9, 1.7, 1H), 2.65 (t, *J* = 6.9, 2H), 3.22 (m, 2H), 3.31 (t, *J* = 7.4, 2H), 3.37 (m, 2H), 6.07 (t, *J* = 1.8, 2H). $^{13}$C {$^1$H} NMR (101 MHz, $CDCl_3$) δ 26.3, 26.6, 27.7, 33.3, 38.3, 42.0, 44.9, 45.7, 52.2, 134.4, 177.7. HRMS (ESI-TOF) m/z: $[M+H]^+$ Calcd for $C_{15}H_{22}N_2O_2$ 263.17540; Found 263.17570.

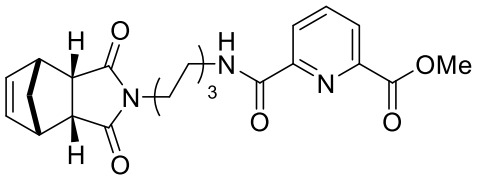

**Methyl 6-((6-((3a*R*,4*S*,7*R*,7a*S*)-1,3-dioxo-1,3,3a,4,7,7a-hexahydro-2*H*-4,7-methanoisoindol-2-yl)hexyl)carbamoyl)picolinate (1.8) RFFII-112**

Precursor **1.7** (10 g, 38.11 mmol) and dimethyl pyridine-2,6-dicarboxylate (11.1581 g, 57.17 mmol) were dissolved in 300 mL of toluene, and 10 mL of acetic acid was added. The solution was heated at reflux for 6 hours, and allowed to cool to room temperature. The volatiles were evaporated off under reduced pressure, and the crude residue was purified by column chromatography using hexanes:ethyl acetate (1:1) as the eluent. The product was isolated as a pale yellow oil (13.1732 g, 81%). $^{1}$H NMR (400 MHz, $CDCl_3$): δ 1.48-1.23 (m, 6H) 1.52 (d, *J* = 8.7, 1H), 1.58-1.74 (m, 3H), 3.23 (m, 2H), 3.31 (t, *J* = 7.3, 2H), 3.37 (m, 2H), 3.46 (q, *J* = 6.8, 2H), 4.01 (s, 3H), 6.09 (t, *J* = 1.8, 2H), 8.00 (t, *J* = 7.8, 1H), 8.12 (t, *J* = 6.1, 1H), 8.21 (dd, *J* = 7.8, 1.1, 1H), 8.39 (dd, *J* = 7.8, 1.1, 1H). $^{13}$C {$^{1}$H} NMR (101 MHz, $CDCl_3$) δ 26.5 26.6, 27.7, 29.5, 38.3, 39.4, 44.9, 45.7, 52.2, 52.9, 125.3, 127.1, 134.4, 138.5, 146.4, 150.3, 163.4, 165.0, 177.8. HRMS (ESI-TOF) m/z: $[M+Na]^+$ Calcd for $C_{23}H_{27}N_3O_5Na$ 448.18430; Found 448.18490.

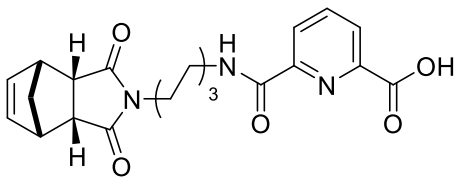

**6-((6-((3a*R*,4*S*,7*R*,7a*S*)-1,3-Dioxo-1,3,3a,4,7,7a-hexahydro-2*H*-4,7-methanoisoindol-2-yl)hexyl)carbamoyl)picolinic acid (1.5) RFFII-4**

Intermediate **1.8** (2.6885 g, 6.32 mmol) and LiOH (0.1564 g, 6.53 mmol) were dissolved in 270 mL of a mixture of $H_2O$/THF (9:1 v/v). This solution was stirred

vigorously for 2.5 hours at room temperature, and was then washed with $CH_2Cl_2$ (3x, 250 mL). The organic layer was discarded, and the aqueous layer was acidified to pH 1 with 2M HCl. This solution was then extracted with $CH_2Cl_2$ (3x, 250 mL), and the organic layer was dried over $Na_2SO_4$. The volatiles were evaporated off under reduced pressure, giving **1.5** as a white solid (2.3050 g, 89%). m.p. 133 °C. $^1$H NMR (400 MHz, $CDCl_3$): δ 1.24 (m, 2H) 1.47-1.61 (m, 5H), 1.67 (q, *J* = 6.1, 2H), 1.77 (dt, *J* = 8.9, 1.8, 1H), 3.37 (m, 2H), 3.37-3.43 (m, 4H), 3.48 (q, *J* = 6.0, 2H), 6.17 (t, *J* = 1.8, 2H), 8.12 (t, *J* = 7.8, 1H), 8.39 (dd, *J* = 7.8, 1.2, 1H), 8.51 (dd, *J* = 7.8, 1.2, 1H), 8.61 (t, *J* = 6.5, 1H). $^{13}$C {$^1$H} NMR (101 MHz, $CDCl_3$) δ 23.9 24.1, 27.2, 28.7, 37.0, 38.0, 45.0, 45.9, 52.5, 126.4, 126.5, 134.5, 139.45, 145.5, 149.6, 163.1, 164.6, 179.3. HRMS (ESI-TOF) m/z: $[M+H]^+$ Calcd for $C_{22}H_{25}N_3O_5$ 412.18670; Found 412.18700.

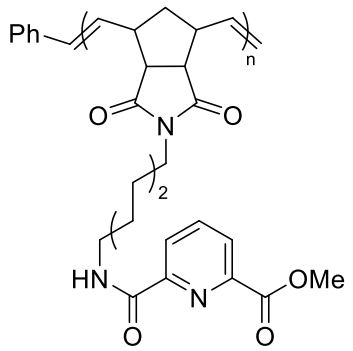


**Poly methyl 6-((6-((3a*R*,4*S*,7*R*,7a*S*)-1,3-dioxo-1,3,3a,4,7,7a-hexahydro-2*H*-4,7-methanoisoindol-2-yl)hexyl)carbamoyl)picolinate (P1.8)**

In a glovebox containing an inert $N_2$ atmosphere, **1.8** was dissolved in dry dichloromethane (0.2 M). To this stirring solution, a desired amount Grubbs 3$^{rd}$ generation catalyst dissolved in dichloromethane (0.02 M) was added, and the solution was allowed to stir overnight (ca. 18 h.). The reaction was then quenched with excess ethyl vinyl ether (ca. 2-3 mL), and allowed to stir for 30 minutes. The solvent was removed *in vacuo*, and

the crude residue redissolved in a minimal quantity of methylene chloride. The polymer was purified by rapidly adding this solution to 50 mL of methanol, and collecting the resulting precipitate. This latter procedure was repeated three times to ensure polymer purity. Yields ranged from 50-90%. $^1$H NMR (400 MHz, $CD_2Cl_2$): δ 1.04-1.64 (b, 10H), 2.85 (b, 1H), 3.15 (b, 3H), 3.38 (b, 4H), 3.29 (s, 4H), 5.45 (b, 1H), 5.62 (b, 1H), 7.96 (t, *J* = 7.6, 1H), 8.13 (b, 2H), 8.28 (b, 1H).

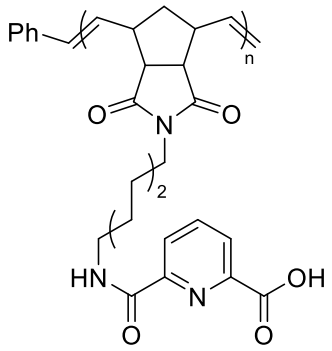


**Poly 6-((6-((3a*R*,4*S*,7*R*,7a*S*)-1,3-Dioxo-1,3,3a,4,7,7a-hexahydro-2*H*-4,7-methanoisoindol-2-yl)hexyl)carbamoyl)picolinic acid (P1.5)**

*Method A:*

In a glovebox containing an inert $N_2$ atmosphere, **1.5** was dissolved in dry DMF (0.2 M). To this stirring solution, a desired amount Grubbs 3$^{rd}$ generation catalyst dissolved in dichloromethane (0.02 M) was added, and the solution was allowed to stir overnight (ca. 18 h). The reaction was then quenched with excess ethyl vinyl ether (ca. 2-3 mL), and allowed to stir for 30 minutes. The volatiles were removed *in vacuo*, and the crude residue redissolved in a minimal quantity of methylene chloride/MeOH (9:1 v/v). The polymer was purified by rapidly adding this solution to 50 mL of diethyl ether, and collecting the resulting precipitate. This latter procedure was repeated three times to ensure polymer

purity. Yields ranged from 50-90%. $^1$H NMR (400 MHz, DMSO-$d_6$): 0.96-1.74 (b, 10H), 3.22 (b, 8H), 5.30 (b, 1H), 5.47 (b, 1H), 8.15 (b, 1H), 9.11 (b, 1H), 12.95 (b, 1H).

*Method B:*

**P1.8** was suspended in a solution of $H_2O$/THF (9:1 v/v, ca. 0.25 M). NaOH (1.05 equivalents) was added, and the solution was stirred vigorously until all of the polymer had dissolved. Small aliquots were taken at this point and the reaction was monitored by NMR spectroscopy, until the complete disappearance of the methyl ester peak was observed (about 3 hours). The reaction mixture was then washed with excess $CH_2Cl_2$, and the aqueous phase was taken to pH 1 with 1 M HCl. The resulting precipitate was filtered and washed with excess $H_2O$, and dried under vacuum, giving a light orange solid. $^1$H NMR (400 MHz, DMSO-$d_6$): 0.94-1.55 (b, 10H), 3.30 (b, 8H), 5.30 (b, 1H), 5.47 (b, 1H), 9.14 (b, 1H) 12.97 (b, 1H).

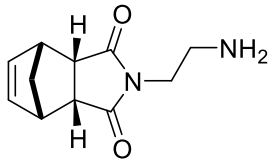


**(3aR,4S,7R,7aS)-2-(2-Aminoethyl)-3a,4,7,7a-tetrahydro-1H-4,7-methanoisoindole-1,3(2H)-dione (1.9) RFFII-180**

A solution of **1.6** (1.0000 g, 6.09 mmol) and ethylene diamine (1.0998 g, 18.3 mmol) in 30 mL of glacial acetic acid was heated at reflux for 3 h. The solution was allowed to cool to room temperature and 50 mL water was added. The resulting mixture was extracted with $CH_2Cl_2$ (3x, 50 mL), and the organic layers collected and washed with water (3x, 50 mL). The aqueous layers were combined and neutralized to pH 9 using 1 M NaOH, and extracted with excess $CH_2Cl_2$ (3x, 50 mL). The organic layers were collected and dried over $Na_2SO_4$. The volatiles were evaporated off under reduced pressure and the residue

purified by column chromatography using $CH_2Cl_2$:MeOH:MeCN:TEA (94:2:2:2) as eluent to give the product as a pale yellow oil (0.5902 g, 47%). $^1$H NMR (400 MHz, $CDCl_3$): δ 1.55 (d, *J* = 8.8 Hz, 1H), 1.74 (d, *J* = 8.8 Hz, 1H), 2.78 (t, *J* = 6.3 Hz, 2H), 3.29 (dd, *J* = 3.0, 1.6 Hz, 0H), 3.39 (dq, *J* = 3.5, 1.7 Hz, 2H), 3.43 (t, *J* = 6.3 Hz, 2H), 6.12 (t, *J* = 1.9 Hz, 2H).

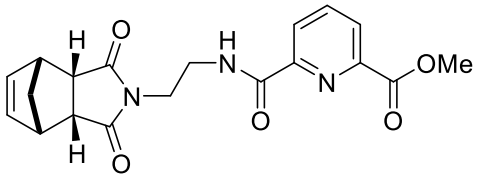


**Methyl 6-((2-((3aR,4S,7R,7aS)-1,3-dioxo-1,3,3a,4,7,7a-hexahydro-2H-4,7-methanoisoindol-2-yl)ethyl)carbamoyl)picolinate (1.10) RFFII-184**

Precursor **1.9** (0.2000 g, 0.970 mmol) and dimethyl pyridine-2,6-dicarboxylate (0.3405 g, 1.74 mmol) were dissolved in 5 mL of toluene, and 3 drop of glacial acetic acid were added. The solution was heated at reflux for 5 h., and allowed to cool to room temperature. The volatiles were evaporated off under reduced pressure, and the crude residue was purified by column chromatography using hexanes:ethyl acetate (1:1). The product was isolated as a pale yellow oil (0.1642 g, 46%). $^1$H NMR (400 MHz, $CDCl_3$): δ 1.47 (dt, *J* = 8.7, 1.5 Hz, 1H), 1.66 (dt, *J* = 8.8, 1.7 Hz, 1H), 3.21 (dd, *J* = 3.0, 1.5 Hz, 2H), 3.30 (dq, *J* = 3.5, 1.7 Hz, 2H), 3.52 (qd, *J* = 5.7, 5.2, 1.2 Hz, 2H), 3.61 (dd, *J* = 6.9, 4.5 Hz, 2H), 6.15 (t, *J* = 1.9 Hz, 2H), 7.94 (t, *J* = 7.8 Hz, 1H), 8.11 (t, *J* = 6.1 Hz, 1H), 8.16 (dd, *J* = 7.8, 1.2 Hz, 1H), 8.29 (dd, *J* = 7.8, 1.2 Hz, 1H). $^{13}$C {$^1$H} NMR (101 MHz, $CDCl_3$) δ 37.9, 37.9, 45.1, 46.0, 52.4, 53.0, 125.5, 127.5, 134.8, 135.5, 138.8, 146.7, 150.0, 163.9, 165.0, 177.9.

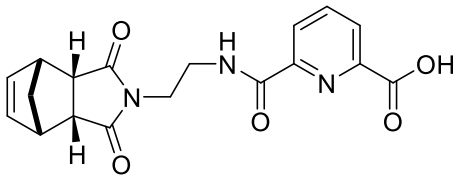

**6-((2-((3aR,4S,7R,7aS)-1,3-Dioxo-1,3,3a,4,7,7a-hexahydro-2H-4,7-methanoisoindol-2-yl)ethyl)carbamoyl)picolinic acid (1.11) RFFII-186**

Precursor **1.10** (0.1642 g, 0.445 mmol) and LiOH (0.0110 g, 0.460 mmol) were dissolved in 18 mL of a mixture of $H_2O$/THF (5:1 v/v). This solution was stirred vigorously for 2 h. at room temperature, and was then washed with $CH_2Cl_2$ (3x, 50 mL). The organic layer was discarded, and the aqueous layer was acidified to pH 1 with 2M HCl. This solution was then extracted with $CH_2Cl_2$ (3x, 50 mL), and the organic layer was dried over $Na_2SO_4$. The volatiles were evaporated off under reduced pressure, giving **1.11** as a white solid (0.1128 g, 71%). $^1$H NMR (400 MHz, $CDCl_3$): δ 1.55 (d, $J$ = 8.9 Hz, 1H), 1.71 (dt, $J$ = 9.0, 1.7 Hz, 1H), 3.33 – 3.43 (m, 4H), 3.47 – 3.56 (m, 2H), 3.72 – 3.83 (m, 2H), 5.95 (t, $J$ = 1.8 Hz, 2H), 8.12 (dd, $J$ = 7.8, 0.6 Hz, 1H), 8.38 (dd, $J$ = 7.8, 0.8 Hz, 2H), 8.82 (s, 1H). $^{13}$C {$^1$H} NMR (101 MHz, $CDCl_3$) δ 37.6, 40.8, 45.3, 46.2, 52.6, 126.2, 126.9, 134.6, 135.5, 140.1, 145.5, 149.0, 163.3, 164.3, 179.6.

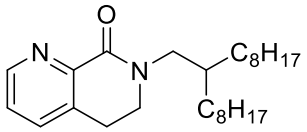

**7-(2-Octyldecyl)-6,7-dihydro-1,7-naphthyridin-8(5H)-one (2.47) RFF-ORNL-85**

6,7-dihydro-1,7-naphthyridin-8(5H)-one (2.5000 g, 17.0 mmol) and sodium hydride as a 60% dispersion in mineral oil (2.0386 g, 51.0 mmol) were dissolved in 90 mL dry DMF under argon atmosphere, and stirred at room temperature for 30 min. Then, 9-(bromomethyl)heptadecane (7.5 mL, 25.6 mmol) was added dropwise via syringe, and the

reaction mixture was heated to 100 °C overnight. Upon cooling, 100 mL of water was added, and the solution was extracted with $Et_2O$ (3x, 250 mL). The organic phase was then washed with water (3x, 250 mL), and dried over $Na_2SO_4$. The volatiles were evaporated off under reduced pressure and the residue purified by column chromatography using $CH_2Cl_2$:Acetone (9:1) as eluent to give the product as a pale yellow oil (5.5125 g, 81%). $^1$H NMR (400 MHz, $CDCl_3$) δ 0.89 (m, 6H), 1.23 – 1.38 (m, 28H), 1.70 – 1.83 (m, 1H), 3.04 (t, *J* = 6.5 Hz, 2H), 3.54 (d, *J* = 7.4 Hz, 2H), 3.58 (t, *J* = 6.5 Hz, 2H), 7.34 (dd, *J* = 7.7, 4.6 Hz, 1H), 7.57 (dd, *J* = 7.7, 1.6 Hz, 1H), 8.72 (dd, *J* = 4.7, 1.6 Hz, 1H). $^{13}$C {$^1$H} NMR (101 MHz, $CDCl_3$) δ 14.1, 22.7, 22.7, 26.5, 27.4, 29.3, 29.3, 29.6, 29.6, 29.6, 30.0, 31.4, 31.9, 31.9, 36.4, 45.6, 51.4, 125.5, 133.8, 135.3, 146.9, 149.1, 163.0. HRMS (ESI-TOF) m/z: $[M+H]^+$ Calcd for $C_{15}H_{22}N_2O_2$ 401.3526; Found 401.3538.

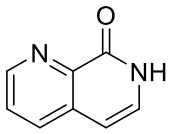


**1,7-Naphthyridin-8(7H)-one (2.49) RFF-ORNL-75**

Compound **2.49** was synthesized according to a literature procedure.[119] 1,7-naphthyridin-8-amine (3.000 g, 20.7 mmol) was dissolved in 30 mL of 6:1 $H_2SO_4$:$H_2O$, and refluxed overnight. The reaction mixture was then poured over ice and neutralized with conc. $NH_4OH$. This solution was extracted with $CHCl_3$ (3x, 250 mL) and 9:1 $CHCl_3$:9:1 $^i$PrOH:conc. $NH_4OH$ (3x, 250 mL), and the organic phases combined and dried over $Na_2SO_4$. The volatiles were removed under reduced pressure, and the resulting crystalline solid recrystallized in water to give **2.49** as light tan crystals (2.4269 g, 80%).

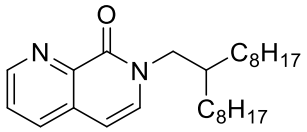

**7-(2-Octyldecyl)-1,7-naphthyridin-8(7H)-one (2.50) RFF-ORNL-61**

Compound **2.49** (1.0877 g, 7.44 mmol) and sodium hydride as a 60% dispersion in mineral oil (0.5358 g, 22.3 mmol) were dissolved in 35 mL dry DMF under argon atmosphere, and stirred at room temperature for 30 min. Then, 9-(bromomethyl)heptadecane (3.25 mL, 11.2 mmol) was added dropwise via syringe, and the reaction mixture was heated to 100 °C overnight. Upon cooling, 100 mL of water was added, and the solution was extracted with $Et_2O$ (3x, 150 mL). The organic phase was then washed with water (3x, 150 mL), and dried over $Na_2SO_4$. The volatiles were evaporated off under reduced pressure and the residue purified by column chromatography using a gradient of hexanes and ethyl acetate as eluent to give the product as a pale yellow oil (2.1692 g, 73%). $^1$H NMR (400 MHz, $CDCl_3$) δ 0.88 (t, *J* = 6.9 Hz, 6H), 1.17 – 1.44 (m, 28H), 2.01 (q, *J* = 6.5 Hz, 1H), 3.97 (d, *J* = 7.4 Hz, 2H), 6.42 (d, *J* = 7.3 Hz, 1H), 7.13 (d, *J* = 7.3 Hz, 1H), 7.54 (dd, *J* = 8.1, 4.4 Hz, 1H), 7.88 (dd, *J* = 8.1, 1.7 Hz, 1H), 8.89 (dd, *J* = 4.4, 1.7 Hz, 1H).

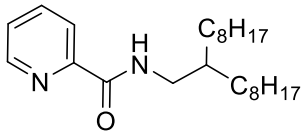

**N-(2-Octyldecyl)picolinamide (2.55) RFF-ORNL-81**

The requisite amine starting material was synthesized via a Gabriel synthesis. 9-(Bromomethyl)heptadecane (8.8 mL, 30.0 mmol) and potassium phthalimide (5.9259 g, 32.0 mmol) were dissolved in 45 mL dry DMF and heated at 90 °C overnight. The reaction mixture was allowed to cool to room temperature and 50 mL water was added.

The solution was extracted with $Et_2O$ (3x, 300 mL) and the organic phases were combined and washed with water (3x 300 mL). The volatiles were evaporated off under reduced pressure and the residue purified on a silica gel plug using hexanes:ethyl acetate (4:1) as eluent to give the product as a pale yellow oil. This product was then dissolved in 100 mL MeOH with hydrazine hydrate (4.38 mL, 90.0 mmol), and the solution was refluxed overnight. The solvent was then removed, and the resulting oil was taken up in excess $CH_2Cl_2$ and washed with 0.1 M KOH and brine (250 mL). The organic phase was dried over $Na_2SO_4$ and evaporated to dryness, give the requisite primary amine as a clear oil. This amine (5.2400 g, 19.5 mmol) and methyl picolinate (1.56 mL, 13.0 mmol) were dissolved in 100 mL toluene and 3.5 mL glacial acetic acid, and the reaction mixture was refluxed overnight. The volatiles were evaporated off under reduced pressure and the residue purified by column chromatography using Hexanes:Ethyl acetate (4:1) as eluent to give the product as a pale yellow oil (4.4687 g, 92%). $^1$H NMR (400 MHz, $CDCl_3$) δ 0.82 – 0.96 (m, 6H), 1.19 – 1.43 (m, 28H), 1.59 – 1.71 (m, 1H), 3.42 (t, $J$ = 6.1 Hz, 2H), 7.44 (ddd, $J$ = 7.6, 5.1, 1.2 Hz, 1H), 7.87 (td, $J$ = 7.7, 1.7 Hz, 1H), 8.12 (t, $J$ = 6.1 Hz, 1H), 8.23 (d, $J$ = 7.8 Hz, 1H), 8.57 (dd, $J$ = 5.0, 1.5 Hz, 1H). $^{13}$C NMR (101 MHz, $CDCl_3$) δ 14.1, 22.7, 26.7, 29.3, 29.6, 30.0, 31.9, 31.9, 38.1, 42.8, 122.3, 126.0, 137.5, 147.8, 150.0, 164.1.

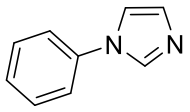


**1-Phenyl-1H-imidazole (3.2) RFFIII-94**

Compound **3.2** was purified by column chromatography using methylene chloride:ethyl acetate (3:1). The product was isolated as a pale yellow oil (4.4693 g,

31%). $^1$H NMR (300 MHz, $CDCl_3$) δ 7.23 (q, $J$ = 1.0 Hz, 1H), 7.31 (q, $J$ = 1.6 Hz, 1H), 7.33 – 7.48 (m, 3H), 7.44 – 7.58 (m, 2H), 7.88 (s, 1H).

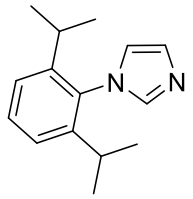

**1-(2,6-Diisopropylphenyl)-1H-imidazole (3.3) RFFIII-269**

Compound **3.3** was purified by column chromatography using methylene chloride:ethyl acetate (3:1). The product was isolated as an off-white solid (0.9735 g, 43%). $^1$H NMR (400 MHz, $CDCl_3$) δ 1.10 (d, $J$ = 6.9 Hz, 12H), 2.38 (d, $J$ = 6.7 Hz, 2H), 6.92 (s, 1H), 7.16 – 7.28 (m, 3H), 7.36 – 7.47 (m, 2H).

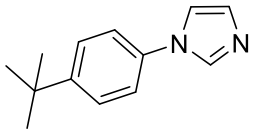

**1-(4-(Tert-butyl)phenyl)-1H-imidazole (3.4) RFFIII-275**

Compound **3.4** was purified by column chromatography using methylene chloride:ethyl acetate (9:1). The product was isolated as a pale yellow oil (0.6832 g, 34%). $^1$H NMR (400 MHz, $CDCl_3$) δ 1.35 (s, 9H), 7.19 (t, $J$ = 1.1 Hz, 1H), 7.26 (d, $J$ = 1.5 Hz, 1H), 7.29 – 7.34 (m, 2H), 7.45 – 7.52 (m, 2H), 7.82 (t, $J$ = 1.1 Hz, 1H).

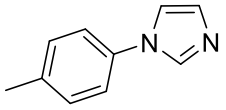

**1-(p-Tolyl)-1H-imidazole (3.5) RFFIII-276**

Compound **3.5** was purified by column chromatography using methylene chloride:ethyl acetate (9:1). The product was isolated as a pale yellow oil (0.6539 g,

41%). $^{1}$H NMR (400 MHz, $CDCl_3$) δ 2.39 (s, 3H), 7.18 (t, *J* = 1.2 Hz, 1H), 7.24 (t, *J* = 1.3 Hz, 1H), 7.26 (s, 4H), 7.80 (t, *J* = 1.2 Hz, 1H).

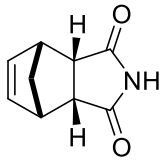


**(3aR,4S,7R,7aS)-3a,4,7,7a-Tetrahydro-1H-4,7-methanoisoindole-1,3(2H)-dione (3.6) RFFI-287**

(3aR,4S,7R,7aS)-3a,4,7,7a-Tetrahydro-4,7-methanoisobenzofuran-1,3-dione (5.7910 g, 35.28 mmol) and urea (4.2374 g, 70.553 mmol) were heated to 145 °C for 4 hours. Water (36 mL) was added, and the solution was heated until it turned clear. The clear solution was then allowed to cool, and the resulting pale brown crystals were collected by vacuum filtration, and washed with cold water to give **3.6** as a light brown solid (4.7608 g, 83%). m.p. 186 °C; $^{1}$H NMR (400 MHz, $CDCl_3$): δ 1.51 (d, *J* = 8.8, 1H), 1.74 (dt, *J* = 8.8, 1.6, 1H), 3.30 (m, 2H), 3.37 (m, 2H), 6.19 (t, *J* = 1.8, 1H), 8.05 (s, 1H); $^{13}$C {$^{1}$H} NMR (101 MHz, $CDCl_3$) δ 44.9, 47.3, 52.3, 134.6, 178.3.

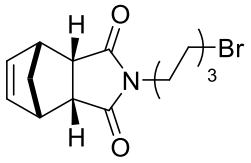


**(3aR,4S,7R,7aS)-2-(6-Bromohexyl)-3a,4,7,7a-tetrahydro-1H-4,7-methanoisoindole-1,3(2H)-dione (3.7) RFFII-144**

Compound **3.6** (0.8078 g, 4.95 mmol), potassium carbonate (6.8416 g, 49.5 mmol), and 1,6-dibromohexane (12.0774 g, 49.5 mmol) were dissolved in 100 mL dry DMF and heated to 50 °C for 6 h.. The volatiles were evaporated off under reduced

pressure, and the crude residue was purified by column chromatography using hexanes:ethyl acetate (2:1). The product was isolated as a clear colorless oil (1.4312 g, 83%). $^1$H NMR (400 MHz, $CDCl_3$): δ 1.21 – 1.30 (m, 2H), 1.37 – 1.48 (m, 4H), 1.53 (dt, *J* = 8.8, 1.6 Hz, 1H), 1.72 (dt, *J* = 8.8, 1.8 Hz, 1H), 1.82 (dq, *J* = 8.7, 6.8, 5.8 Hz, 2H), 3.23 (dd, *J* = 2.9, 1.5 Hz, 2H), 3.31 (dd, *J* = 8.0, 6.7 Hz, 2H), 3.34 – 3.45 (m, 2H), 6.08 (t, *J* = 1.9 Hz, 2H).

*General procedure for the synthesis of N-aryl imidazoles:*

Aryl aniline (1 eq.) and glyoxal (40%, 1 eq.) were dissolved in MeOH (2M) and allowed to stir at room temperature overnight. The solution was then diluted with MeOH (0.2 M) and $NH_4Cl$ (2 equiv.) and formaldehyde (40%, 2 equiv.) were added, and the mixture was refluxed for 1 h. $H_3PO_4$ (85%, 3 eq.) was added dropwise to the refluxing mixture over 10 min., and the reaction was allowed to reflux overnight. The reaction was allowed to cool, and the volatiles were evaporated off under reduced pressure. Ice was added to the crude residue, and a solution of KOH (40%) was added until a pH = 9 was achieved. This solution was extracted with $Et_2O$ (3x 150 mL), and the organic phases were combined and dried over $Na_2SO_4$. The volatiles were evaporated off under reduced pressure, and the crude residue was purified by column chromatography to give the desired N-aryl imidazole.

*General procedure for the synthesis of norbornene functionalized N-aryl imidazolium bromides:*

**3.7** (1 equiv.) and the desired N-aryl imidazole were dissolved in THF (1 M) and heated to 90 °C overnight. The crude residue was purified by column chromatography using silica gel previously soaked in 6% NaBr in MeOH. The desired product was typically obtained as the second band off of the column.

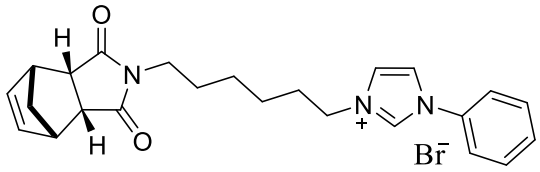

**3-(6-((3aR,4S,7R,7aS)-1,3-Dioxo-1,3,3a,4,7,7a-hexahydro-2H-4,7-methanoisoindol-2-yl)hexyl)-1-phenyl-1H-imidazol-3-ium bromide (3.8) RFFII-159**

Compound **3.8** was purified by column chromatography using methylene chloride:MeOH (95:5). The product was isolated as an off-white foam (0.2729 g, 84%). $^1$H NMR (400 MHz, $CDCl_3$): δ 1.08 – 1.37 (m, 6H), 1.43 (d, *J* = 8.9 Hz, 1H), 1.59 (dt, *J* = 8.8, 1.7 Hz, 1H), 1.88 (p, *J* = 7.3 Hz, 2H), 3.09 – 3.26 (m, 6H), 4.47 (t, *J* = 7.2 Hz, 2H), 5.95 (t, *J* = 1.9 Hz, 2H), 7.35 – 7.50 (m, 3H), 7.73 (d, *J* = 8.0 Hz, 2H), 7.77 (t, *J* = 1.8 Hz, 1H), 7.87 (t, *J* = 1.9 Hz, 1H), 10.77 (d, *J* = 1.7 Hz, 1H).

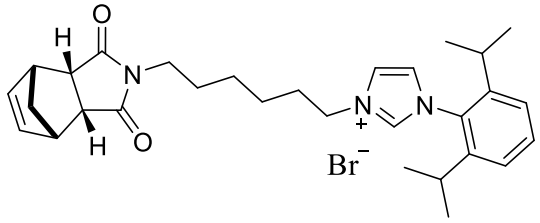

**1-(2,6-Diisopropylphenyl)-3-(6-((3a*R*,4*S*,7*R*,7a*S*)-1,3-dioxo-1,3,3a,4,7,7a-hexahydro-2*H*-4,7-methanoisoindol-2-yl)hexyl)-1*H*-imidazol-3-ium bromide (3.9) RFFIII-290**

Compound **3.9** was purified by column chromatography using methylene chloride:MeOH (95:5). The product was isolated as an off-white foam (0.9110 g, 60%). $^1$H NMR (400 MHz, $CDCl_3$): δ 1.12 (d, *J* = 6.8 Hz, 5H), 1.20 (d, *J* = 6.8 Hz, 5H), 1.23 – 1.45 (m, 4H), 1.51 (d, *J* = 8.7 Hz, 1H), 1.69 (dt, *J* = 8.8, 1.6 Hz, 1H), 1.96 (p, *J* = 7.2 Hz, 2H), 2.25 (hept, *J* = 6.8 Hz, 2H), 3.23 (dd, *J* = 2.9, 1.6 Hz, 2H), 3.26 (t, 2H), 3.33 (dq, *J* = 3.3, 1.7 Hz, 2H), 4.77 (t, *J* = 7.1 Hz, 1H), 6.04 (t, *J* = 1.8 Hz, 3H), 7.19 (t, *J* = 1.8 Hz, 1H), 7.27 (d, *J* = 7.9 Hz, 9H), 7.50 (t, *J* = 7.8 Hz, 1H), 7.94 (t, *J* = 1.7 Hz, 1H), 10.43 (t, *J* = 1.5

Hz, 1H); $^{13}C$ {$^{1}H$} NMR (101 MHz, $CDCl_3$): δ 24.3, 24.4, 25.3, 26.1, 27.4, 28.7, 30.4, 37.8, 44.8, 45.7, 50.2, 52.2, 122.9, 124.2, 124.64, 130.1, 131.9, 134.4, 138.4, 145.3, 177.7; HRMS (ESI-TOF) m/z: $[M]^+$ Calcd for $C_{30}H_{40}N_3O_2$ 474.31150; Found 474.31190.

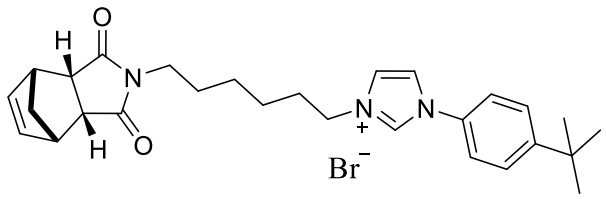


**1-(4-(Tert-butyl)phenyl)-3-(6-((3a*R*,4*S*,7*R*,7a*S*)-1,3-dioxo-1,3,3a,4,7,7a-hexahydro-2*H*-4,7-methanoisoindol-2-yl)hexyl)-1*H*-imidazol-3-ium bromide (3.10) RFFIII-298**

Compound **3.10** was purified by column chromatography using methylene chloride:MeOH (95:5). The product was isolated as a clear tacky solid (0.6506 g, 59%). $^{1}H$ NMR (400 MHz, $CDCl_3$) δ 1.49-1.28 (m, 15H), 1.52 (d, *J*=8.8 Hz, 1H), 1.71 (dt, *J*=8.7, 1.6 Hz, 1H), 1.98 (p, *J*=7.4 Hz, 2H), 7.54 (t, *J*=1.7 Hz, 1H), 7.46 (t, *J*=1.7 Hz, 1H), 6.06 (t, *J*=1.8 Hz, 2H), 4.61 (t, *J*=7.2 Hz, 1H), 3.33 (dq, *J*=3.3, 1.7 Hz, 2H), 3.31-3.24 (m, 4H), 7.58 (dt, *J*=8.8, 2.4 Hz, 2H), 7.70 (dt, *J*=8.8, 2.4 Hz, 2H), 11.22 (s, 1H); $^{13}C$ NMR (101 MHz, $CDCl_3$) δ 25.2, 25.9, 27.2, 30.0, 31.0, 34.7, 37.7, 44.7, 45.6, 50.0, 52.1, 120.9, 121.2, 123.3, 127.2, 131.9, 134.2, 135.1, 153.4, 177.7; HRMS (ESI-TOF) m/z: $[M]^+$ Calcd for $C_{28}H_{36}N_3O_2$ 446.28020; Found 446.28090.

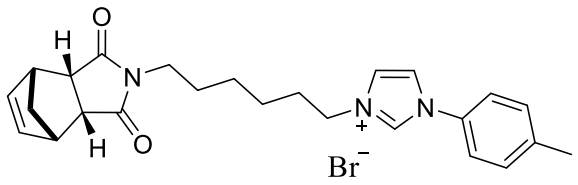

**3-(6-((3a*R*,4*S*,7*R*,7a*S*)-1,3-dioxo-1,3,3a,4,7,7a-hexahydro-2*H*-4,7-methanoisoindol-2-yl)hexyl)-1-(p-tolyl)-1*H*-imidazol-3-ium bromide (3.11) RFFIII-299**

Compound **3.11** was purified by column chromatography using methylene chloride:MeOH (95:5). The product was isolated as a clear tacky solid (0.8233 g, 70%). $^{1}$H NMR (400 MHz, $CDCl_3$): δ 1.24-1.00 (m, 6H), 1.32 (d, *J*, 8.7 Hz, 1H), 1.46 (dt, *J* = 8.8, 1.5 Hz, 1H), 1.76 (p, *J* = 7.4 Hz, 2H), 2.15 (s, 3H), 3.10-2.99 (m, 6H), 4.32 (t, *J* = 7.2 Hz, 2H), 5.82 (t, *J* = 1.8 Hz, 2H), 7.09 (d, *J* = 8.2 Hz, 2H), 7.47 (d, *J* = 8.5 Hz, 2H), 7.71 (t, *J* = 1.8 Hz, 1H), 7.74 (t, *J* = 1.9 Hz, 1H), 10.38 (s, 1H); $^{13}$C NMR (101 MHz, $CDCl_3$) δ 21.0, 25.2, 25.8, 27.1, 29.9, 37.7, 44.6, 45.5, 49.9, 52.0, 120.9, 121.4, 123.4, 130.7, 132.0, 134.4, 134.9, 140.1, 177.7; HRMS (ESI-TOF) m/z: $[M]^+$ Calcd for $C_{25}H_{30}N_3O_2$ 404.23330; Found 404.23350.

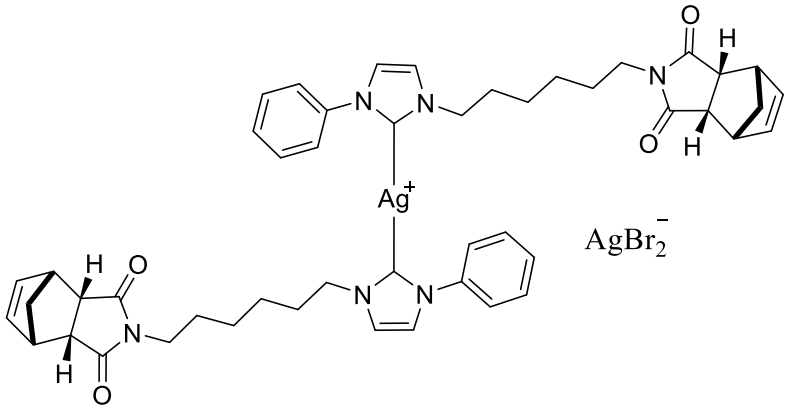


**Bis(1-(6-((3aR,4S,7R,7aS)-1,3-dioxo-1,3,3a,4,7,7a-hexahydro-2H-4,7-methanoisoindol-2-yl)hexyl)-3-phenyl-2,3-dihydro-1H-imidazol-2-yl)silver(I) dibromoargenate(I) (3.12) RFFII-197**

Compound **3.8** (0.1000 g, .213 mmol) and silver(I) oxide (0.0246 g, 0.106 mmol) were dissolved in 2 mL methylene chloride. The reaction vessel was covered with foil and the reaction was allowed to stir at room temperature overnight. The reaction mixture was filtered and the volatiles were evaporated under reduced pressure, giving **3.12** as an off-white solid; complete conversion inferred from the disappearance of the C2 proton at ca. 9 ppm in the $^1$H NMR spectrum (0.0794 g, 59%). $^1$H NMR (400 MHz, $CDCl_3$): δ 1.23 – 1.37 (m, 4H), 1.36 – 1.48 (m, 2H), 1.54 (dt, *J* = 8.8, 1.5 Hz, 1H), 1.69 (dt, *J* = 8.7, 1.8 Hz, 1H), 1.84 (p, *J* = 7.3 Hz, 2H), 3.24 (dd, *J* = 3.0, 1.6 Hz, 2H), 3.28 (dd, *J* = 8.0, 6.7 Hz, 2H), 3.33 (dp, *J* = 3.4, 1.7 Hz, 2H), 6.07 (t, *J* = 1.9 Hz, 2H), 7.24 (d, *J* = 1.8 Hz, 1H), 7.35 (d, *J* = 1.9 Hz, 1H), 7.46 – 7.65 (m, 5H).

*General procedure for the synthesis of norbornene functionalized N-aryl imidazolium hexafluorophosphates:*

The desired imidazolium bromide (1 equiv.) and potassium hexafluorophosphate (50 equiv.) were dissolved in methylene chloride (0.035 M) and stirred at room temperature overnight. The reaction mixture was filtered, washed with excess water, and the organic

phase was dried over $Na_2SO_4$. The volatiles were evaporated off under reduced pressure to give the desired hexafluorophosphate salt. Salt metathesis was inferred from an $^{19}F$ NMR spectroscopic analysis.

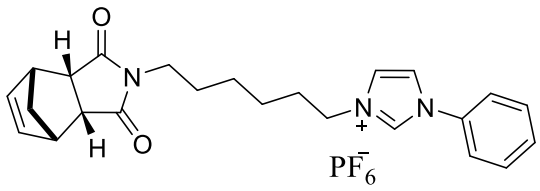

**3-(6-((3aR,4S,7R,7aS)-1,3-Dioxo-1,3,3a,4,7,7a-hexahydro-2H-4,7-methanoisoindol-2-yl)hexyl)-1-phenyl-1H-imidazol-3-ium hexafluorophosphate (3.13) RFFII-170**

Compound **3.13** was isolated as a white foam (1.1413 g, 99%). $^1H$ NMR (400 MHz, $CDCl_3$): δ 1.20 – 1.49 (m, 6H), 1.49 – 1.57 (m, 1H), 1.71 (dt, *J* = 8.8, 1.7 Hz, 1H), 1.90 (p, *J* = 7.5 Hz, 2H), 3.22 – 3.31 (m, 4H), 3.33 (dq, *J* = 3.3, 1.7 Hz, 2H), 4.27 (t, *J* = 7.4 Hz, 2H), 6.06 (t, *J* = 1.9 Hz, 2H), 7.49 (t, *J* = 1.8 Hz, 1H), 7.51 – 7.62 (m, 6H), 8.92 (t, *J* = 1.7 Hz, 1H).

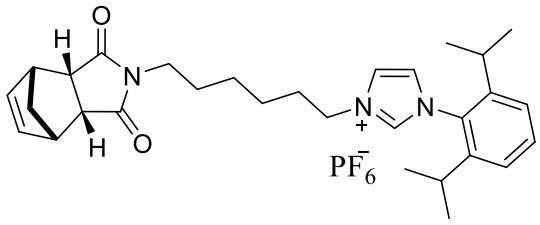

**1-(2,6-Diisopropylphenyl)-3-(6-((3aR,4S,7R,7aS)-1,3-dioxo-1,3,3a,4,7,7a-hexahydro-2H-4,7-methanoisoindol-2-yl)hexyl)-1H-imidazol-3-ium hexafluorophosphate (3.14) RFFIV-1**

Compound **3.14** was isolated as a white foam (0.5843 g, 86%). $^1H$ NMR (400 MHz, $CDCl_3$): δ 1.05 (d, *J* = 6.8 Hz, 12H), 1.12 – 1.37 (m, 6H), 1.44 (d, *J* = 8.7 Hz, 1H), 1.59 (d, *J* = 7.4 Hz, 1H), 1.83 (p, *J* = 7.3 Hz, 2H), 2.16 (hept, *J* = 6.7 Hz, 2H), 3.14 – 3.24 (m, 6H),

4.26 (t, $J$ = 7.2 Hz, 2H), 5.95 (t, $J$ = 1.8 Hz, 2H), 7.19 – 7.25 (m, 3H), 7.45 (t, $J$ = 7.8 Hz, 1H), 7.61 (t, $J$ = 1.7 Hz, 1H), 8.56 (t, $J$ = 1.4 Hz, 1H); $^{13}$C {$^{1}$H} NMR (101 MHz, $CDCl_3$): δ 23.9, 24.0, 25.2, 25.8, 27.3, 28.5, 29.9, 37.7, 44.7, 45.6, 50.2, 52.1, 53.6, 123.2, 124.5, 125.1, 129.9, 131.9, 134.3, 136.2, 145.3, 177.8; $^{19}$F NMR (376 MHz, $CDCl_3$): δ -72.08 (d, $J$ = 712.7 Hz); HRMS (ESI-TOF) m/z: $[M]^+$ Calcd for $C_{30}H_{40}N_3O_2$ 474.31205; Found 474.31190.

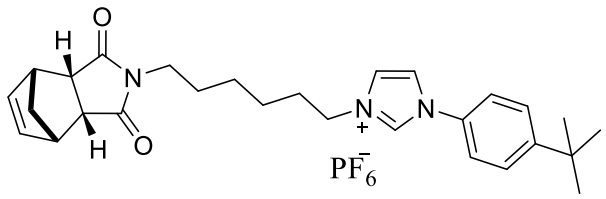


**3-(4-(Tert-butyl)phenyl)-1-(6-((3a*R*,4*S*,7*R*,7a*S*)-1,3-dioxo-1,3,3a,4,7,7a-hexahydro-2*H*-4,7-methanoisoindol-2-yl)hexyl)-1*H*-imidazol-3-ium hexafluorophosphate (3.15) RFFIII-292**

**3.15** was isolated as a clear tacky solid (0.5639 g, 77%). $^{1}$H NMR (400 MHz, $CDCl_3$): δ 1.15 – 1.40 (m, 5H), 1.46 (d, $J$ = 8.6 Hz, 0H), 1.61 (d, $J$ = 8.7 Hz, 0H), 1.86 (p, $J$ = 7.5 Hz, 1H), 3.12 – 3.24 (m, 26H), 4.24 (t, $J$ = 7.3 Hz, 1H), 7.44 – 7.52 (m, 1H); $^{13}$C {$^{1}$H} NMR (101 MHz, $CDCl_3$): δ 25.2, 25.8, 27.2, 29.7, 31.1, 34.9, 37.7, 44.7, 45.6, 50.2, 52.1, 121.6, 121.6, 123.3, 127.4, 132.0, 133.5, 134.3, 153.9, 177.9; $^{19}$F NMR (376 MHz, $CDCl_3$): δ -71.93 (d, $J$=712.7 Hz); HRMS (ESI-TOF) m/z: $[M]^+$ Calcd for $C_{28}H_{36}N_3O_2$ 446.28020; Found 46.28040.

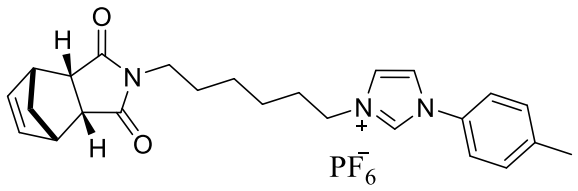

**3-(6-((3a*R*,4*S*,7*R*,7a*S*)-1,3-Dioxo-1,3,3a,4,7,7a-hexahydro-2*H*-4,7-methanoisoindol-2-yl)hexyl)-1-(p-tolyl)-1*H*-imidazol-3-ium hexafluorophosphate (3.16) RFFIII-293**

Compound **3.16** was isolated as a clear tacky solid (0.730 g, 79%). $^{1}$H NMR (400 MHz, $CDCl_3$): δ 1.15 – 1.43 (m, 2H), 1.48 (d, *J* = 8.7 Hz, 1H), 1.64 (d, *J* = 8.7 Hz, 1H), 1.85 (p, *J* = 7.6 Hz, 2H), 3.16 – 3.28 (m, 3H), 4.21 (t, *J* = 7.4 Hz, 1H), 6.00 (t, *J* = 1.7 Hz, 2H), 7.28 (d, *J* = 8.3 Hz, 1H), 7.41 (d, *J* = 8.5 Hz, 1H), 7.50 (t, *J* = 1.8 Hz, 1H), 7.59 (t, *J* = 1.8 Hz, 1H), 8.83 (t, *J* = 1.4 Hz, 1H); $^{13}$C NMR (101 MHz, $CDCl_3$) δ 21.0, 25.3, 25.8, 27.22, 29.7, 37.7, 44.8, 45.6, 50.2, 52.2, 121.54, 121.8, 123.2, 130.9, 132.1, 133.5, 134.3, 140.8, 177.9; $^{19}$F NMR (376 MHz, $CDCl_3$) δ -71.94 (d, *J*=712.7 Hz); HRMS (ESI-TOF) m/z: $[M]^+$ Calcd for $C_{25}H_{30}N_3O_2$ 404.23330; Found 404.23370.

*General procedure for the synthesis of silver (I) complexes with norbornene functionalized N-aryl imidazolium hexafluorophosphates:*

The hexafluorophosphate salt (1 equiv.) and silver(I) oxide (2 equiv.) were dissolved in MeCN (0.04 M) and 1 M NaOH (10 eq.). The reaction vessel was covered with foil and the reaction was allowed to stir at room temperature overnight. The reaction mixture was filtered and the volatiles were evaporated under reduced pressure giving the desired product. Complete conversion was inferred from the disappearance of the C2 proton at ca. 9 ppm in the $^{1}$H NMR spectrum.

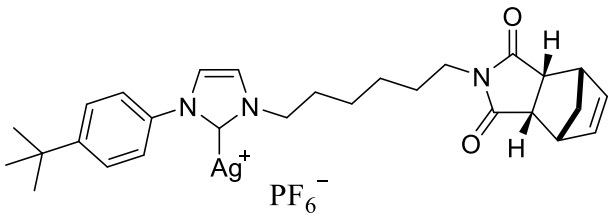

**(1-(4-(Tert-butyl)phenyl)-3-(6-((3a*R*,4*S*,7*R*,7a*S*)-1,3-dioxo-1,3,3a,4,7,7a-hexahydro-2*H*-4,7-methanoisoindol-2-yl)hexyl)-2,3-dihydro-1*H*-imidazol-2-yl)silver(I) hexafluorophosphate (3.17) RFFIII-295**

Compound **3.17** was isolated as an off-white solid (0.1113 g, 63%). $^{1}$H NMR (400 MHz, $CDCl_3$): δ 1.15 – 1.41 (m, 3H), 1.52 (d, J = 8.8 Hz, 0H), 1.69 (dt, *J* = 8.8, 1.7 Hz, 0H), 3.20 – 3.26 (m, 1H), 3.33 (dq, *J* = 3.5, 1.7 Hz, 1H), 4.02 (t, *J* = 7.0 Hz, 1H), 6.02 (t, *J* = 1.8 Hz, 1H), 7.24 – 7.29 (m, 1H), 7.38 (d, *J* = 8.7 Hz, 0H), 7.44 (d, *J* = 8.8 Hz, 1H); $^{13}$C {$^{1}$H} NMR (101 MHz, $CDCl_3$): δ 25.9, 26.3, 27.4, 31.3, 34.8, 37.9, 44.8, 45.7, 52.1, 52.2, 53.5, 122.1, 123.5, 123.7, 126.7, 134.4, 137.5, 152.3, 177.7. Carbene carbon missing; $^{19}$F NMR (376 MHz, $CDCl_3$) δ -73.27 (d, *J* = 712.7 Hz); HRMS (ESI-TOF) m/z: $[M]^+$ Calcd for $C_{28}H_{35}AgN_3O_2$ 552.17750; Found 552.17720.

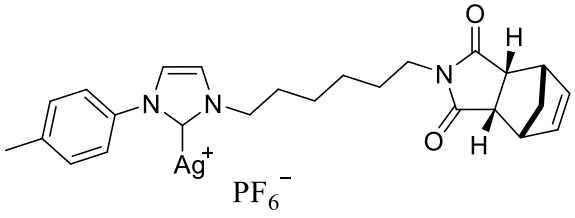

**(1-(6-((3a*R*,4*S*,7*R*,7a*S*)-1,3-Dioxo-1,3,3a,4,7,7a-hexahydro-2*H*-4,7-methanoisoindol-2-yl)hexyl)-3-(p-tolyl)-2,3-dihydro-1*H*-imidazol-2-yl)silver(I) hexafluorophosphate (3.18) RFFIII-296**

Compound **3.18** was isolated as an off-white solid (0.0984 g, 61%). $^{1}$H NMR (400 MHz, $CDCl_3$): δ 1.14 – 1.26 (m, 4H), 1.31 – 1.40 (m, 2H), 1.52 (dt, *J* = 8.9, 1.5 Hz, 1H), 1.64 – 1.77 (m, 3H), 2.38 (s, 3H), 3.18 – 3.27 (m, 4H), 3.32 (m, 2H), 4.00 (t, *J* = 7.2 Hz,

2H), 6.02 (t, $J$ = 1.9 Hz, 2H), 7.12 – 7.44 (m, 6H); $^{13}C$ {$^{1}H$} NMR (101 MHz, $CDCl_3$) δ 21.1, 25.9, 26.3, 27.4, 31.2, 37.9, 44.8, 45.7, 52.2, 53.4, 122.2, 124.0, 130.2, 134.4, 137.5, 139.1, 177.7. Carbene carbon missing; $^{19}F$ NMR (376 MHz, $CDCl_3$) δ -73.21 (d, $J$ = 712.6 Hz); HRMS (ESI-TOF) m/z: $[M]^+$ Calcd for $C_{25}H_{29}AgN_3O_2$ 510.13050; Found 510.13060.

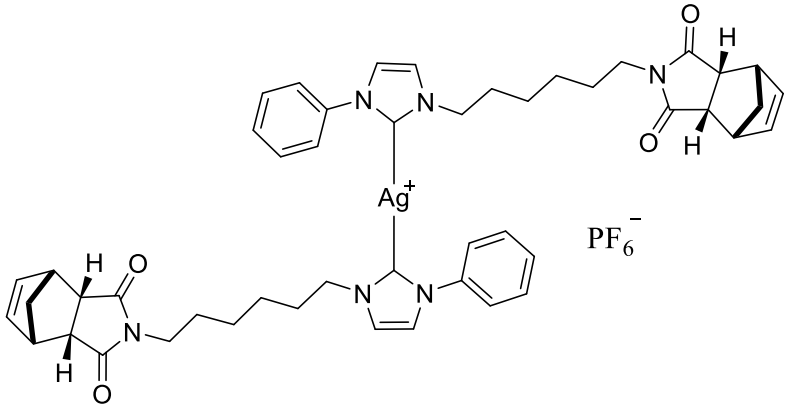


**Bis(1-(6-((3aR,4S,7R,7aS)-1,3-dioxo-1,3,3a,4,7,7a-hexahydro-2H-4,7-methanoisoindol-2-yl)hexyl)-3-phenyl-2,3-dihydro-1H-imidazol-2-yl)silver(I) hexafluorophosphate (3.19) RFFII-204**

Compound **3.19** was isolated as an off-white solid (0.0272 g, 92%). $^{1}H$ NMR (400 MHz, $CDCl_3$): δ 1.23 – 1.37 (m, 4H), 1.36 – 1.48 (m, 2H), 1.54 (dt, $J$ = 8.8, 1.5 Hz, 1H), 1.69 (dt, $J$ = 8.7, 1.8 Hz, 1H), 1.84 (p, $J$ = 7.3 Hz, 2H), 3.24 (dd, $J$ = 3.0, 1.6 Hz, 2H), 3.28 (dd, $J$ = 8.0, 6.7 Hz, 2H), 3.33 (dp, $J$ = 3.4, 1.7 Hz, 2H), 6.07 (t, $J$ = 1.9 Hz, 2H), 7.24 (d, $J$ = 1.8 Hz, 1H), 7.35 (d, $J$ = 1.9 Hz, 1H), 7.46 – 7.65 (m, 5H).

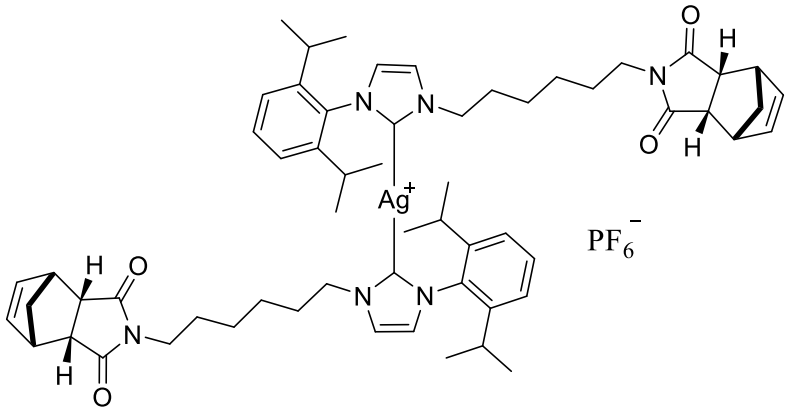


**Bis(1-(2,6-diisopropylphenyl)-3-(6-((3aR,4S,7R,7aS)-1,3-dioxo-1,3,3a,4,7,7a-hexahydro-2H-4,7-methanoisoindol-2-yl)hexyl)-2,3-dihydro-1H-imidazol-2-yl)silver(I) hexafluorophosphate (3.20) RFFIII-289**

Compound **3.20** was isolated as an off-white solid (0.0760 g, 65%). $^{1}$H NMR (400 MHz, $CDCl_3$): δ 1.05 (d, *J* = 6.8 Hz, 12H), 1.12 – 1.37 (m, 6H), 1.44 (d, *J* = 8.7 Hz, 1H), 1.59 (d, *J* = 7.4 Hz, 1H), 1.83 (p, *J* = 7.3 Hz, 2H), 2.16 (hept, *J* = 6.7 Hz, 2H), 3.14 – 3.24 (m, 6H), 4.26 (t, *J* = 7.2 Hz, 2H), 5.95 (t, *J* = 1.8 Hz, 2H), 7.19 – 7.25 (m, 3H), 7.45 (t, *J* = 7.8 Hz, 1H), 7.61 (t, *J* = 1.7 Hz, 1H), 8.56 (t, *J* = 1.4 Hz, 1H); $^{13}$C {$^{1}$H} NMR (101 MHz, $CDCl_3$): δ 23.9, 24.0, 25.2, 25.8, 27.3, 28.5, 29.9, 37.7, 44.7, 45.6, 50.2, 52.1, 53.6, 123.2, 124.5, 125.1, 129.9, 131.9, 134.3, 136.2, 145.3, 177.8. Carbene carbon missing; $^{19}$F NMR (376 MHz, $CDCl_3$): δ -72.08 (d, *J* = 712.7 Hz); HRMS (ESI-TOF) m/z: $[M]^+$ Calcd for $C_{30}H_{40}N_3O_2$ 474.31205; Found 474.31190.

**CRYSTALLOGRAPHIC DATA**

**Table 4.1**: Crystal data and structure refinement for **1.5** complexed with Cu(II)

| | |
|---|---|
| Empirical formula | C44 H52 Cu N6 O12 |
| Formula weight | 920.45 |
| Temperature | 100(2) K |

| | | |
|---|---|---|
| Wavelength | 1.54184 Å | |
| Crystal system | Monoclinic | |
| Space group | P 21/n | |
| Unit cell dimensions | a = 11.3467(4) Å | α= 90°. |
| | b = 32.3727(12) Å | β= 108.319(4)°. |
| | c = 13.0107(4) Å | γ= 90°. |
| Volume | 4536.9(3) $Å^3$ | |
| Z | 4 | |
| Density (calculated) | 1.348 $Mg/m^3$ | |
| Absorption coefficient | 1.247 $mm^{-1}$ | |
| F(000) | 1932 | |
| Crystal size | 0.4422 x 0.0824 x 0.0333 $mm^3$ | |
| Theta range for data collection | 2.730 to 66.597°. | |
| Index ranges | -13<=h<=13, -25<=k<=38, -15<=l<=14 | |
| Reflections collected | 16212 | |
| Independent reflections | 7966 [R(int) = 0.0538] | |
| Completeness to theta = 66.597° | 99.2 % | |
| Absorption correction | Semi-empirical from equivalents | |
| Max. and min. transmission | 1.00000 and 0.77692 | |
| Refinement method | Full-matrix least-squares on $F^2$ | |
| Data / restraints / parameters | 7966 / 7 / 587 | |
| Goodness-of-fit on $F^2$ | 1.010 | |
| Final R indices [I>2sigma(I)] | R1 = 0.0491, wR2 = 0.1025 | |
| R indices (all data) | R1 = 0.0792, wR2 = 0.1165 | |
| Extinction coefficient | n/a | |
| Largest diff. peak and hole | 0.314 and -0.571 $e.Å^{-3}$ | |
| CCDC number | 1570007 | |

**Table 4.2**: Crystal data and structure refinement for **1.5** complexed with Ni(II)

| | | |
|---|---|---|
| Identification code | shelx | |
| Empirical formula | C88 H104 N12 Ni2 O24 | |
| Formula weight | 1831.25 | |
| Temperature | 100(2) K | |
| Wavelength | 1.54184 Å | |
| Crystal system | Triclinic | |
| Space group | P -1 | |
| Unit cell dimensions | a = 9.7941(3) Å | α = 89.839(2)°. |
| | b = 18.0616(5) Å | β = 86.549(2)°. |
| | c = 25.9141(5) Å | γ = 81.820(3)°. |
| Volume | 4529.2(2) Å3 | |
| Z | 2 | |
| Density (calculated) | 1.343 Mg/m3 | |
| Absorption coefficient | 1.187 mm-1 | |
| F(000) | 1928 | |
| Crystal size | 0.189 x 0.060 x 0.022 mm3 | |
| Theta range for data collection | 2.471 to 66.595°. | |
| Index ranges | -11<=h<=11, -21<=k<=21, -30<=l<=30 | |
| Reflections collected | 63893 | |
| Independent reflections | 15980 [R(int) = 0.0759] | |
| Completeness to theta = 66.595° | 99.8 % | |
| Absorption correction | Gaussian | |
| Max. and min. transmission | 1.000 and 0.718 | |
| Refinement method | Full-matrix least-squares on F2 | |
| Data / restraints / parameters | 15980 / 65 / 1171 | |
| Goodness-of-fit on F2 | 1.019 | |
| Final R indices [I>2sigma(I)] | R1 = 0.0497, wR2 = 0.1057 | |
| R indices (all data) | R1 = 0.0822, wR2 = 0.1195 | |
| Extinction coefficient | n/a | |
| Largest diff. peak and hole | 0.461 and -0.382 e.Å-3 | |
| CCDC Number | 1570287 | |

**Table 4.3:** Crystal data and structure refinement for **1.5** complexed with Zn(II)

| | | |
|---|---|---|
| Identification code | shelx | |
| Empirical formula | C110 H129 N15 O29 Zn2 | |
| Formula weight | 2256.01 | |
| Temperature | 100(2) K | |
| Wavelength | 1.54184 Å | |
| Crystal system | Triclinic | |
| Space group | P -1 | |
| Unit cell dimensions | a = 13.8159(3) Å | α= 73.471(2)°. |
| | b = 18.9784(5) Å | β= 89.547(2)°. |
| | c = 23.4074(5) Å | γ = 69.612(2)°. |
| Volume | 5486.8(2) Å3 | |
| Z | 2 | |
| Density (calculated) | 1.366 Mg/m3 | |
| Absorption coefficient | 1.238 mm-1 | |
| F(000) | 2372 | |
| Crystal size | 0.326 x 0.110 x 0.027 mm3 | |
| Theta range for data collection | 2.604 to 66.601°. | |
| Index ranges | -16<=h<=16, -21<=k<=22, -27<=l<=27 | |
| Reflections collected | 50631 | |
| Independent reflections | 18905 [R(int) = 0.0459] | |
| Completeness to theta = 66.601° | 97.4 % | |
| Absorption correction | Gaussian | |
| Max. and min. transmission | 1.000 and 0.589 | |
| Refinement method | Full-matrix least-squares on F2 | |
| Data / restraints / parameters | 18905 / 376 / 1488 | |
| Goodness-of-fit on F2 | 1.019 | |
| Final R indices [I>2sigma(I)] | R1 = 0.0396, wR2 = 0.0918 | |
| R indices (all data) | R1 = 0.0536, wR2 = 0.0998 | |
| Extinction coefficient | n/a | |
| Largest diff. peak and hole | 0.675 and -0.401 e.Å-3 | |
| CCDC Number | 1570856 | |

**Table 4.4**: Crystal data and structure refinement for **1.5** complexed with Pb(II)

| | | |
|---|---|---|
| Empirical formula | C44 H56 N6 O14 Pb | |
| Formula weight | 1100.13 | |
| Temperature | 123(2) K | |
| Wavelength | 0.71073 Å | |
| Crystal system | monoclinic | |
| Space group | C 2/c | |
| Unit cell dimensions | a = 26.065(2) Å | α= 90°. |
| | b = 10.5416(8) Å | β= 94.018(2)°. |
| | c = 16.2407(12) Å | γ = 90°. |
| Volume | 4451.5(6) $Å^3$ | |
| Z | 4 | |
| Density (calculated) | 1.642 $Mg/m^3$ | |
| Absorption coefficient | 3.865 $mm^{-1}$ | |
| F(000) | 2224 | |
| Crystal size | 0.320 x 0.160 x 0.100 $mm^3$ | |
| Theta range for data collection | 2.406 to 29.708°. | |
| Index ranges | -36<=h<=36, -14<=k<=14, -22<=l<=22 | |
| Reflections collected | 31399 | |
| Independent reflections | 6273 [R(int) = 0.0833] | |
| Completeness to theta = 25.242° | 99.9 % | |
| Absorption correction | Semi-empirical from equivalents | |
| Max. and min. transmission | 1.00 and 0.743 | |
| Refinement method | Full-matrix least-squares on $F^2$ | |
| Data / restraints / parameters | 6273 / 0 / 314 | |
| Goodness-of-fit on $F^2$ | 1.029 | |
| Final R indices [I>2sigma(I)] | R1 = 0.0337, wR2 = 0.0809 | |
| R indices (all data) | R1 = 0.0379, wR2 = 0.0824 | |
| Extinction coefficient | n/a | |
| Largest diff. peak and hole | 2.133 and -1.902 $e.Å^{-3}$ | |
| CCDC number | 1570082 | |

**Table 4.5**: Crystal data and structure refinement for **3.8**

| | | |
|---|---|---|
| Empirical formula | C24 H28 Br N3 O2 | |
| Formula weight | 470.40 | |
| Temperature | 100(2) K | |
| Wavelength | 0.71073 Å | |
| Crystal system | monoclinic | |
| Space group | I 2/a | |
| Unit cell dimensions | a = 20.7033(11) Å | α= 90°. |
| | b = 10.2870(6) Å | β= 106.432(3)°. |
| | c = 21.5102(19) Å | γ = 90°. |
| Volume | 4394.0(5) $Å^3$ | |
| Z | 8 | |
| Density (calculated) | 1.422 $Mg/m^3$ | |
| Absorption coefficient | 1.897 $mm^{-1}$ | |
| F(000) | 1952 | |
| Crystal size | 0.800 x 0.360 x 0.180 $mm^3$ | |
| Theta range for data collection | 1.974 to 24.997°. | |
| Index ranges | -24<=h<=24, -12<=k<=12, -25<=l<=25 | |
| Reflections collected | 99673 | |
| Independent reflections | 3871 [R(int) = 0.1317] | |
| Completeness to theta = 24.997° | 100.0 % | |
| Absorption correction | Numerical | |
| Max. and min. transmission | 1.00 and 0.466 | |
| Refinement method | Full-matrix least-squares on $F^2$ | |
| Data / restraints / parameters | 3871 / 308 / 298 | |
| Goodness-of-fit on $F^2$ | 1.028 | |
| Final R indices [I>2sigma(I)] | R1 = 0.0443, wR2 = 0.0833 | |
| R indices (all data) | R1 = 0.0734, wR2 = 0.0954 | |
| Extinction coefficient | 0.00056(8) | |
| Largest diff. peak and hole | 0.649 and -0.393 $e.Å^{-3}$ | |

**Table 4.6**: Crystal data and structure refinement for **3.19**

| | | |
|---|---|---|
| Empirical formula | C24 H27 Ag0.50 F3 N3 O2 P0.50 | |
| Formula weight | 515.90 | |
| Temperature | 100(2) K | |
| Wavelength | 0.71073 Å | |
| Crystal system | Monoclinic | |
| Space group | C 2/c | |
| Unit cell dimensions | a = 18.6622(16) Å | α= 90°. |
| | b = 11.3451(9) Å | β= 91.035(6)°. |
| | c = 21.1959(14) Å | γ = 90°. |
| Volume | 4487.0(6) $Å^3$ | |
| Z | 8 | |
| Density (calculated) | 1.527 $Mg/m^3$ | |
| Absorption coefficient | 0.563 $mm^{-1}$ | |
| F(000) | 2128 | |
| Crystal size | 0.486 x 0.385 x 0.282 $mm^3$ | |
| Theta range for data collection | 1.922 to 25.026°. | |
| Index ranges | -21<=h<=22, -13<=k<=13, -25<=l<=25 | |
| Reflections collected | 18532 | |
| Independent reflections | 3949 [R(int) = 0.0628] | |
| Completeness to theta = 25.026° | 99.9 % | |
| Absorption correction | Numerical | |
| Refinement method | Full-matrix least-squares on $F^2$ | |
| Data / restraints / parameters | 3949 / 18 / 300 | |
| Goodness-of-fit on $F^2$ | 1.041 | |
| Final R indices [I>2sigma(I)] | R1 = 0.0552, wR2 = 0.1352 | |
| R indices (all data) | R1 = 0.0777, wR2 = 0.1486 | |
| Extinction coefficient | n/a | |
| Largest diff. peak and hole | 1.591 and -1.449 $e.Å^{-3}$ | |

# References


(1) Davenport, W. G.; King, M.; Schlesinger, M.; Biswas, A. K. *Extractive Metallurgy of Copper*, 5th ed.; Pergamon Press: Oxford, UK, 2002.

(2) Habashi, F. Extractive Metallurgy and National Policy. *Int. J. Nonferrous Metall.* **2013**, *2*, 31–34.

(3) Agrawal, A.; Kumari, S.; Bagchi, D.; Kumar, V.; Pandey, B. D. Hydrogen Reduction of Copper Bleed Solution from an Indian Copper Smelter for Producing High Purity Copper Powders. *Hydrometallurgy* **2006**, *84* (3–4), 218–224.

(4) Sörme, L.; Lagerkvist, R. Sources of Heavy Metals in Urban Wastewater in Stockholm. *Sci. Total Environ.* **2002**, *298* (1–3), 131–145.

(5) Flett, D. S. Solvent Extraction in Hydrometallurgy: The Role of Organophosphorus Extractants. *J. Organomet. Chem.* **2005**, *690* (10), 2426–2438.

(6) Gotfryd, L.; Pietek, G.; Szolomicki, Z.; Becker, K.; Piwowonska, J. Neodecanoic Acid as Extractant of Selected Non-Ferrous Metals. *Physiochemical Probl. Miner. Process.* **2015**, *51* (2), 435–445.

(7) Alexandratos, S. D. New Polymer-Supported Ion-Complexing Agents: Design, Preparation and Metal Ion Affinities of Immobilized Ligands. *J. Hazard. Mater.* **2007**, *139* (3), 467–470.

(8) Koide, Y.; Tsujimoto, K.; Shosenji, H.; Maeda, M.; Takagi, M. Adsorption of Metal Ions to Surface-Template Resins Prepared with Amphiphilic Styrene Monomers Bearing Amino Carboxylic Acid. *Bull. Chem. Soc. Jpn.* **1998**, *71* (4), 789–796.

(9) Akita, S.; Maeda, T.; Takeuchi, H. Metal Sorption Characteristics of a Macromolecular Resin Containing D2EHPA. *J. Chem. Eng. Jpn.* **1994**, *27* (1), 126–129.

(10) Wang, X.; Chen, L.; Xu, X.; Li, Y. Synthesis of Molecularly Imprinted Polymers via Ring-Opening Metathesis Polymerization for Solid-Phase Extraction of Bisphenol A. *Anal. Bioanal. Chem.* **2011**, *401* (4), 1423.

(11) Al-Degs, Y. S.; Abu-Surrah, A. S.; Ibrahim, K. A. Preparation of Highly Selective Solid-Phase Extractants for Cibacron Reactive Dyes Using Molecularly Imprinted Polymers. *Anal. Bioanal. Chem.* **2009**, *393* (3), 1055–1062.

(12) Hande, P. E.; Samui, A. B.; Kulkarni, P. S. Highly Selective Monitoring of Metals by Using Ion-Imprinted Polymers. *Environ. Sci. Pollut. Res.* **2015**, *22* (10), 7375–7404.

(13) Lorenzo, A. R.; Carro, M. A.; Alvarez-Lorenzo, C.; Concheiro, A. To Remove or Not to Remove? The Challenge of Extracting the Template to Make the Cavities Available in Molecularly Imprinted Polymers (MIPs). *Int. J. Mol. Sci.* **2011**, *12* (7).

(14) Aydogan, A.; Coady, D. J.; Lynch, V. M.; Akar, A.; Marquez, M.; Bielawski, C. W.; Sessler, J. L. Poly(Methyl Methacrylate)s with Pendant Calixpyrroles:

Polymeric Extractants for Halide Anion Salts. *Chem. Commun.* **2008**, No. 12, 1455–1457.
(15) Abd-El-Aziz, A. S.; Shipman, P. O.; Neeland, E. G.; Corkery, T. C.; Mohammed, S.; Harvey, P. D.; Mohamed, H. M.; Bedair, A. H.; El-Agrody, A. M.; Aguiar, P. M.; et al. Benzo[f]- and Benzo[h]Coumarin-Containing Poly(Methyl Methacrylate)s and Poly(Methyl Methacrylate)s with Pendant Coumarin-Containing Azo Dyes. *Macromol. Chem. Phys.* **2008**, *209* (1), 84–103.
(16) Evanoff, D. D.; Carroll, J. B.; Roeder, R. D.; Hunt, Z. J.; Lawrence, J. R.; Foulger, S. H. Poly(Methyl Methacrylate) Copolymers Containing Pendant Carbazole and Oxadiazole Moieties for Applications in Single-layer Organic Light Emitting Devices. *J. Polym. Sci. Part Polym. Chem.* **2008**, *46* (23), 7882–7897.
(17) Matyjaszewski, K.; Xia, J. Atom Transfer Radical Polymerization. *Chem. Rev.* **2001**, *101* (9), 2921–2990.
(18) Sanford, M. S.; Love, J. A.; Grubbs, R. H. A Versatile Precursor for the Synthesis of New Ruthenium Olefin Metathesis Catalysts. *Organometallics* **2001**, *20* (25), 5314–5318.
(19) Ulman, M.; Grubbs, R. H. Ruthenium Carbene-Based Olefin Metathesis Initiators: Catalyst Decomposition and Longevity. *J. Org. Chem.* **1999**, *64* (19), 7202–7207.
(20) Buchmeiser, M. R.; Atzl, N.; Bonn, G. K. Ring-Opening-Metathesis Polymerization for the Preparation of Carboxylic-Acid-Functionalized, High-Capacity Polymers for Use in Separation Techniques. *J. Am. Chem. Soc.* **1997**, *119* (39), 9166–9174.
(21) Sinner, F.; Buchmeiser, M. R.; Tessadri, R.; Mupa, M.; Wurst, K.; Bonn, G. K. Dipyridyl Amide-Functionalized Polymers Prepared by Ring-Opening-Metathesis Polymerization (ROMP) for the Selective Extraction of Mercury and Palladium. *J. Am. Chem. Soc.* **1998**, *120* (12), 2790–2797.
(22) Mitchell, L. A.; Holliday, B. J. Polymeric Materials for the Separation of F-Elements Utilizing Carbamoylmethylphosphine Oxide Chelating Ligands. *ACS Macro Lett.* **2016**, 1100–1103.
(23) Irving, H.; Williams, R. J. P. 637. The Stability of Transition-Metal Complexes. *J. Chem. Soc. Resumed* **1953**, No. 0, 3192–3210.
(24) Tasaki, T.; Oshima, T.; Baba, Y. Selective Extraction and Transport of Copper(II) with New Alkylated Pyridinecarboxylic Acid Derivatives. *Talanta* **2007**, *73* (2), 387–93.
(25) Kiriazis, A.; Gennäs, G. B. af; Talman, V.; Ekokoski, E.; Ruotsalainen, T.; Kylänlahti, I.; Rüffer, T.; Wissel, G.; Xhaard, H.; Lang, H.; et al. Stereoselective Synthesis of (3-Aminodecahydro-1,4-Methanonaphthalen-2-Yl)Methanols Targeted to the {C1} Domain of Protein Kinase C. *Tetrahedron* **2011**, *67* (45), 8665–8670.

(26) Jahn, H. A.; Teller, E. Stability of Polyatomic Molecules in Degenerate Electronic States. I. Orbital Degeneracy. *Proc. R. Soc. Lond. Math. Phys. Eng. Sci.* **1937**, *161* (905), 220–235.
(27) Haas, K. L.; Franz, K. J. Application of Metal Coordination Chemistry to Explore and Manipulate Cell Biology. *Chem. Rev.* **2009**, *109* (10), 4921–4960.
(28) Viéville, J.; Tanty, M.; Delsuc, M.-A. Polydispersity Index of Polymers Revealed by {DOSY} {NMR}. *J. Magn. Reson.* **2011**, *212* (1), 169–173.
(29) Augé, S.; Schmit, P.-O.; Crutchfield, C. A.; Islam, M. T.; Harris, D. J.; Durand, E.; Clemancey, M.; Quoineaud, A.-A.; Lancelin, J.-M.; Prigent, Y.; et al. NMR Measure of Translational Diffusion and Fractal Dimension. Application to Molecular Mass Measurement. *J. Phys. Chem. B* **2009**, *113* (7), 1914–1918.
(30) Tasaki, T.; Oshima, T.; Baba, Y. Selective Extraction and Transport of Copper(II) with New Alkylated Pyridinecarboxylic Acid Derivatives. *Talanta* **2007**, *73* (2), 387–393.
(31) Silverman, D. C. Technical Note: Presence of Solid Fe(OH)2 in EMF-PH Diagram for Iron. *CORROSION* **1982**, *38* (8), 453–455.
(32) Asabella, A. N.; Cascini, G. L.; Paparella, D.; Notaristefano, A.; Rubini, G. The Copper Radioisotopes: A Systematic Review with Special Interest to 64Cu. *BioMed Res. Int. 2014* (Article ID 786463), 9 pages.
(33) Toyota, T.; Hanafusa, T.; Oda, T.; Koumura, I.; Sasaki, T.; Matsuura, E.; Kumon, H.; Yano, T.; Ono, T. A Purification System for (64)Cu Produced by a Biomedical Cyclotron for Antibody PET Imaging. *J. Radioanal. Nucl. Chem.* **2013**, *298* (1), 295–300.
(34) Martell, A. E.; Smith, R. M. Pyridenecarboxylic Acids. In *Critical Stability Constants: First Supplement*; Martell, A. E., Smith, R. M., Eds.; Springer US: Boston, MA, 1982; pp 129–131.
(35) Hofmeister, F. Zur Lehre von Der Wirkung Der Salze. *Arch. Für Exp. Pathol. Pharmakol.* **1888**, *24* (4), 247–260.
(36) Bielawski, C. W.; Benitez, D.; Morita, T.; Grubbs, R. H. Synthesis of End-Functionalized Poly(Norbornene)s via Ring-Opening Metathesis Polymerization. *Macromolecules* **2001**, *34* (25), 8610–8618.
(37) Q3D Elemental Impurities Guidance for Industry. U.S Department of Health and Human Services Food and Drug Administration Center for Drug Evaluation and research (CDER) Center for Biologics Evaluation and research (CBER) September 2015.
(38) *Fuel Cycle Stewardship in a Nuclear Renaissance*; The Royal Society Science Policy Centre Report 10/11; The Royal Society: London, 2011.
(39) Baumgärtner, F.; Ertel, D. The Modern Purex Process and Its Analytical Requirements. *J. Radioanal. Chem.* **1980**, *58* (1), 11–28.
(40) Wigeland, R. A.; Bauer, T. H.; Fanning, T. H.; Morris, E. E. Separations and Transmutation Criteria to Improve Utilization of a Geologic Repository. *Nucl. Technol.* **2006**, *154* (1), 95–106.

(41) Moyer, B. A.; Lumetta, G. J.; Mincher, B. J. 11 - Minor Actinide Separation in the Reprocessing of Spent Nuclear Fuels: Recent Advances in the United States A2 - Taylor, Robin. In *Reprocessing and Recycling of Spent Nuclear Fuel*; Woodhead Publishing: Oxford, 2015; pp 289–312.
(42) Shannon, R. D. Revised Effective Ionic Radii and Systematic Studies of Interatomic Distances in Halides and Chalcogenides. *Acta Crystallogr. Sect. A* **1976**, *32* (5), 751–767.
(43) Runde, W. H.; Mincher, B. J. Higher Oxidation States of Americium: Preparation, Characterization and Use for Separations. *Chem. Rev.* **2011**, *111* (9), 5723–5741.
(44) Pearson, R. G. Hard and Soft Acids and Bases. *J. Am. Chem. Soc.* **1963**, *85* (22), 3533–3539.
(45) Weaver, B.; Kappelmann, F. A. Preferential Extraction of Lanthanides over Trivalent Actinides by Monoacidic Organophosphates from Carboxylic Acids and from Mixtures of Carboxylic and Aminopolyacetic Acids. *J. Inorg. Nucl. Chem.* **1968**, *30* (1), 263–272.
(46) Svantesson, I.; Hangstroem, I.; Persson, G.; Liljenzin, J. O. Separation of Americium and Neodymium by Selective Stripping and Subsequent Extraction with HDEHP Using DTPA-Lactic Acid Solution in a Closed Loop. *Radiochem. Radioanal. Lett.* **1979**, *37* (4–5), 215–222.
(47) Braley, J. C.; Grimes, T. S.; Nash, K. L. Alternatives to HDEHP and DTPA for Simplified TALSPEAK Separations. *Ind. Eng. Chem. Res.* **2012**, *51* (2), 629–638.
(48) Lumetta, G. J.; Casella, A. J.; Rapko, B. M.; Levitskaia, T. G.; Pence, N. K.; Carter, J. C.; Niver, C. M.; Smoot, M. R. An Advanced TALSPEAK Concept Using 2-Ethylhexylphosphonic Acid Mono-2-Ethylhexyl Ester as the Extractant. *Solvent Extr. Ion Exch.* **2015**, *33* (3), 211–223.
(49) Philip Horwitz, E.; Kalina, D. C.; Diamond, H.; Vandegrift, G. F.; Schulz, W. W. THE TRUEX PROCESS - A PROCESS FOR THE EXTRACTION OF THE TKANSURANIC ELEMENTS EROM NITRIC AC In WASTES UTILIZING MODIFIED PUREX SOLVENT*. *Solvent Extr. Ion Exch.* **1985**, *3* (1–2), 75–109.
(50) Braley, J. C.; Lumetta, G. J.; Carter, J. C. Combining CMPO and HEH[EHP] for Separating Trivalent Lanthanides from the Transuranic Elements. *Solvent Extr. Ion Exch.* **2013**, *31* (6), 567–577.
(51) Lumetta, G. J.; Gelis, A. V.; Braley, J. C.; Carter, J. C.; Pittman, J. W.; Warner, M. G.; Vandegrift, G. F. The TRUSPEAK Concept: Combining CMPO and HDEHP for Separating Trivalent Lanthanides from the Transuranic Elements. *Solvent Extr. Ion Exch.* **2013**, *31* (3), 223–236.
(52) Dhami, P. S.; Chitnis, R. R.; Gopalakrishnan, V.; Wattal, P. K.; Ramanujam, A.; Bauri, A. K. Studies on the Partitioning of Actinides from High Level Waste Using a Mixture of HDEHP and CMPO as Extractant. *Sep. Sci. Technol.* **2001**, *36* (2), 325–335.
(53) Courson, O.; Malmbeck, R.; Pagliosa, G.; Roemer, K.; Saetmark, B.; Glatz, J. P.; Baron, P.; Madic, C. *Separation of Minor Actinides from Genuine HLLW Using*

*the DIAMEX Process*; OECD-NEA: Nuclear Energy Agency of the OECD (NEA), 1999.
(54) Lumetta, G. J.; Gelis, A. V.; Carter, J. C.; Niver, C. M.; Smoot, M. R. The Actinide-Lanthanide Separation Concept. *Solvent Extr. Ion Exch.* **2014**, *32* (4), 333–347.
(55) *Lanthanides and Trivalent Actinides Complexation by Tripyridyl Triazine, Applications to Liquid-Liquid Extraction*; CEA-R--5270; France, 1984; p 210.
(56) Cordier, P. Y.; Hill, C.; Baron, P.; Madic, C.; Hudson, M. J.; Liljenzin, J. O. Am (III)/Eu (III) Separation at Low PH Using Synergistic Mixtures Composed of Carboxylic Acids and Neutral Nitrogen Polydendate Ligands. *J. Alloys Compd.* **1998**, *271–273*, 738–741.
(57) Edwards, J. O.; Pearson, R. G. The Factors Determining Nucleophilic Reactivities. *J. Am. Chem. Soc.* **1962**, *84* (1), 16–24.
(58) Kolarik, Z.; Müllich, U.; Gassner, F. Selective Extraction of Am(III) Over Eu(III) by 2,6-Ditriazolyl- and 2,6-Ditriazinylpyridines. *Solvent Extr. Ion Exch.* **1999**, *17* (1), 23–32.
(59) Hill, C.; Guillaneux, D.; Berthon, L.; Madic, C. Sanex-Btp Process Development Studies. *J. Nucl. Sci. Technol.* **2002**, *39* (sup3), 309–312.
(60) Hudson, M. J.; Boucher, C. E.; Braekers, D.; Desreux, J. F.; Drew, M. G. B.; Foreman, M. R. S. J.; Harwood, L. M.; Hill, C.; Madic, C.; Marken, F.; et al. New Bis(Triazinyl) Pyridines for Selective Extraction of Americium(Iii). *New J. Chem.* **2006**, *30* (8), 1171–1183.
(61) Colette, S.; Amekraz, B.; Madic, C.; Berthon, L.; Cote, G.; Moulin, C. Trivalent Lanthanide Interactions with a Terdentate Bis(Dialkyltriazinyl)Pyridine Ligand Studied by Electrospray Ionization Mass Spectrometry. *Inorg. Chem.* **2003**, *42* (7), 2215–2226.
(62) Drew, M. G. B.; Foreman, M. R. S. J.; Hill, C.; Hudson, M. J.; Madic, C. 6,6′-Bis-(5,6-Diethyl-[1,2,4]Triazin-3-Yl)-2,2′-Bipyridyl the First Example of a New Class of Quadridentate Heterocyclic Extraction Reagents for the Separation of Americium(III) and Europium(III). *Inorg. Chem. Commun.* **2005**, *8* (3), 239–241.
(63) Harwood, L. M.; Lewis, F. W.; Hudson, M. J.; John, J.; Distler, P. The Separation of Americium(III) from Europium(III) by Two New 6,6'-Bistriazinyl-2,2'-Bipyridines in Different Diluents. *Solvent Extr. Ion Exch.* **2011**, *29* (4), 551–576.
(64) Lewis Frank W.; Harwood Laurence M.; Hudson Michael J.; Distler Petr; John Jan; Stamberg Karel; Núñez Ana; Galán Hitos; Espartero Amparo G. Synthesis and Evaluation of Lipophilic BTBP Ligands for An/Ln Separation in Nuclear Waste Treatment: The Effect of Alkyl Substitution on Extraction Properties and Implications for Ligand Design. *Eur. J. Org. Chem.* **2012**, *2012* (8), 1509–1519.
(65) Lewis, F. W.; Harwood, L. M.; Hudson, M. J.; Drew, M. G. B.; Modolo, G.; Sypula, M.; Desreux, J. F.; Bouslimani, N.; Vidick, G. Interaction of 6,6[Prime or Minute][Prime or Minute]-Bis(5,5,8,8-Tetramethyl-5,6,7,8-Tetrahydro-1,2,4-Benzotriazin-3-Yl)-2,2[Prime or Minute]:6[Prime or Minute],2[Prime or Minute][Prime or Minute]-Terpyridine (CyMe4-BTTP) with Some Trivalent Ions

Such as Lanthanide(Iii) Ions and Americium(Iii). *Dalton Trans.* **2010**, *39* (21), 5172–5182.

(66) Lewis, F. W.; Harwood, L. M.; Hudson, M. J.; Drew, M. G. B.; Desreux, J. F.; Vidick, G.; Bouslimani, N.; Modolo, G.; Wilden, A.; Sypula, M.; et al. Highly Efficient Separation of Actinides from Lanthanides by a Phenanthroline-Derived Bis-Triazine Ligand. *J. Am. Chem. Soc.* **2011**, *133* (33), 13093–13102.

(67) Higginson, M. A.; Kyle, N. D.; Marsden, O. J.; Thompson, P.; Livens, F. R.; Heath, S. L. Synthesis of Functionalised BTPhen Derivatives - Effects on Solubility and Americium Extraction. *Dalton Trans.* **2015**, *44* (37), 16547–16552.

(68) Benay, G.; Wipff, G. Oil-Soluble and Water-Soluble BTPhens and Their Europium Complexes in Octanol/Water Solutions: Interface Crossing Studied by MD and PMF Simulations. *J. Phys. Chem. B* **2013**, *117* (4), 1110–1122.

(69) Higginson, M. A.; Marsden, O. J.; Thompson, P.; Livens, F. R.; Heath, S. L. Separation of Americium from Complex Radioactive Mixtures Using a BTPhen Extraction Chromatography Resin. *React. Funct. Polym.* **2015**, *91–92*, 93–99.

(70) Afsar, A.; Distler, P.; Harwood, L. M.; John, J.; Westwood, J. Extraction of Minor Actinides, Lanthanides and Other Fission Products by Silica-Immobilized BTBP/BTPhen Ligands. *Chem. Commun.* **2017**, *53* (28), 4010–4013.

(71) Lewis, F. W.; Harwood, L. M.; Hudson, M. J.; Geist, A.; Kozhevnikov, V. N.; Distler, P.; John, J. Hydrophilic Sulfonated Bis-1,2,4-Triazine Ligands Are Highly Effective Reagents for Separating Actinides(Iii) from Lanthanides(Iii) via Selective Formation of Aqueous Actinide Complexes †Electronic Supplementary Information (ESI) Available: Procedures and Characterization Data for All Compounds. Tables and Graphs of Solvent Extraction Data. See DOI: 10.1039/C5sc01328c Click Here for Additional Data File. *Chem. Sci.* **2015**, *6* (8), 4812–4821.

(72) Xiao, C.-L.; Wang, C.-Z.; Yuan, L.-Y.; Li, B.; He, H.; Wang, S.; Zhao, Y.-L.; Chai, Z.-F.; Shi, W.-Q. Excellent Selectivity for Actinides with a Tetradentate 2,9-Diamide-1,10-Phenanthroline Ligand in Highly Acidic Solution: A Hard–Soft Donor Combined Strategy. *Inorg. Chem.* **2014**, *53* (3), 1712–1720.

(73) Jansone-Popova, S.; Ivanov, A. S.; Bryantsev, V. S.; Sloop, F. V.; Custelcean, R.; Popovs, I.; Dekarske, M. M.; Moyer, B. A. Bis-Lactam-1,10-Phenanthroline (BLPhen), a New Type of Preorganized Mixed N,O-Donor Ligand That Separates Am(III) over Eu(III) with Exceptionally High Efficiency. *Inorg. Chem.* **2017**, *56* (10), 5911–5917.

(74) Berthon, L.; Condamines, N.; Y. Cordier, P.; Livet, J.; Madic, C.; Cuillerdier, C.; Musikas, C.; Hudson, M. *Recent Advances in the Treatment of Nuclear Wastes by the Use of Diamide and Picolinamide Extractants*; 1995; Vol. 30.

(75) Casnati, A.; Ca', N. D.; Fontanella, M.; Sansone, F.; Ugozzoli, F.; Ungaro, R.; Liger, K.; Dozol, J. Calixarene-Based Picolinamide Extractants for Selective An/Ln Separation from Radioactive Waste. *Eur. J. Org. Chem.* **2005**, *2005* (11), 2338–2348.

(76) Galletta, M.; Baldini, L.; Sansone, F.; Ugozzoli, F.; Ungaro, R.; Casnati, A.; Mariani, M. Calix[6]Arene-Picolinamide Extractants for Radioactive Waste: Effect of Modification of the Basicity of the Pyridine N Atom on the Extraction Efficiency and An/Ln Separation. *Dalton Trans.* **2010**, *39* (10), 2546–2553.
(77) Macerata, E.; Sansone, F.; Baldini, L.; Ugozzoli, F.; Brisach, F.; Haddaoui, J.; Hubscher-Bruder, V.; Arnaud-Neu, F.; Mariani, M.; Ungaro, R.; et al. Calix[6]Arene-Picolinamide Extractants for Radioactive Waste Treatment: Effect of Additional Carboxy Binding Sites in the Pyridine 6-Positions on Complexation, Extraction Efficiency and An/Ln Separation. *Eur. J. Org. Chem.* **2010**, *2010* (14), 2675–2686.
(78) Bisson, J.; Dehaudt, J.; Charbonnel, M.; Guillaneux, D.; Miguirditchian, M.; Marie, C.; Boubals, N.; Dutech, G.; Pipelier, M.; Blot, V.; et al. 1,10-Phenanthroline and Non-Symmetrical 1,3,5-Triazine Dipicolinamide-Based Ligands For Group Actinide Extraction. *Chem. - Eur. J.* **2014**, *20* (25), 7819–7829.
(79) Hebel, W.; Cottone, G. Management Modes for Iodine-129: Proceedings of a Meeting. In *Radioactive Waste Management*; Harwood Academic Publishers, 1982; Vol. 7, pp 306–310.
(80) International Atomic Energy Agency. *Treatment, Conditioning and Disposal of Iodine-129*; Technical Reports Series; International Atomic Energy Agency: Vienna, 1987.
(81) International Atomic Energy Agency. *Control of Iodine in the Nuclear Industry*; Technical Reports Series; International Atomic Energy Agency, 1973.
(82) Jubin, R. T.; Soelberg, N. R.; Strachan, D. M.; Ilas, G. *Fuel Age Impacts on Gaseous Fission Product Capture During Separations*; United States, 2012.
(83) Burger, L. L.; Scheele, R. D. *HWVP Iodine Trap Evaluation*; United States, 2004.
(84) Jubin, R. T. *Airborne Waste Management Technology Applicable for Use in Reprocessing Plants for Control of Iodine and Other Off-Gas Constituents*; United States, 1988.
(85) Holladay, D. W. *Literature Survey: Methods for the Removal of Iodine Species from Off-Gases and Liquid Waste Streams of Nuclear Power and Nuclear Fuel Reprocessing Plants, with Emphasis on Solid Sorbents*; 1979.
(86) Mailen, J. C.; Horner, D. E. Removal of Radioiodine from Gas Streams by Electrolytic Scrubbing. *Nucl. Technol.* **1976**, *30* (3), 317–324.
(87) Haefner, D. *Methods of Gas Phase Capture of Iodine from Fuel Reprocessing Off-Gas: A Literature Survey*; Idaho National Laboratory, 2007.
(88) Pence, D. T.; Duce, F. A.; Maeck, W. J.; First, M. W. Developments in the Removal of Airborne Iodine Species with Metal- Substituted Zeolites; Research Org.: Allied Chemical Corp., Idaho Falls, ID; Harvard Univ., Boston, Mass. (USA). Harvard Air Cleaning Lab., 1973.
(89) Moore, J. G.; Howerton, W. B. *LMFBR Fuel Cycle Studies Progress Report For July 1970, No. 17*; ORNL/TM-3095; Oak Ridge National Laboratory, 1970.

(90) Patil, K. C.; Rao, C. N. R.; Lacksonen, J. W.; Dryden, C. E. The Silver Nitrate-Iodine Reaction: Iodine Nitrate as the Reaction Intermediate. *J. Inorg. Nucl. Chem.* **1967**, *29* (2), 407–412.
(91) Wilhelm, J. G.; Schuettelkopf, H.; First, M. W. (ed. . Inorganic Adsorber Material for Off-Gas Cleaning in Fuel Reprocessing Plants; Research Org.: Kernforschungszentrum, Karlsruhe, Ger.; Harvard Univ., Boston, Mass. (USA). Harvard Air Cleaning Lab.; Oak Ridge National Lab., Tenn. (USA), 1973.
(92) Herrmann, F. J.; Herrman, B.; Hoeflich, V. *Removal Efficiency of Silver Impregnated Filter Materials and Performance of Iodine Filters in the Off-Gas of the Karlsruhe Reprocessing Plant WAK*; NUREG-CP--0153; United States, 1997; pp 609–617.
(93) Fukasawa, T.; Funabashi, K.; Kondo, Y. *Influences of Impurities on Iodine Removal Efficiency of Silver Alumina Adsorbent*; NUREG-CP--0153; United States, 1997; pp 563–575.
(94) Brown, R. A.; Christian, J. D.; Thomas, T. R. *Airborne Radionuclide Waste-Management Reference Document*; ENICO--1133; Idaho National Laboratory: United States, 1983; p 361.
(95) Chapman, K. W.; Chupas, P. J.; Nenoff, T. M. Radioactive Iodine Capture in Silver-Containing Mordenites through Nanoscale Silver Iodide Formation. *J. Am. Chem. Soc.* **2010**, *132* (26), 8897–8899.
(96) Murphy, L. P.; Staples, B. A.; Thomas, T. R. *Development of Ag0Z for Bulk 129I Removal from Nuclear Fuel Reprocessing Plants and PbX for 129I Storage*; ICP--1135; United States, 1977; p 26.
(97) Jubin, R. T. *Organic Iodine Removal from Simulated Dissolver Off-Gas Streams Using Silver-Exchanged Mordenite*; CONF-801038--1 (Draft); United States, 1980; p 31.
(98) Gurav, J. L.; Jung, I.-K.; Park, H.-H.; Kang, E. S.; Nadargi, D. Y. Silica Aerogel: Synthesis and Applications. *J. Nanomater.* **2010**, *2010*, 11.
(99) Soleimani Dorcheh, A.; Abbasi, M. H. Silica Aerogel; Synthesis, Properties and Characterization. *J. Mater. Process. Technol.* **2008**, *199* (1), 10–26.
(100) Matyáš, J. *Silver-Functionalized Silica Aerogels for Iodine Capture and Immobilization*; Separations and Waste Forms Research and Development FY 2012 Accomplishments Report; FCRD-SWF-2013-000073; Idaho National Laboratory: United States, 2013; pp 63–64.
(101) Mohanan, J. L.; Arachchige, I. U.; Brock, S. L. Porous Semiconductor Chalcogenide Aerogels. *Science* **2005**, *307* (5708), 397.
(102) Bag, S.; Gaudette, A. F.; Bussell, M. E.; Kanatzidis, M. G. Spongy Chalcogels of Non-Platinum Metals Act as Effective Hydrodesulfurization Catalysts. *Nat. Chem.* **2009**, *1*, 217.
(103) Kanatzidis, M. G.; Bag, S. Semiconducting Aerogels from Chalcogenido Clusters with Broad Applications.
(104) Riley, B. J.; Chun, J.; Ryan, J. V.; Matyas, J.; Li, X. S.; Matson, D. W.; Sundaram, S. K.; Strachan, D. M.; Vienna, J. D. Chalcogen-Based Aerogels as a

Multifunctional Platform for Remediation of Radioactive Iodine. *RSC Adv.* **2011**, *1* (9), 1704–1715.
(105) Riley, B. J.; Chun, J.; Um, W.; Lepry, W. C.; Matyas, J.; Olszta, M. J.; Li, X.; Polychronopoulou, K.; Kanatzidis, M. G. Chalcogen-Based Aerogels as Sorbents for Radionuclide Remediation. *Environ. Sci. Technol.* **2013**, *47* (13), 7540–7547.
(106) Bag, S.; Kanatzidis, M. G. Chalcogels: Porous Metal−Chalcogenide Networks from Main-Group Metal Ions. Effect of Surface Polarizability on Selectivity in Gas Separation. *J. Am. Chem. Soc.* **2010**, *132* (42), 14951–14959.
(107) Szente, L.; Fenyvesi, É.; Szejtli, J. Entrapment of Iodine with Cyclodextrins: Potential Application of Cyclodextrins in Nuclear Waste Management. *Environ. Sci. Technol.* **1999**, *33* (24), 4495–4498.
(108) Sessler, J. L.; An, D.; Cho, W.-S.; Lynch, V. Calix[n]Bipyrroles: Synthesis, Characterization, and Anion-Binding Studies. *Angew. Chem. Int. Ed.* **2003**, *42* (20), 2278–2281.
(109) Garner, M. E.; Niu, W.; Chen, X.; Ghiviriga, I.; Abboud, K. A.; Tan, W.; Veige, A. S. N-Heterocyclic Carbene Gold(i) and Silver(i) Complexes Bearing Functional Groups for Bio-Conjugation. *Dalton Trans.* **2015**, *44* (4), 1914–1923.
(110) Liu, J.; Chen, J.; Zhao, J.; Zhao, Y.; li, L.; Zhang, H. *A Modified Procedure for the Synthesis of 1-Arylimidazoles*; 2003; Vol. 35.
(111) Ranke, J.; Othman, A.; Fan, P.; Müller, A. Explaining Ionic Liquid Water Solubility in Terms of Cation and Anion Hydrophobicity. *Int. J. Mol. Sci.* **2009**, *10* (3).
(112) de Frémont, P.; Scott, N. M.; Stevens, E. D.; Ramnial, T.; Lightbody, O. C.; Macdonald, C. L. B.; Clyburne, J. A. C.; Abernethy, C. D.; Nolan, S. P. Synthesis of Well-Defined N-Heterocyclic Carbene Silver(I) Complexes. *Organometallics* **2005**, *24* (26), 6301–6309.
(113) *CrysAlisPro Ref*; CrysAlisPro; Rigaku Americas Corporation: The Woodlands, TX 77381, USA.
(114) Altomare, A.; Burla, M. C.; Camalli, M.; Cascarano, G. L.; Giacovazzo, C.; Guagliardi, A.; Moliterni, A. G. G.; Polidori, G.; Spagna, R. It SIR97: A New Tool for Crystal Structure Determination and Refinement. *J. Appl. Crystallogr.* **1999**, *32* (1), 115–119.
(115) Sheldrick, G. M. A Short History of It SHELX. *Acta Crystallogr. Sect. A* **2008**, *64* (1), 112–122.
(116) Spek, A. L. Single-Crystal Structure Validation with the Program It PLATON. *J. Appl. Crystallogr.* **2003**, *36* (1), 7–13.
(117) Farrugia, L. J. It WinGX and It ORTEP for Windows: An Update. *J. Appl. Crystallogr.* **2012**, *45* (4), 849–854.
(118) *Mercury*; The Cambridge Crystallographic Data Centre: Cambridge, UK, 2016.
(119) Woźaniak, M.; van der Plas, H. C. On the Synthesis and Animation of 5-Chloro- and 5-Bromo-1,7-Naphthyridine. *J. Heterocycl. Chem.* **1978**, *15* (5), 731–736.